BED LOAD TRANSPORT IN GRAVEL-BED RIVERS

A Dissertation

Presented in Partial Fulfillment of the Requirements for the

Degree of Doctor of Philosophy

with a major in

Civil Engineering

in the

College of Graduate Studies

University of Idaho

by

Jeffrey J. Barry

July 2007

Major Professor: John M. Buffington

AUTHORIZATION TO SUBMIT

DISSERTATION

This dissertation of Jeffrey J. Barry, submitted for the degree of Doctor of Philosophy (Ph.D.) with a major in Civil Engineering in the College of Graduate Studies titled “Bed load transport in gravel-bed rivers,” has been reviewed in final form. Permission, as indicated by the signatures and dates given below, is now granted to submit final copies to the College of Graduate Studies for approval.

Major Professor	_____ John M. Buffington	Date	_____
Committee Members	_____ Peter Goodwin	Date	_____
	_____ John G. King	Date	_____
	_____ William W. Emmett	Date	_____
Department Administrator	_____ Sunil Sharma	Date	_____
College of Engineering Dean	_____ Aicha Elshabini	Date	_____

Final Approval and Acceptance by the College of Graduate Studies

_____ Date _____

Margrit von Braun

ABSTRACT

Bed load transport is a fundamental physical process in alluvial rivers, building and maintaining a channel geometry that reflects both the quantity and timing of water and the volume and caliber of sediment delivered from the watershed. A variety of formulae have been developed to predict bed load transport in gravel-bed rivers, but testing of the equations in natural channels has been fairly limited. Here, I assess the performance of 4 common bed load transport equations (the *Meyer-Peter and Müller* [1948], *Ackers and White* [1973], *Bagnold* [1980], and *Parker* [1990] equations) using data from a wide range of gravel-bed rivers in Idaho. Substantial differences were found in equation performance, with the transport data best described by a simple power function of discharge. From this, a new bed load transport equation is proposed in which the coefficient and exponent of the power function are parameterized in terms of channel and watershed characteristics. The accuracy of this new equation was evaluated at 17 independent test sites, with results showing that it performs as well or better than the other equations examined.

However, because transport measurements are typically taken during lower flows it is unclear whether this and other previous assessments of equation performance apply to higher, geomorphically significant flows. To address this issue, the above transport equations were evaluated in terms of their ability to predict the effective discharge, an index flow used in stream restoration projects. It was found that accurate effective discharge predictions are not particularly sensitive to the choice of bed load transport equation. A framework is presented for standardizing the transport equations to explain

observed differences in performance and to explore sensitivity of effective discharge predictions.

Finally, a piecewise regression was used to identify transitions between phases of bed load transport that are commonly observed in gravel-bed rivers. Transitions from one phase of motion to another are found to vary by size class, and equal mobility (defined as $p_i/f_i \approx 1$, the proportion of a size class in the bed load relative to that of the subsurface) was not consistently associated with any specific phase of transport. The identification of phase transitions provides a physical basis for defining size-specific reference transport rates (W^*_{ri}). In particular, the transition from Phase I to II transport may be an alternative to *Parker*'s [1990] constant value of W^*_{ri} =0.0025, and the transition from Phase II to III transport could be used for defining flushing flows or channel maintenance flows.

ACKNOWLEDGEMENTS

Above all I want to thank my wife Ginger for her amazing patience and understanding during this process that took years longer than anticipated. I also apologize to her and my two young boys for the time spent away from them while I completed this project.

I would like to thank my supervisor John Buffington for making this research possible and for his advice. The quality of work improved immensely with every comment and correction John made and without which this work could not have been possible.

I would like to mention my committee members, Peter Goodwin, Jack King and Bill Emmett. Thanks go to Peter Goodwin who initially convinced me to return to academia after two bliss filled years away. My interest in bed load transport is largely due to the time spent with Jack and Bill at the Boise River Adjudication Team.

I would like to mention that this work was, in part, supported by the USDA Forest Service Yankee Fork Ranger District (grant number 00-PA-11041303-071).

Table of Contents

List of Tables

List of Figures

Introduction

Bed load transport in alluvial rivers is the principle link between river hydraulics and river form [*Parker*, 1978; *Leopold*, 1994; *Gomez*, 2006] and is responsible for building and maintaining the channel geometry [*Parker*, 1978; *Leopold*, 1994]. Furthermore, the reproductive success of salmonids and other riverine communities are influenced by the size of sediment eroded from and deposited on the channel bed and banks [*Montgomery et al.*, 1996; *Reiser*, 1998]. Projects aimed at restoring the physical processes and ecological function of rivers increasingly recognize the importance of a quasi-stable channel geometry and the role of bed load transport in forming and maintaining it [*Goodwin*, 2004].

However, because the collection of good quality bed load transport data is expensive and time consuming, we frequently must rely on predicted bed load transport rates determined from existing equations [*Gomez*, 2006]. But the evaluation of equation performance in coarse gravel-bed rivers has been limited due to the small number of available data sets, and those assessments that have been made are discouraging, commonly reporting orders of magnitude error [*Gomez and Church*, 1989; *Yang and Huang*, 2001]. It appears that despite over a century of effort, we are unable to consistently and reliably predict bed load transport rates [*Gomez*, 2006]. This is particularly difficult in gravel-bed rivers where the presence of a coarse surface layer acts to constrain the availability and mobility of the finer subsuface bed material [*Parker et al.*, 1982; *Gomez*, 2006].

An extensive set of over 2,000 bed load transport data obtained by *King et al.* [2004] from 24 mountain gravel-bed rivers in central Idaho present a unique opportunity

to assess the performance of different bed load transport equations across a wide range of gravel-bed rivers and to further examine the effects of armoring on bed load transport.. Based on this work I present a new bed load transport equation which explicitly accounts for channel armoring, and I evaluate the accuracy of this new equation at 17 independent test sites.

However, the data collected by *King et al.* [2004] were typically taken during lower flows and, therefore, it is unclear whether my assessment of equation performance applies to higher, geomorphically significant flows. This is a problem common to most previous assessments of equation performance [e.g., *Gomez and Church*, 1989; *Yang and Huang*, 2001; *Bravo-Espinosa et al*., 2003; *Barry et al*., 2004]. To address this issue, I evaluate a number of common transport equations (including my own) in terms of their ability to predict the effective discharge, a geomorphically important flow often used to size stream channels in restoration projects.

I also explore in greater detail the effect of the armor layer on controlling bed load transport rates over a wide range of flows in two channels representing very different geomorphic conditions.

References

Barry, J. J., J. M. Buffington, and, J. G. King (2004), A general power equation for predicting bed load transport rates in gravel bed rivers, *Water Resour. Res.*, 40, W104001, doi:10.1029/2004WR003190.

Bravo-Espinosa, M., W. R. Osterkamp, and, V. L. Lopes (2003), Bed load transport in alluvial channels, *J. Hydraul. Eng.*, 129, 783-795.

Gomez, B., and M. Church (1989), An assessment of bed load sediment transport formulae for gravel bed rivers, *Water Resour. Res.*, *25*, 1161-1186.

Gomez, B. (2006), The potential rate of bed-load transport, *Proceedings, National Academy of Sciences, 73, 103*, 17170-17173.

Goodwin, P. (2004), Analytical solutions for estimating effective discharge, *J. Hydraul. Eng., 130*, 729-738.

King, J. G., W. W. Emmett, P. J. Whiting, R. P. Kenworthy, and, J. J. Barry (2004), Sediment transport data and related information for selected gravel-bed streams and rivers in Idaho, *U.S. Forest Service Tech. Rep. RMRS-GTR-131*, 26 pp.

Leopold, L. B. (1994). *A view of the river*, Harvard University Press, Cambridge, Mass..

Montgomery, D. R., J. M. Buffington, N. P. Peterson, D. Schuett-Hames, and, T. P. Quinn (1996), Stream-bed scour, egg burial depths, and the influence of salmonids spawning on bed surface mobility and embryo survival, *Can. J. Fish Aquat. Sci. 53* 1061-1070, 1996.

Parker, G. (1978), Self-formed straight rivers with equilibrium banks and mobile bed. Part 2. The gravel river, *J. Fluid Mech., 89*, 127-146.

Parker, G., P. C. Klingeman, and, D. G. McLean (1982), Bed load and size distribution in paved gravel-bed streams, *J. Hydraul. Div., Amer. Soc. Civ. Eng.*, *108*, 544-571.

Reiser, D.W. (1998), Sediment in gravel bed rivers: ecological and biological considerations, in *Gravel Bed Rivers in the Environment*, ed. P.C. Klingeman, R.L. Beschta, P.D. Komar and J.B. Bradley, 1, 199-225, Highland Ranch, CO: Water Res., 896 pp.

Yang, C. T., and, C. Huang (2001), Applicability of sediment transport formulas, *Int. J. Sed. Res.*, *16*, 335-353.

Chapter 1. A General Power Equation for Predicting Bed Load Transport Rates in Gravel-Bed Rivers[1]

1.1 Abstract

A variety of formulae have been developed to predict bed load transport in gravel-bed rivers, ranging from simple regressions to complex multi-parameter formulations. The ability to test these formulae across numerous field sites has, until recently, been hampered by a paucity of bed load transport data for gravel-bed rivers. We use 2104 bed load transport observations in 24 gravel-bed rivers in Idaho to assess the performance of 8 different formulations of 4 bed load transport equations. Results show substantial differences in performance, but no consistent relationship between formula performance and degree of calibration or complexity. However, formulae containing a transport threshold typically exhibit poor performance. Furthermore, we find that the transport data are best described by a simple power function of discharge. From this we propose a new bed load transport equation and identify channel and watershed characteristics that control the exponent and coefficient of the proposed power function. We find that the exponent is principally a factor of supply-related channel armoring (transport capacity in excess of sediment supply), whereas the coefficient is related to drainage area (a surrogate for absolute sediment supply). We evaluate the accuracy of the proposed power function at 17 independent test sites.

[1] Co-authored paper with John M. Buffington and John G. King published in Water Resources Research, 2004.

1.2 Introduction

Fang [1998] remarked on the need for a critical evaluation and comparison of the plethora of sediment transport formulae currently available. In response, *Yang and Huang* [2001] evaluated the performance of 13 sediment transport formulae in terms of their ability to describe the observed sediment transport from 39 datasets (a total of 3391 transport observations). They concluded that sediment transport formulae based on energy dissipation rates or stream power concepts more accurately described the observed transport data and that the degree of formula complexity did not necessarily translate into increased model accuracy. Although the work of *Yang and Huang* [2001] is helpful in evaluating the applicability and accuracy of many popular sediment transport equations, it is necessary to extend their analysis to coarse-grained natural rivers. Of the 39 datasets used by *Yang and Huang* [2001] only 5 included observations from natural channels (166 transport observations) and these were limited to sites with a fairly uniform grain-size distribution (gradation coefficient ≤ 2).

Prior to the extensive work of *Yang and Huang* [2001], *Gomez and Church* [1989] performed a similar analysis of 12 bed load transport formulae using 88 bed load transport observations from 4 natural gravel-bed rivers and 45 bed load transport observations from 3 flumes. The authors concluded that none of the selected formulae performed consistently well, but they did find that formula calibration increases prediction accuracy. However, similar to *Yang and Huang* [2001], *Gomez and Church* [1989] had limited transport observations from natural gravel-bed rivers.

Reid et al. [1996] assessed the performance of several popular bed load formulae in the Negev Desert, Israel, and found that the *Meyer-Peter and Müller* [1948] and

Parker [1990] equations performed best, but their analysis considered only one gravel-bed river. Due to small sample sizes, these prior investigations leave the question unresolved as to the performance of bed load transport formulae in coarse-grained natural channels.

Recent work by *Martin* [2003], *Bravo-Espinosa et al.* [2003] and *Almedeij and Diplas* [2003] has begun to address this deficiency. *Martin* [2003] took advantage of 10 years of sediment transport and morphologic surveys on the Vedder River, British Columbia, to test the performance of the *Meyer-Peter and Müller* [1948] equation and two variants of the *Bagnold* [1980] equation. The author concluded that the formulae generally under-predict gravel transport rates and suggested that this may be due to loosened bed structure or other disequilibria resulting from channel alterations associated with dredge mining within the watershed.

Bravo-Espinosa et al. [2003] considered the performance of seven bed load transport formulae on 22 alluvial streams (including a sub-set of the data examined here) in relation to a site-specific "transport category" (i.e., transport limited, partially transport limited and supply limited). The authors found that certain formulae perform better under certain categories of transport and that, overall, the *Schoklitsch* [1962] equation performed well at eight of the 22 sites, while the *Bagnold* [1980] equation performed well at seven of the 22 sites.

Almedeij and Diplas [2003] considered the performance of the *Meyer-Peter and Müller* [1948], Einstein and Brown [*Brown*, 1950], *Parker* [1979] and *Parker et al.* [1982] bed load transport equations on three natural gravel-bed streams, using a total of 174 transport observations. The authors found that formula performance varied between

sites, in some cases over-predicting observed bed load transport rates by one to three orders of magnitude, while at others under-predicting by up to two orders of magnitude.

Continuing these recent studies of bed load transport in gravel-bed rivers, we examine 2104 bed load transport observations from 24 study sites in mountain basins of Idaho to assess the performance of four bed load transport equations. We also assess accuracy in relation to the degree of formula calibration and complexity.

Unlike *Gomez and Church* [1989] and *Yang and Huang* [2001], we find no consistent relationship between formula performance and the degree of formula calibration and complexity. However, we find that the observed transport data are best fit by a simple power function of total discharge. We propose this power function as a new bed load transport equation and explore channel and watershed characteristics that control the exponent and coefficient of the observed bed load power functions. We hypothesize that the exponent is principally a function of supply-related channel armoring, such that mobilization of the surface material in a well armored channel is followed by a relatively larger increase in bed load transport rate (i.e., steeper rating curve) than that of a similar channel with less surface armoring. We use *Dietrich et al.*'s [1989] dimensionless bed load transport ratio (q^*) to quantify channel armoring in terms of upstream sediment supply relative to transport capacity, and relate q^* values to the exponents of the observed bed load transport functions. We hypothesize that the power-function coefficient depends on absolute sediment supply, which we parameterize in terms of drainage area.

The purpose of this paper is four-fold: 1) assess the performance of four bed load transport formulae in mountain gravel-bed rivers, 2) use channel and watershed

characteristics to parameterize the coefficient and exponent of our bed load power function to make it a predictive equation, 3) test the parameterization equations, and 4) compare the performance of our proposed bed load transport function to that of the other equations in item (1).

1.3. Bed Load Transport Formulae

We compare predicted total bed load transport rates to observed values at each study site using four common transport equations, and we examine how differences in formula complexity and calibration influence performance. In each equation we use the characteristic grain size as originally specified by the author(s) to avoid introducing error or bias. We also examine several alternative definitions to investigate the effects of grain-size calibration on formula performance. Variants of other parameters in the bed load equations are not examined, but could also influence performance.

Eight variants of four formulae were considered: the *Meyer-Peter and Müller* [1948] equation (calculated both by median subsurface grain size, d_{50ss}, and by size class, d_i), the *Ackers and White* [1973] equation as modified by *Day* [1980] (calculated by d_i), the *Bagnold* [1980] equation (calculated by the modal grain size of each bed load event, d_{mqb}, and by the mode of the subsurface material, d_{mss}), and the *Parker et al.* [1982] equation as revised by *Parker* [1990] (calculated by d_{50ss} and two variants of d_i). We use the subsurface-based version of the *Parker* [1990] equation because the surface-based one requires site-specific knowledge of how the surface size distribution evolves with discharge and bed load transport (information that was not available to us and that we did not feel confident predicting). The formulae are further described in Appendix 1.1 and

are written in terms of specific bed load transport rate, defined as dry mass per unit width and time (q_b, kg/m•s).

Two variants of the size-specific (d_i) *Parker et al.* [1982] equation are considered, one using a site-specific hiding function following *Parker et al.*'s [1982] method, and the other using *Andrews'* [1983] hiding function. These two variants allow comparison of site-specific calibration versus use of an "off-the-shelf" hiding function for cases where bed load transport data are not available. We selected the *Andrews* [1983] hiding function because it was derived from channel types and physiographic environments similar to those examined in this study. We also use single grain size (d_{50ss}) and size-specific (d_i) variants of the *Meyer-Peter and Müller* [1948] and *Parker et al.* [1982] equations to further examine effects of grain-size calibration. In this case, we compare predictions based on a single grain size (d_{50ss}) versus those summed over the full range of size classes available for transport (d_i). We also consider two variants of the *Bagnold* [1980] equation, one where the representative grain size is defined as the mode of the observed bed load data (d_{mqb}, as specified by *Bagnold* [1980]) and one based on the mode of the subsurface material (d_{mss}, an approach that might be used where bed load transport observations are unavailable). The latter variant of the *Bagnold* [1980] equation is expected to be less accurate because it uses a static grain size (the subsurface mode), rather than the discharge-specific mode of the bed load.

The transport equations were solved for flow and channel conditions present during bed load measurements and are calibrated to differing degrees to site-specific conditions. For example, the *Meyer-Peter and Müller* [1948] formula includes a shear stress correction based on the ratio of particle roughness to total roughness, where

particle roughness is determined from surface grain size and the *Strickler* [1923] equation, and total roughness is determined from the *Manning* [1891] equation for observed values of hydraulic radius and water-surface slope (Appendix 1.1).

Except for the *Parker et al.* [1982] equation, each of the formulae used in our analysis are similar in that they contain a threshold for initiating bed load transport. The *Meyer-Peter and Müller* [1948] equation is a power function of the difference between applied and critical shear stresses, the *Ackers and White* [1973] equation is a power function of the ratio of applied to critical shear stress minus 1, and the *Bagnold* [1980] equation is a power function of the difference between applied and critical unit stream power (Appendix 1.1). In contrast, the *Parker et al.* [1982] equation lacks a transport threshold and predicts some degree of transport at all discharges, similar to *Einstein*'s [1950] equation.

1.4. Study Sites and Methods

Data obtained by *King et al.* [2004] from 24 mountain gravel-bed rivers in central Idaho were used to assess the performance of different bed load transport equations and to develop our proposed power-function for bed load transport (Figure 1.1). The 24 study sites are single-thread channels with pool-riffle or plane-bed morphology [as defined by *Montgomery and Buffington*, 1997]. Banks are typically composed of sand, gravel and cobbles with occasional boulders, are densely vegetated and appear stable. An additional 17 study sites in Oregon, Wyoming and Colorado were used to test our new bed load transport equation (Figure 1.1). Selected site characteristics are given in Table 1.1.

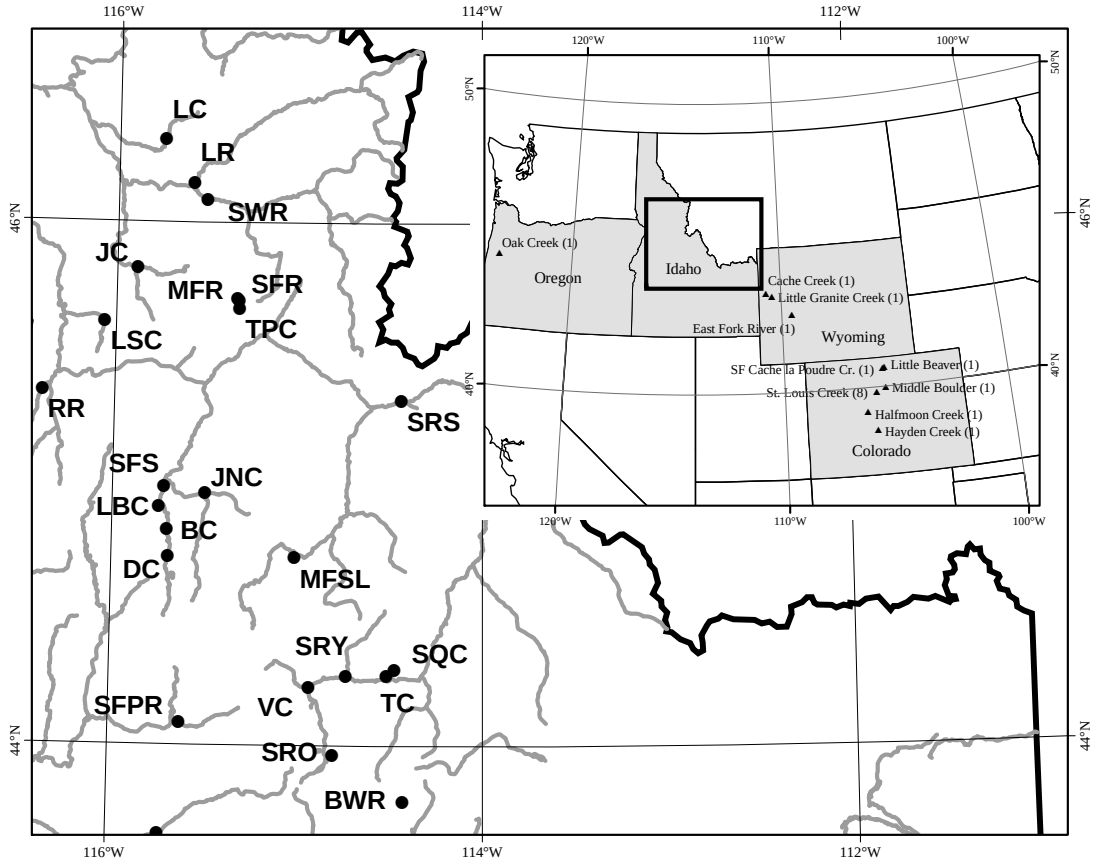

Figure 1.1. Location of bed load transport study sites. Table 1.1 lists river names abbreviated here. Inset box shows the location of test sites outside of Idaho. Parentheses next to test site names indicate number of data sets at each site.

Whiting and King [2003] describes the field methods at 11 of our 24 Idaho sites (also see *Moog and Whiting* [1998], *Whiting et al.* [1999] and *King et al.* [2004] for further information on the sites). Bed load samples were obtained using a 3-inch Helley-Smith [*Helley and Smith*, 1971] sampler, which limits the sampled bed load material to particle sizes less than about 76 mm. Multiple lines of evidence, including movement of painted rocks and bed load captured in large basket samplers at a number of the 24 Idaho

Table 1.1. Study-and test site characteristics.

Study Site (abbreviation)	Drainage Area (km^2)	Average Slope (m/m)	Subsurface d_{50ss} (mm)	Surface d_{50s} (mm)	2-yr flood (cms)
Little Buckhorn Creek (LBC)	16	0.0509	15	74	2.79
Trapper Creek (TPC)	21	0.0414	17	75	2.21
Dollar Creek (DC)	43	0.0146	22	83	11.8
Blackmare Creek (BC)	46	0.0299	25	101	6.95
Thompson Creek (TC)	56	0.0153	44	62	3.10
SF Red River (SFR)	99	0.0146	25	95	8.7
Lolo Creek (LC)	106	0.0097	19	85	16.9
MF Red River (MFR)	129	0.0059	18	57	12.8
Little Slate Creek (LSC)	162	0.0268	24	134	16.0
Squaw Creek (SQC)	185	0.0100	29	46	6.62
Salmon R. near Obsidian (SRO)	243	0.0066	26	61	14.8
Rapid River (RR)	280	0.0108	16	75	20.3
Johns Creek (JC)	293	0.0207	36	204	36.8
Big Wood River (BWR)	356	0.0091	25	119	26.2
Valley Creek (VC)	386	0.0040	21	50	28.3
Johnson Creek (JNC)	560	0.0040	14	62	83.3
SF Salmon River (SFS)	853	0.0025	14	38	96.3
SF Payette River (SFPR)	1164	0.0040	20	95	120
Salmon R. blw Yankee Fk (SRY)	2101	0.0034	25	104	142
Boise River (BR)	2154	0.0038	21	60	188
MF Salmon R. at Lodge (MFSL)	2694	0.0041	36	146	258
Lochsa River (LR)	3055	0.0023	27	132	532
Selway River (SWR)	4955	0.0021	24	185	731
Salmon River at Shoup (SRS)	16154	0.0019	28	96	385
Test Sites					
Fool Cr. (St. Louis Cr Test Site)	2.9	0.0440	14.7	38.2	0.320
Oak Creek	6.7	0.0095	19.5	53.0	2.98
East St. Louis Creek	8.0	0.0500	13.4	51.1	0.945
St. Louis Creek Site 5	21.3	0.0480	14.4	146	2.52
Cache Creek	27.5	0.0210	20.2	45.6	2.2
St. Louis Creek Site 4a	33.5	0.0190	12.9	71.7	3.96
St. Louis Creek Site 4	33.8	0.0190	12.8	90.5	3.99
Little Beaver Creek	34	0.2300	9.88	46.7	2.24
Hayden Creek	46.5	0.0250	19.7	68	2.28
St. Louis Creek Site 3	54	0.0160	16.4	81.9	5.07
St. Louis Creek Site 2	54.2	0.0170	14.8	76.2	5.08
Little Granite Creek	54.6	0.0190	17.8	55.0	8.41
St. Louis Creek Site 1	55.6	0.0390	16.5	129.3	5.21
Halfmoon Creek	61.1	0.0150	18.4	61.5	7.3
Middle Boulder Creek	83.0	0.0128	24.7	74.5	12.6
SF Cache la Poudre	231	0.0070	12.3	68.5	13.79
East Fork River	466.0	0.0007	1.0	5.00	36.0

sites, indicate that during the largest flows almost all sizes found on the streambed are mobilized, including sizes larger than the orifice of the Helley-Smith sampler. However, transport-weighted composite samples across all study sites indicate that only a very small percentage of the observed particles in motion approached the size limit of the Helley-Smith sampler. Therefore, though larger particles are in motion during flood flows, the motion of these particles is infrequent and the likelihood of sampling these larger particles is small.

Each bed load observation is a composite of all sediment collected over a 30 to 60 second sample period, depending on flow conditions, at typically 20 equally-spaced positions across the width of the wetted channel [*Edwards and Glysson*, 1999]. Between 43 and 192 non-zero bed load transport measurements were collected over a 1 to 7 year period and over a range of discharges from low flows to those well in excess of the bankfull flood at each of the 24 Idaho sites.

Channel geometry and water surface profiles were surveyed following standard field procedures [*Williams et al.*, 1988]. Surveyed reaches were typically 20 channel widths in length. At eight sites water surface slopes were measured over a range of discharges and did not vary significantly. Hydraulic geometry relations for channel width, average depth and flow velocity were determined from repeat measurements over a wide range of discharges.

Surface and subsurface particle size distributions were measured at a minimum of three locations at each of the study sites during low flows between 1994 and 2000. Where surface textures were fairly uniform throughout the study reach, three locations were systematically selected for sampling surface and subsurface material. If major

textural differences were observed, two sample sites were located within each textural patch, and measurements were weighted by patch area [e.g., *Buffington and Montgomery*, 1999a]. *Wolman* [1954] pebble counts of 100^{+} surface grains were conducted at each sample site. Subsurface samples were obtained after removing the surface material to a depth equal to the d_{90} of surface grains and were sieved by weight. The *Church et al.* [1987] sampling criterion was generally met, such that the largest particle in the sample comprised, on average, about 5% of the total sample weight. However, at three sites (Johns Creek, Big Wood River and Middle Fork Salmon River) the largest particle comprised 13%-14% of the total sample weight; the Middle Fork Salmon River is later excluded for other reasons.

Estimates of flood frequency were calculated using a Log Pearson III analysis [*USGS*, 1982] at all study sites that had at least a 10 year record of instantaneous stream flow. Only five years of flow data were available at Dollar and Blackmare creeks and, therefore, estimates of flood frequency were calculated using a two-station comparison [*USGS*, 1982] based on nearby, long-term USGS stream gages. A regional relationship between drainage area and flood frequency was used at Little Buckhorn Creek due to a lack instantaneous peak flow data.

Each sediment transport observation at the 24 Idaho sites was reviewed for quality. At nine of the sites all observations were included. Of the remaining 15 sites, a total of 284 transport observations (out of 2,388) were removed (between 2 and 51 observations per site). The primary reasons for removal were differences in sampling method prior to 1994, or because the transport observations were taken at a different, or unknown, location compared to the majority of bed load transport samples. Only 41

transport observations (out of 284) from nine sites were removed due to concerns regarding sample quality (i.e., significant amounts of measured transport at extremely low discharges indicative of "scooping" during field sampling).

Methods of data collection varied greatly among the additional 17 test sites outside of Idaho and are described in detail elsewhere (see *Ryan and Emmett* [2002] for Little Granite Creek, Wyoming; *Leopold and Emmett* [1997] for the East Fork River, Wyoming; *Milhous* [1973] for Oak Creek, Oregon; *Ryan et al.* [2002] for the eight sites on the St. Louis River, Colorado; and *Gordon* [1995] for both Little Beaver and Middle Boulder creeks, Colorado). Data collection methods at Halfmoon Creek, Hayden Creek and South Fork Cache la Poudre Creek, Colorado and Cache Creek, Wyoming were similar to the 8 test sites from St. Louis Creek. Both the East Fork River and Oak Creek sites used channel-spanning slot traps to catch the entire bed load, while the remaining 15 test sites used a 3-inch Helley-Smith bed load sampler spanning multiple years (typically 1 to 5 years, with a maximum of 14 years at Little Granite Creek). Estimates of flood frequency were determined using either standard flood-frequency analyses [*USGS*, 1982] or from drainage area – discharge relationships derived from nearby stream gages.

1.5. Results and Discussion

1.5.1. Performance of the Bed load Transport Formulae

1.5.1.1. Log-Log Plots

Predicted total bed load transport rates for each formula were compared to observed values, with a $\log_{10}$-transformation applied to both. A logarithmic transformation is commonly applied in bed load studies because transport rates typically span a large range of values (6^{+} orders of magnitude on a $\log_{10}$ scale), and the data tend to

be skewed toward small transport rates without this transformation. To provide more rigorous support for the transformation we used the ARC program [*Cook and Weisberg*, 1999] to find the optimal Box-Cox transformation [*Neter et al.*, 1974] (i.e., one that produces a near-normal distribution of the data). Results indicate that a $\log_{10}$ transformation is appropriate, and conforms with the traditional approach for analyzing bed load transport data.

Figure 1.2 provides an example of observed versus predicted transport rates from the Rapid River study site and indicates that some formulae produced fairly accurate, but biased, predictions of total transport. That is, predicted values were generally tightly clustered and sub-parallel to the 1:1 line of perfect agreement, but were typically larger than the observed values (e.g., Figure 1.2c). Other formulae exhibited either curvilinear bias (e.g., Figures 1.2b, f and g) or rotational bias (constantly trending departure from accuracy) (e.g., Figures 1.2a, d, e and h). Based on visual inspection of similar plots from all 24 sites, the *Parker et al.* [1982] equations (d_i and d_{50ss}) best describe the observed transport rates, typically within an order of magnitude of the observed values. In contrast, the *Parker et al.* [1982] (d_i via *Andrews* [1983]), *Meyer-Peter and Müller* [1948] (d_i and d_{50ss}) and *Bagnold* [1980] (d_{mss} and d_{mqb}) equations did not perform as well, usually over two orders of magnitude from the observed values. The *Ackers and White* [1973] equation was typically one to three orders of magnitude from the observed values.

1.5.1.2. Transport Thresholds

The above assessment of performance can be misleading for those formulae that contain a transport threshold (i.e., the *Meyer-Peter and Müller* [1948], *Ackers and White*

[1973] and *Bagnold* [1980] equations). Formulae of this sort often erroneously predict zero transport at low to moderate flows that are below the predicted threshold for transport. These incorrect zero-transport predictions cannot be shown in the log-log plots of observed versus predicted transport rates (Figure 1.2). However, frequency distributions of the erroneous zero-transport predictions reveal substantial error for both variants of the *Meyer-Peter and Müller* [1948] equation and the *Bagnold* [1980] (d_{mss}) equation (Figure 1.3). These formulae incorrectly predict zero transport for about 50% of all observations at our study sites. In contrast, the *Bagnold* [1980] (d_{mqb}) and *Ackers and White* [1973] equations incorrectly predict zero transport for only 2% and 4% of the observations, respectively, at only one of the 24 study sites. Formulae that lack transport thresholds (i.e., the *Parker et al.* [1982] equation) do not predict zero transport rates.

The significance of the erroneous zero-transport predictions depends on the magnitude of the threshold discharge and the portion of the total bed load that is excluded by the prediction threshold. To examine this issue we calculated the maximum discharge at which each threshold-based transport formula predicted zero transport (Q_{max}) normalized by the 2-year flood discharge (Q_2). Many authors report that significant bed load movement begins at discharges that are 60% to 100% of bankfull flow [*Leopold et al.*, 1964; *Carling*, 1988; *Andrews and Nankervis*, 1995; *Ryan and Emmett*, 2002; *Ryan et al.*, 2002]. Bankfull discharge at the Idaho sites has a recurrence interval of 1-4.8 years, with an average of 2 years [*Whiting et al.*, 1999], hence Q_2 is a bankfull-like flow. We use Q_2 rather than the bankfull discharge because it can be determined objectively from flood frequency analyses (Section 1.4) without the uncertainty inherent in field identification of bankfull stage. As Q_{max}/Q_2 increases the significance of incorrectly

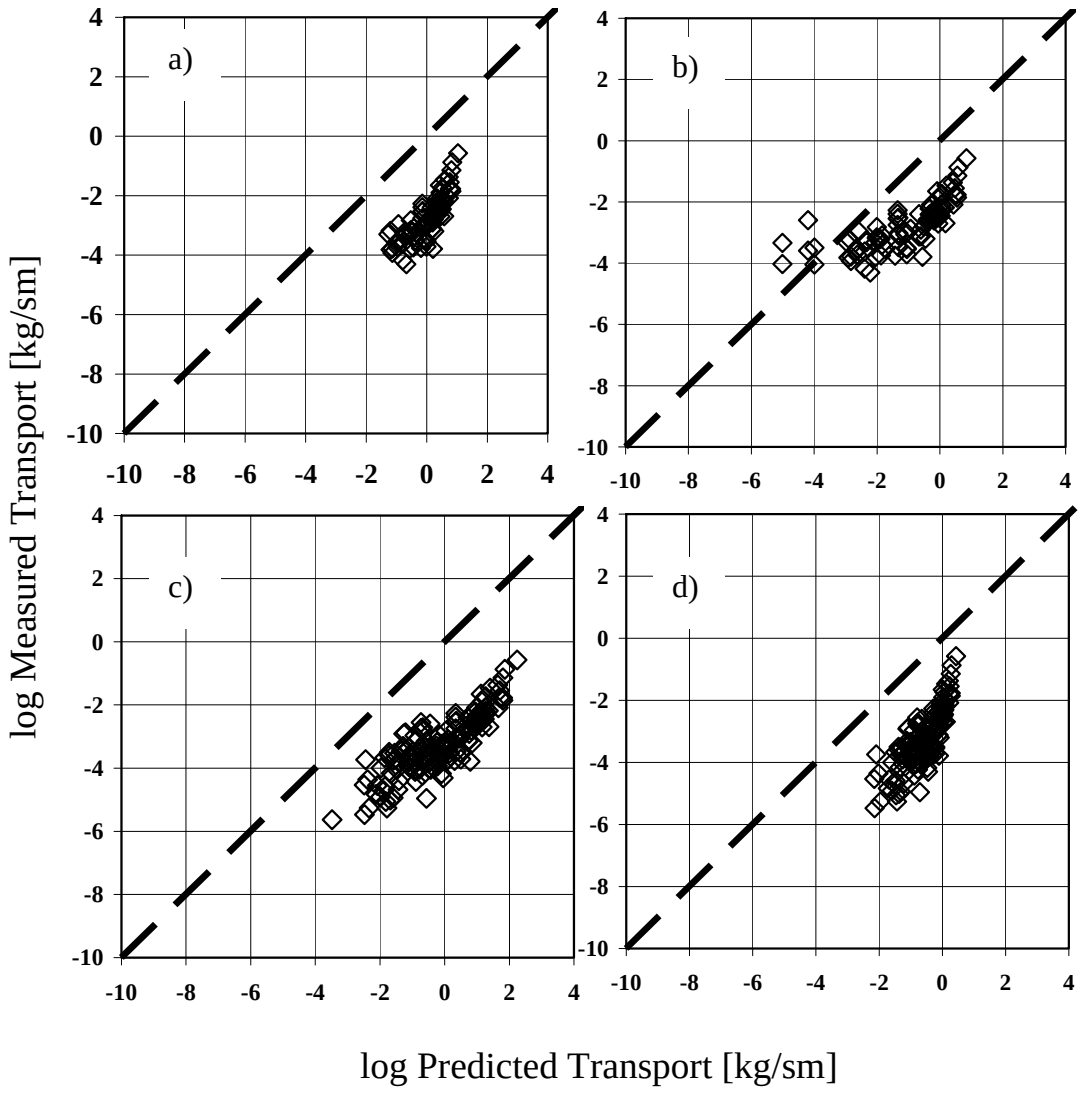

Figure 1.2. Comparison of measured versus computed total bed load transport rates for Rapid River (typical of the Idaho study sites): a) *Meyer-Peter and Müller* [1948] equation by d_{50ss}, b) Meyer-Peter and Müller equation by d_i c) *Ackers and White* [1973] equation by d_i, d) Bagnold equation by d_{mss}, e) Bagnold equation by d_{mqb}, f) *Parker et al.* [1982] equation by d_{50ss}, g) *Parker et al.* [1982] equation by d_i (hiding function defined by *Parker et al.* [1982] and h) *Parker et al.* [1982] equation by d_i (hiding function defined by *Andrews* [1983]).

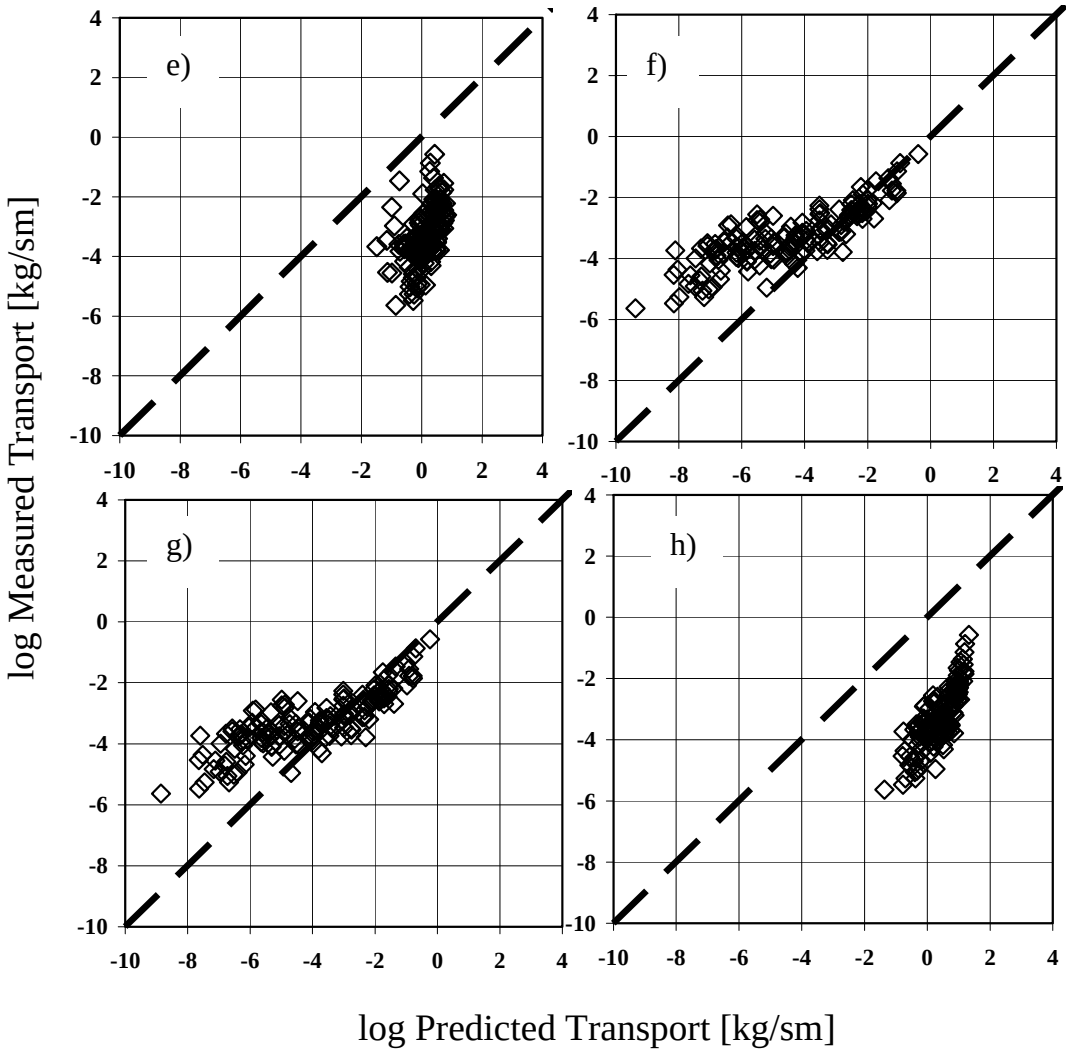

Figure 1.2, continued. Comparison of measured versus computed total bed load transport rates for Rapid River (typical of the Idaho study sites): a) *Meyer-Peter and Müller* [1948] equation by d_{50ss}, b) Meyer-Peter and Müller equation by d_i c) *Ackers and White* [1973] equation by d_i, d) Bagnold equation by d_{mss}, e) Bagnold equation by d_{mqb}, f) *Parker et al.* [1982] equation by d_{50ss}, g) *Parker et al.* [1982] equation by d_i (hiding function defined by *Parker et al.* [1982] and h) *Parker et al.* [1982] equation by d_i (hiding function defined by *Andrews* [1983]).

predicting zero transport increases as well. For instance, at the Boise River study site, both variants of the *Meyer-Peter and Müller* [1948] equation incorrectly predicted zero transport rates for approximately 10% of the transport observations. However, because this error occurred for flows approaching only 19% of Q_2, only 2% of the cumulative total transport is lost due to this prediction error. The significance of incorrectly predicting zero transport is greater at Valley Creek where, again, both variants of the *Meyer-Peter and Müller* [1948] equation incorrectly predict zero transport rates for approximately 90% of the transport observations and at flows approaching 75% of Q_2. This prediction error translates into a loss of 48% of the cumulative bed load transport.

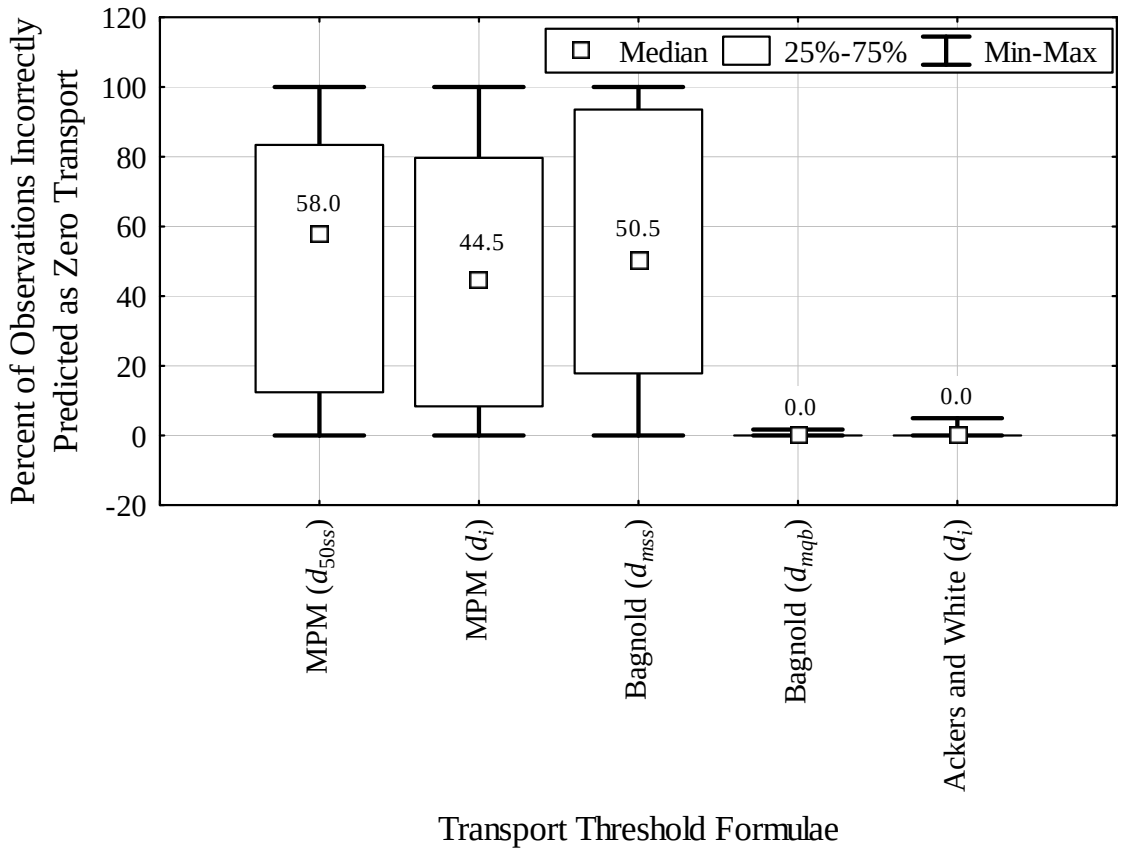

Figure 1.3. Box plots of the distribution of incorrect predictions of zero transport for the 24 Idaho sites. Median values are specified. MPM stands for Meyer-Peter and Müller.

Box plots of Q_{max}/Q_2 values show that incorrect zero predictions are most significant for the *Meyer-Peter and Müller* [1948] equations and the *Bagnold* [1980] (d_{mss}) equation, while the *Bagnold* [1980] (d_{mqb}) and *Ackers and White* [1973] equations have few incorrect zero predictions and less significant error (lower Q_{max}/Q_2 ratios) (Figure 1.4).

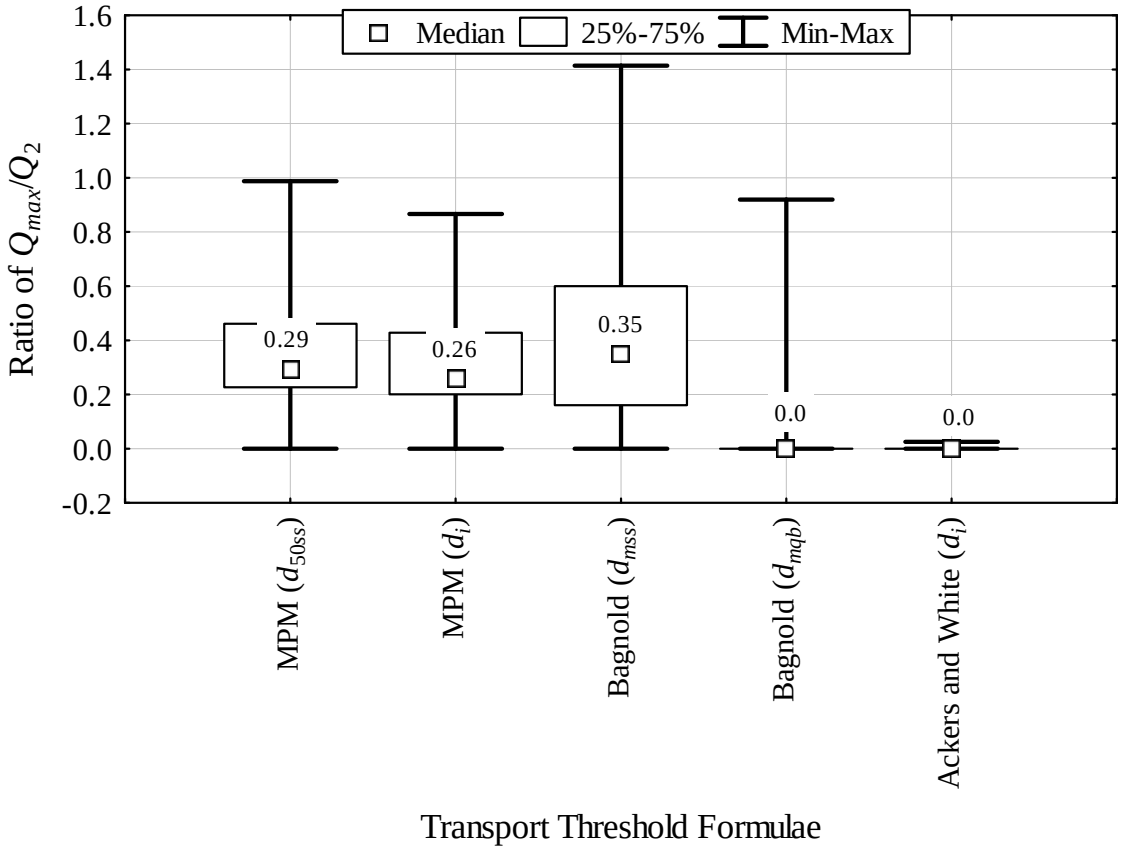

Figure 1.4. Box plots of the distribution of Q_{max}/Q_2 (maximum discharge at which each threshold-based transport formula predicted zero transport normalized by the 2-year flood discharge) for the 24 Idaho sites. Median values are specified. MPM stands for Meyer-Peter and Müller.

Because coarse-grained rivers typically transport most of their bed load at near-bankfull discharges [e.g., *Andrews and Nankervis*, 1995], failure of the threshold equations at low flows may not be significant in terms of the annual bed load transport. However, our analysis indicates that in some instances the threshold equations fail at moderate to high discharges ($Q_{max}/Q_2 > 0.8$), potentially excluding a significant portion of the annual bed load transport (e.g., Valley Creek as discussed above). Moreover, the frequency of incorrect zero predictions varies widely by transport formula (Figure 1.4). To better understand the performance of these equations it is useful to examine the nature of their threshold formulations.

As discussed in Section 1.3, the *Meyer-Peter and Müller* [1948] equation is a power function of the difference between applied and critical shear stresses. A shear stress correction is used to account for channel roughness and to determine that portion of the total stress applied to the bed (Appendix 1.1). However, the *Meyer-Peter and Müller* [1948] stress correction may be too severe, causing the high number of zero-transport predictions. Bed stresses predicted from the *Meyer-Peter and Müller* [1948] method are typically only 60-70% of the total stress at our sites. Moreover, because armored gravel-bed rivers tend to exhibit a near-bankfull threshold for significant bed load transport [*Leopold et al.*, 1964; *Parker* 1978; *Carling*, 1988; *Andrews and Nankervis*, 1995], the range of transporting shear stresses may be narrow, causing transport predictions to be particularly sensitive to the accuracy of stress corrections.

The *Bagnold* [1980] equation is a power function of the difference between applied and critical unit stream powers. The modal grain size of the subsurface material (d_{mss}) is typically 32 mm to 64 mm (geometric mean of 45 mm) at our study sites,

whereas the modal grain size of the bed load observations varied widely with discharge and was typically between 1.5 mm at low flows and 64 mm during flood flows. Not surprisingly the *Bagnold* [1980] equation performs well when critical stream power is based on the modal grain size of each measured bed load event (d_{mqb}), but not when it is defined from the mode of the subsurface material (d_{mss}) (Figures 1.3 and 1.4). When calibrated to the observed bed load data, the critical unit stream power scales with discharge such that at low flows when the measured bed load is fine (small d_{mqb}) the critical stream power is reduced. Conversely, as discharge increase and the measured bed load data coarsens (larger d_{mqb}) the critical unit stream power increases. However, the mode of the subsurface material (d_{mss}) does not scale with discharge and consequently the critical unit discharge is held constant for all flow conditions when based on d_{mss}. Consequently, threshold conditions for transport based on d_{mss} are often not exceeded, while those of d_{mqb} were exceeded over 90% of the time.

In contrast, the *Ackers and White* [1973] equation is a power function of the ratio of applied to critical shear stress minus 1, where the critical shear stress is, in part, a function of d_{50ss}, rather than d_{mss}. At the Idaho sites, d_{50ss} is typically about 20 mm and, therefore, the critical shear stress is exceeded at most flows, resulting in a low number of incorrect zero predictions (Figure 1.3).

1.5.1.3. Statistical Assessment

The performance of each formula was also assessed statistically using the $\log_{10}$-difference between predicted and observed total bed load transport. To include the incorrect zero predictions in this analysis we added a constant value, ε, to all observed

and predicted transport rates prior to taking the logarithm. The lowest non-zero transport rate predicted for the study sites ($1 \cdot 10^{-15}$ kg/m·s) was chosen for this constant.

Formula performance changes significantly compared to that of Section 1.5.1.1 when we include the incorrect zero-transport predictions. The distribution of $\log_{10}$ differences across all 24 study sites from each formula is shown in Figure 1.5. Both versions of the *Meyer-Peter and Müller* [1948] equation and the *Bagnold* [1980] (d_{mss}) equation typically underpredict total transport due to the large number of incorrect zero predictions, with the magnitude of this underprediction set by ε. All other equations included in this analysis have few, if any, incorrect zero predictions and tend to predict total transport values within 2 to 3 orders of magnitude of the observed values.

To further examine formula performance, we conducted paired-sample χ^2 tests to compare observed versus predicted transport rates for each equation across the 24 study sites. We use *Freese's* [1960] approach, which differs slightly from the traditional paired-sample χ^2 analysis in that the χ^2 statistic is calculated as

$$\chi^2 = \frac{\sum_{i=1}^{n} (x_i - \mu_i)^2}{\sigma^2} \tag{1.1}$$

where x_i is the i^{th} predicted value, μ_i is the i^{th} observed value, n is the number of observations, and σ^2 is the required accuracy defined as

$$\sigma^2 = \frac{E^2}{(1.96)^2} \tag{1.2}$$

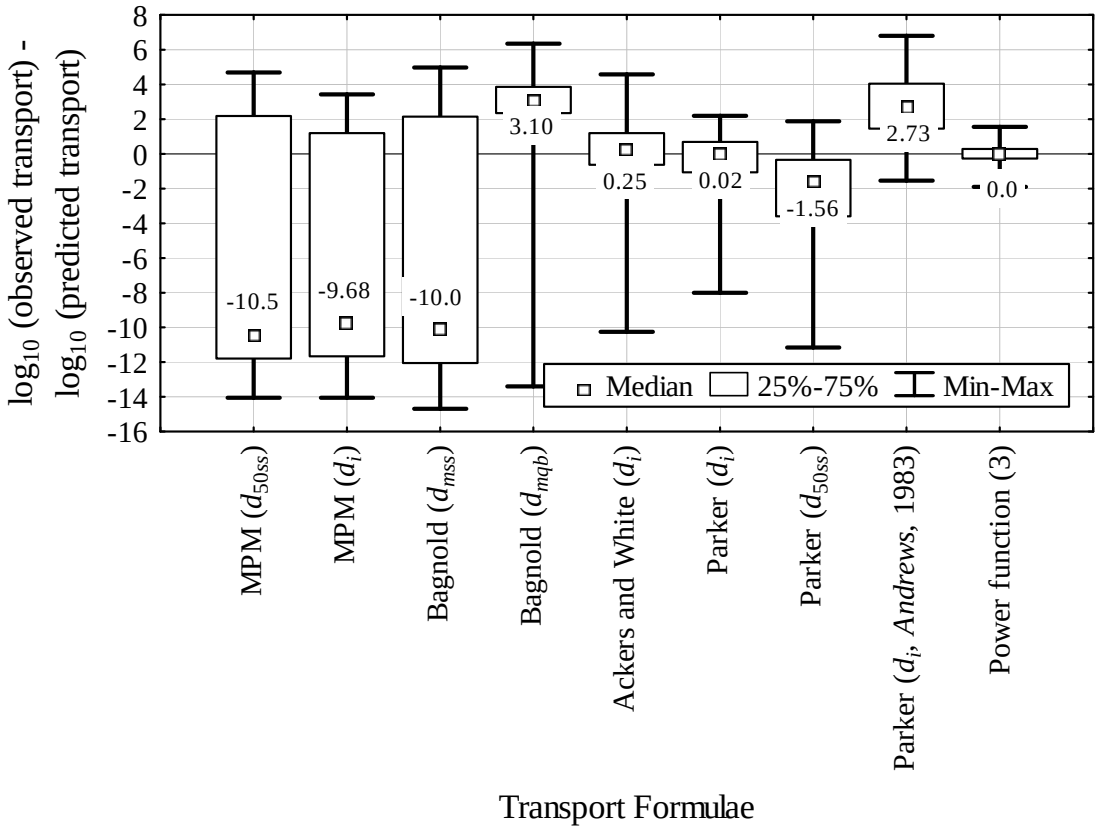

Figure 1.5. Box plots of the distribution of $\log_{10}$ differences between observed and predicted bed load transport rates for the 24 Idaho study sites. Median values are specified. MPM stands for Meyer-Peter and Müller. Power function is discussed in Section 1.5.3.

where E is the user-specified acceptable error, and 1.96 is the value of the standard normal deviate corresponding to a two-tailed probability of 0.05. We evaluate χ^2 using log-transformed values of bed load transport, with ε added to both x_i and μ_i prior to taking the logarithm, and E defined as one log unit (i.e., ± an order of magnitude error).

Freese's [1960] χ^2 test shows that none of the equations perform within the specified accuracy (± an order of magnitude error, $\alpha = 0.05$). Nevertheless, some

equations are clearly better than others (Figure 1.5). To further quantify equation performance, we calculated the critical error, e^*, at each of the 24 study sites (Figure 1.6), where e^* is the smallest value of E that will lead to adequate model performance (i.e., acceptance of the null hypothesis of equal distributions of observed and predicted bed load transport rates assessed via *Freese's* [1960] χ^2 test). Hence, we are asking how much error would have to be tolerated to accept a given model (bed load transport equation) [*Reynolds*, 1984].

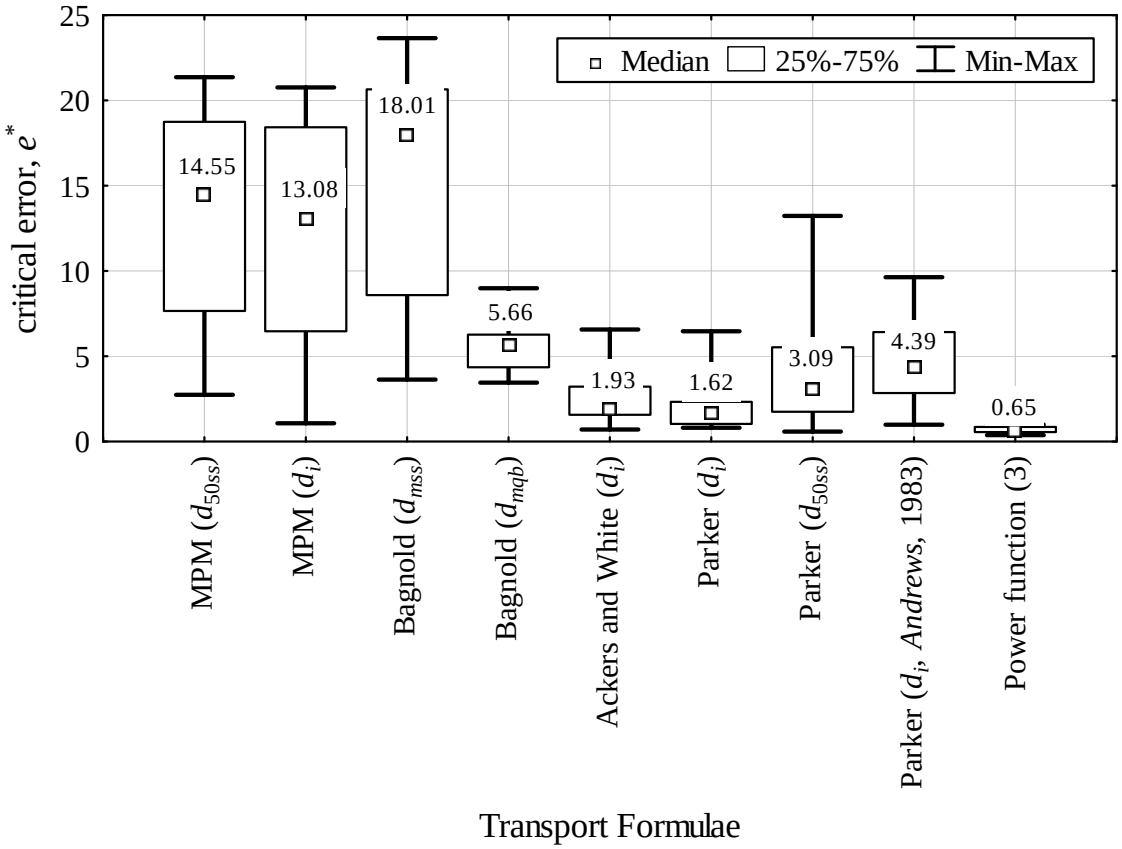

Figure 1.6. Box plots of the distribution of critical error, e^*, for the 24 Idaho sites. Median values are specified. MPM stands for Meyer-Peter and Müller. Power function is discussed in Section 1.5.3.

Results show that at best, median errors of less than 2 orders of magnitude would have to be tolerated for acceptance of the best-performing equations (*Ackers and White* [1973] and *Parker et al.* [1982] (d_i) equations), while at worst, median errors of more than 13 orders of magnitude would have to be tolerated for acceptance of the poorest-performing equations (Figure 1.6). In detail, we find that the *Parker et al.* [1982] (d_i) equation outperformed all others except for the *Ackers and White* [1973] formula (paired χ^2 test of e^* values, $\alpha = 0.05$). However, the median critical errors of these two equations were quite poor (1.62 and 1.93, respectively). The *Bagnold* [1980] (d_{mss}) equation and both variants of the *Meyer-Peter and Müller* [1948] equation had the largest critical errors, with the latter not statistically different from one another (paired χ^2 test, $\alpha = 0.05$). The *Parker et al.* [1982] (d_{50ss}) and the *Parker et al.* [1982] (d_i via *Andrews* [1983]) equations were statistically similar to each other and performed better than the *Bagnold* [1980] (d_{mqb}) equation (paired χ^2 test, $\alpha = 0.05$).

Although the χ^2 statistic is sensitive to the magnitude of ε, specific choice of ε between $1 \cdot 10^{-15}$ and $1 \cdot 10^{-7}$ kg/m·s does not change the relative performance of the equations or the significance of the differences in performance between them. Nor does it alter the finding that none of the median critical errors, e^*, are less than or equal to E; the formulae with the lowest critical errors have little to no incorrect zero transport predictions and are, thus, least affected by ε (c.f. Figures 1.3 and 1.6).

It should be noted that our analysis of performance does not weight transport events by their proportion of the annual bed load transport [sensu *Wolman and Miller*, 1960], but by the number of transport observations. Because there are more low-flow

transport events than high-flow ones during a given period of record, the impact of the low-flow events (and any error associated with them) is emphasized. This analysis artifact is common to all previous studies that have examined the performance of bed load transport equations. Hence, geomorphic performance [sensu *Wolman and Miller*, 1960] remains to be tested in future studies.

1.5.2. Effects of Formula Calibration and Complexity

Accuracy was also considered in relation to degree of formula calibration and complexity. The number and nature of calibrated parameters determines the degree of formula calibration which, in turn, determines equation complexity. In general, formulae computed by grain size fraction (d_i), using site-specific particle-size distributions, are more calibrated and more complex than those determined from a single characteristic particle size. Moreover, formulae that are fit to observed bed load transport rates and that use site-specific hiding functions (e.g., *Parker et al.* [1982] (d_i) equation) are more calibrated and complex than those that that use a hiding function derived from another site (e.g., our use of the *Andrews* [1983] function in variants of the *Parker et al.* [1982] and *Meyer-Peter and Müller* [1948] equations). The *Bagnold* [1980] formula does not contain a hiding function, is based on a single grain size, has a limited number of user-calibrated parameters and is, therefore, ranked lowest in terms of both calibration and complexity. However, we have ranked the *Bagnold* [1980] (d_{mqb}) variant higher in terms of calibration because the modal grain size varied with discharge and was calculated from the observed bed load transport data. We consider the *Ackers and White* [1973] equation equal in terms of calibration and complexity to both the *Meyer-Peter and Müller* [1948] (d_i) equation and the *Parker et al.* [1982] (d_i via *Andrews* [1983]) equation because all

three are calculated by d_i, have a similar number of calibrated parameters and contain "off the shelf" particle-hiding functions that are calibrated to other sites, rather than to site-specific conditions.

Results from our prior analyses (Figures 1.5 and 1.6) indicate that the most complex and calibrated equation (i.e., *Parker et al.* [1982] (d_i)) outperforms all other formulae except for the *Ackers and White* [1973] equation. However, we find no consistent relationship between formula performance and degree of calibration and complexity. Size-specific formulae (those calculated by d_i) do not consistently outperform those based on a single characteristic particle size (d_{50ss}, d_{mqb} or d_{mss}), nor does a site-specific hiding function (i.e., *Parker et al.* [1982] (d_{50ss})) guarantee better performance than an "off the shelf" hiding function (i.e., *Parker et al.* [1982] (d_i) via *Andrews* [1983]).

1.5.3. A New Bed load Transport Equation

The bed load equations examined in Sections 1.5.1-2 are some of the most common and popular equations used for gravel-bed rivers. However, their performance is disconcerting and makes us ask whether there is a better alternative?

We find that bed load transport at our sites is generally well described in $\log_{10}$ space ($0.50 < r^2 < 0.90$) by a simple power function of total discharge (Q)

$$q_b = \alpha Q^{\beta} \tag{1.3}$$

where q_b is bed load transport per unit width, and α and β are empirical values (Leopold et al., 1964, Smith and Bretherton, 1972; Vanoni, 1975). Figure 1.7 shows a sample fit of this function at the Boise River study site. Moreover, we find that (1.3) performs within the accuracy specified in Section 1.5.1.3 (Freese's χ^2 [1960], $\alpha = 0.05$) and is superior to

the other bed load equations examined in terms of describing the observed transport (Figures 1.5 and 1.6). In particular, the median critical error, e^*, for (1.3) is significantly lower than that of the other equations (paired χ^2 test, $\alpha = 0.05$) and is within the specified accuracy (E = 1 $\log_{10}$ unit). We expect this result because (1.3) is empirically fit to the data and, thus, fully calibrated. Nevertheless, the results demonstrate that a power function of discharge may be a viable alternative to the other equations examined in Sections 1.5.1-2. To generalize (1.3) and make it predictive, we next parameterize α and β in terms of channel and watershed characteristics.

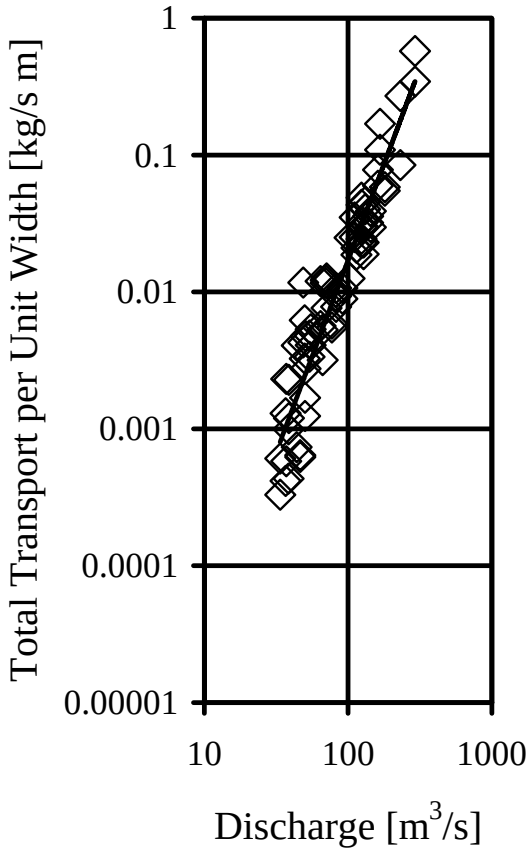

Figure 1.7. Example bed load rating curve from the Boise River study site (q_b=4.1 x 10^8 $Q^{2.81}$, r^2=0.90).

1.5.4. Parameterization of the Bed Load Transport Equation

We hypothesize that the exponent of (3) is principally a factor of supply-related channel armoring. *Emmett and Wolman* [2001] discuss two types of supply limitation in gravel-bed rivers. First, the supply of fine material present on the streambed determines, in part, the magnitude of Phase I transport (motion of finer particles over an immobile armor) [*Jackson and Beschta*, 1982]. Second, supply limitation occurs when the coarse armor layer limits the rate of gravel transport until the larger particles that make up the armor layer are mobilized, thus exposing the finer subsurface material to the flow (Phase II transport [*Jackson and Beschta*, 1982]). Mobilization of the surface material in a well armored channel is followed by a relatively larger increase in bed load transport rate compared to a similar channel with less surface armoring. Consequently, we expect that a greater degree of channel armoring, or supply-limitation, will delay mobilization of the armor layer and result in a steeper bed load rating curve (larger exponent of the bed load function (1.3)) compared to a less armored channel.

Dietrich et al. [1989] proposed that the degree of channel armoring is related to the upstream sediment supply relative to the local transport capacity, and presented a dimensionless bed load transport ratio, q^*, to represent this relationship. Here, we use q^* as an index of supply-related channel armoring and examine its effect on the exponent (β) of the observed bed load rating curves (1.3).

We define q^* as

$$q^* = \left(\frac{\tau_{Q_2} - \tau_{d_{50s}}}{\tau_{Q_2} - \tau_{d_{50ss}}} \right)^{1.5} \tag{1.4}$$

where τ_{Q_2} is the total shear stress at Q_2 calculated from the depth-slope product (ρgDS, where ρ is fluid density, g is gravitational acceleration, D is flow depth at Q_2 calculated from hydraulic geometry relationships, and S is channel slope) and $\tau_{d_{50s}}$ and $\tau_{d_{50ss}}$ are the critical shear stresses necessary to mobilize the surface and subsurface median grain sizes, respectively. Channel morphology and bed load transport are adjusted to bankfull flows in many gravel-bed rivers [e.g., *Leopold et al.*, 1964; *Parker*, 1978; *Andrews and Nankervis*, 1995], hence bankfull is the relevant flow for determining q^* in natural rivers [*Dietrich et al.*, 1989]. However, we use Q_2 because it is a bankfull-like flow that can be determined objectively from flood frequency analyses without the uncertainty inherent in field identification of bankfull stage (Section 1.5.1.2). The critical shear stresses are calculated as

$$\tau_{d_{50s}} = \tau^*_{c50}\left(\rho_s - \rho\right)g d_{50s} \tag{1.5a}$$

$$\tau_{d_{50ss}} = \tau^*_{c50}\left(\rho_s - \rho\right)g d_{50ss} \tag{1.5b}$$

where τ^*_{c50} is the dimensionless critical Shields stress for mobilization of the median grain size. We set this value equal to 0.03, corresponding with the lower limit of dimensionless critical Shield stress values for visually-based determination of incipient motion in coarse-grained channels [*Buffington and Montgomery*, 1997].

Values for q^* range from 0 for low bed load supply and well-armored surfaces ($d_{50s} >> d_{50ss}$ and $\tau_{d_{50s}} \approx \tau_{Q_2}$) to 1 for high bed load supply and unarmored surfaces ($d_{50s} \approx d_{50ss}$ and $\tau_{d_{50s}} \approx \tau_{d_{50ss}}$). As demonstrated by *Dietrich et al.* [1989], q^* does not measure absolute armoring (i.e., it is not uniquely related to d_{50s}/d_{50ss}), but rather relative armoring (a function of transport capacity relative to bed load supply). The

denominator of (1.4) is the equilibrium transport capacity of the unarmored bed and is a reference transport rate (theoretical end-member) that quantifies the maximum bed load transport capacity for the imposed boundary shear stress and the size of supplied bed load material. The numerator is the equilibrium transport rate for the actual bed load supply (equilibrium excess shear stress), with equilibrium transport achieved by textural adjustment of the bed (fining or coarsening in response to bed load supply) [e.g., *Dietrich et al.*, 1989; *Buffington and Montgomery*, 1999b]. Hence, q^* is a relative index of armoring (textural adjustment as a function of excess shear stress that provides equilibrium bed load transport). It describes armoring as a function of bed load supply relative to boundary shear stress and transport capacity. Consequently, q^* is not a measure of absolute armoring (d_{50s}/d_{50ss}). For the same degree of armoring, one can have different values of q^*, depending on the bed load supply and the corresponding equilibrium excess shear stress [*Dietrich et al.*, 1989; *Lisle et al.*, 2000]. Similarly, for a given q^*, a lower degree of armoring will occur for lower values of equilibrium excess shear stress [*Dietrich et al.*, 1989; *Lisle et al.*, 2000].

We determined values of q^* at 21 of the 24 study sites. Values of q^* could not be determined for three of the study sites because their median grain sizes were calculated to be immobile during Q_2 (Salmon River at Shoup, Middle Fork Salmon River at Lodge and Selway River). Results show an inverse relationship between q^* and the exponent of our bed load power function (Figure 1.8) supporting the hypothesis that supply-related changes in armoring relative to the local transport capacity influence the delay in bed load transport and the slope of the bed load rating curve. We parameterize q^* in terms of low-flow bed material for practical reasons (safety during grain-size measurement and

feasibility of future application of our approach). However, surface grain size can change with discharge and transport rate [*Parker and Klingeman*, 1982; *Parker et al.*, 2003], thereby potentially making β discharge dependent. Nevertheless, β is an average value across the range of observed discharges (including channel-forming flows) and any textural changes are empirically incorporated into our relationship between β and q^*.

Two sites (Thompson Creek and Little Buckhorn) appear to be outliers and, therefore, were removed from the analysis (shown as open diamonds in Figure 1.8). The anomalous Thompson Creek q^* value may be due to an extensive network of upstream beaver dams. The availability of sediment at all but the greatest flows is likely influenced by dam storage, delaying transport and increasing β by compressing the effective flows into a smaller portion of the hydrograph. In contrast, the large q^* value for Little Buckhorn may be due to a lack of peak flow information. The Q_2 at this site was calculated from a drainage area versus Q_2 relationship developed from the other 23 Idaho study sites where peak flow information was available. This relationship may over-predict Q_2 at Little Buckhorn, resulting in an anomalously high q^* value.

Because q^* is a relative measure of armoring (i.e., relative to bed load supply and transport capacity), it is unlikely to be biased by site-specific conditions (climate, geology, channel type, etc.). For example, the relative nature of q^* implies that channels occurring in different physiographic settings and possessing different particle size distributions (e.g., a fine gravel-bed stream versus a coarse cobble-bed one) may have identical values of q^*, indicating identical armoring conditions relative to transport capacity and bed load sediment supply and, thus, identical bed load rating-curve slopes. Although, q^* is not uniquely related to absolute armoring (d_{50s}/d_{50ss}), we examined its

effect on the exponent of our transport function (1.3), and found that the relationship was not significant (F-test , $\alpha = 0.05$). Hence, relative armoring (q^*) is more important than absolute armoring (d_{50s}/d_{50ss}). Because q^* is a relative index of armoring, it should be a robust predictor of the exponent of our bed load power function and unbiased by changing physiography and channel morphology.

In contrast, the coefficient of the bed load power function (α) describes the absolute magnitude of bed load transport, which is a function of basin-specific sediment supply and discharge. In general, sediment transport rate (q_b) and discharge (Q) both increase with drainage area (A) [*Leopold et al.*, 1964], however discharge increases faster, such that the coefficient of the bed load power function is inversely related to drainage area (a surrogate for transport rate relative to discharge, $\alpha \propto 1/A \propto q_b/Q$) (Figure 1.8). The rate of downstream increase in unit bed load transport rate (q_b) also depends on 1) downstream changes in channel width (a function of discharge, riparian vegetation, geology and land use) and 2) loss of bed load material to the suspended fraction due to particle abrasion [*Cui and Parker*, in press]. Factors that affect channel width also influence flow depth, boundary shear stress, and surface grain size and, thus, may influence, and be partially compensated by, β. We hypothesize that the Figure 1.8 relationship is a region-specific function of land use and physiography (i.e., topography, geology, and climate). Consequently, care should be taken in applying this function to other regions. In contrast, prediction of the exponent of our bed load transport equation may be less restrictive, as discussed above.

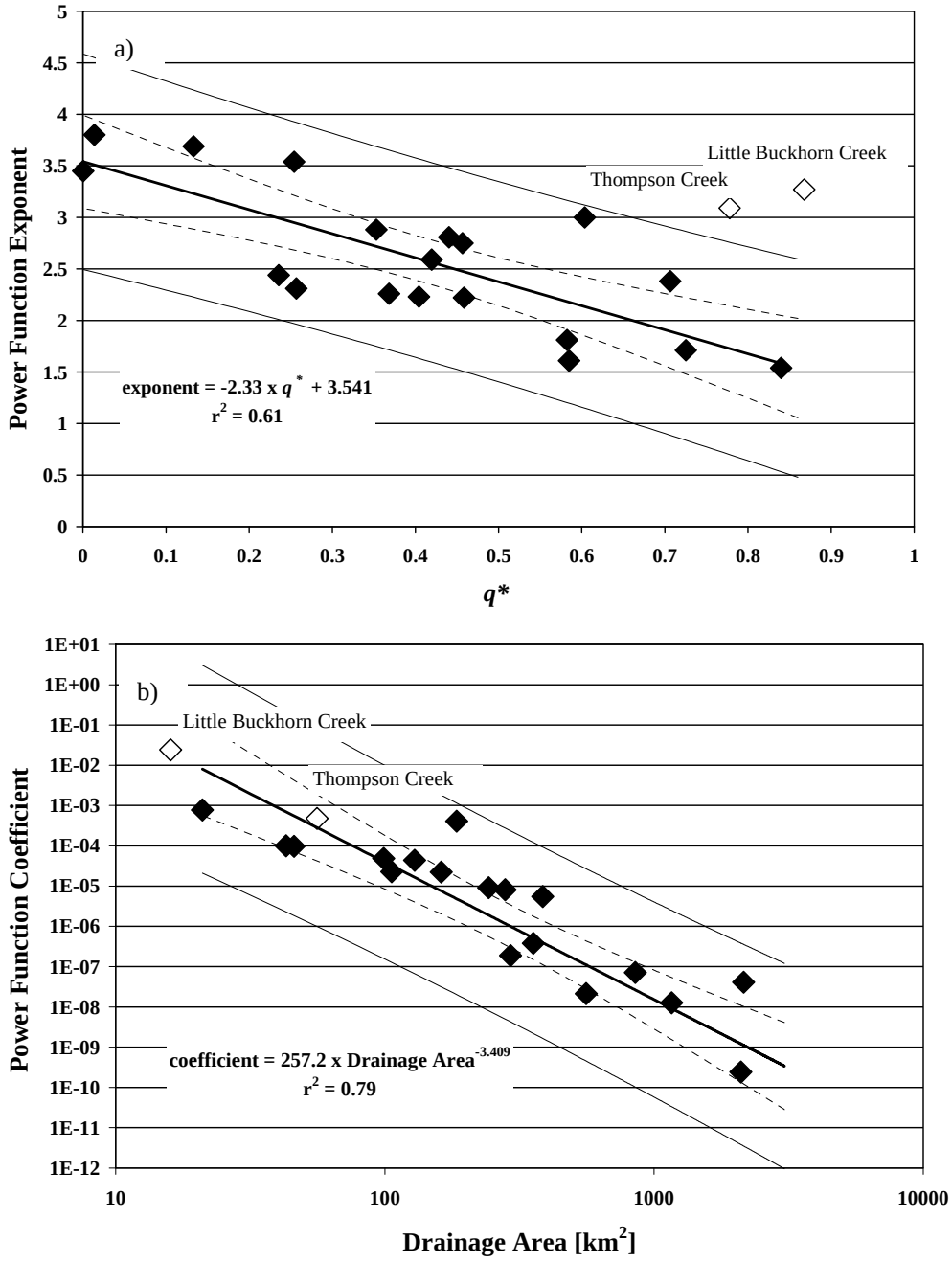

Figure 1.8. Relationships between a) q^* and the exponent of the bed load rating curves (1.3) and b) drainage area and the coefficient of the bed load rating curves (1.3) for the Idaho sites. Dashed line indicates 95% confidence interval about the mean regression line. Solid line indicates 95% prediction interval (observed values) [*Neter et al.*, 1974; *Zar*, 1974].

Based on the relationships shown in Figure 1.8 we propose the following empirically derived total bed load transport function with units of dry mass per unit width and time (kg/m•s).

$$q_b = 257 A^{-3.41} Q^{\left(-2.45 q^* + 3.56\right)} \tag{1.6}$$

where the coefficient and exponent are parameterized in terms of channel and watershed characteristics. The coefficient is a power function of drainage area (a surrogate for the magnitude of basin-specific bed load supply) and the exponent is a linear function of q^* (an index of channel armoring as a function of transport capacity relative to bed load supply).

The 17 independent test sites (Table 1.1) allow us to consider two questions concerning our bed load formula (1.6). First, how well can we predict the coefficient and exponent of the bed load power function at other sites? Second, how does our bed load formula perform relative to those examined in Section 1.5.1? These questions are addressed in the next two sections.

1.5.5. Test of Equation Parameters

We test our parameterization of (1.6) by comparing predicted values of the formula coefficient (α) and exponent (β) to observed values at 17 independent test sites in Wyoming, Colorado and Oregon (Figure 1.1). The independent test sites cover a generally similar range of slopes and particle sizes as the 24 Idaho sites used to develop (1.6) (Table 1.1). However, the East Fork River test site occurs at the gravel/sand transition [e.g., *Sambrook Smith and Ferguson,* 1995*; Ferguson et al*., 1998; *Parker and Cui*, 1998] and is significantly finer than the coarse-grained Idaho study sites. The Idaho study sites and the supplemental test sites are all snowmelt-dominated streams, except for

Oak Creek which is a rainfall-dominated channel. The geology is also similar across the study and test sites. The channels are predominantly underlain by granitics, with some metamorphic and sedimentary geologies, except for Oak Creek which is underlain by basalt. Bed load transport was measured with Helley-Smith samplers at all sites, with the exception of the East Fork and Oak Creek sites, where slot traps were used [*Milhous*, 1973; *Leopold and Emmett*, 1997].

As expected, the exponent of our bed load function is better predicted on average at the 17 test sites than the coefficient (Figure 1.9). The observed exponents are reasonably well predicted by (1.6) with a median error of less than 3%. This suggests that q^*, determined in part through measurements of the surface and subsurface material during low flow, is able to accurately predict the rating-curve exponent over a range of observed discharges (including channel-forming flows) despite any stage-dependent changes in surface grain size [*Parker and Klingeman*, 1982; *Parker et al.*, 2003]. Moreover, the rating-curve exponents are accurately predicted across different climatic regimes (snowmelt- and rainfall-dominated), different lithologies (basalt and granite), and different bed load sampling methods (Helley-Smith and slot samplers), despite the fact that the predictive equation is derived from a subset of these conditions (i.e., snowmelt rivers in granitic basins, sampled via Helley-Smith). In particular, β is reasonably well predicted at the two test sites that are most different from the Idaho study sites (Oak Creek and East Fork; observed β values of 2.55 and 2.19 versus predicted values of 2.43 and 1.82, respectively). We suspect that the success of our exponent function is due to the robust nature of q^* to describe supply-related channel armoring regardless of differences in physiography and channel conditions (Section 1.5.4).

In contrast, the predicted coefficients are considerably less accurate and were over 3 times larger than the observed values at many of the 17 test sites (Figure 1.9). Prediction errors, however, can be significant for both parameters, which is expected given the spread of the 95% prediction intervals shown in Figure 1.8. The largest errors in predicting the coefficient occurred at the Oak Creek and East Fork sites (3 orders of magnitude overprediction, and 2 orders of magnitude under-prediction, respectively). The cause of the error at these sites is examined below.

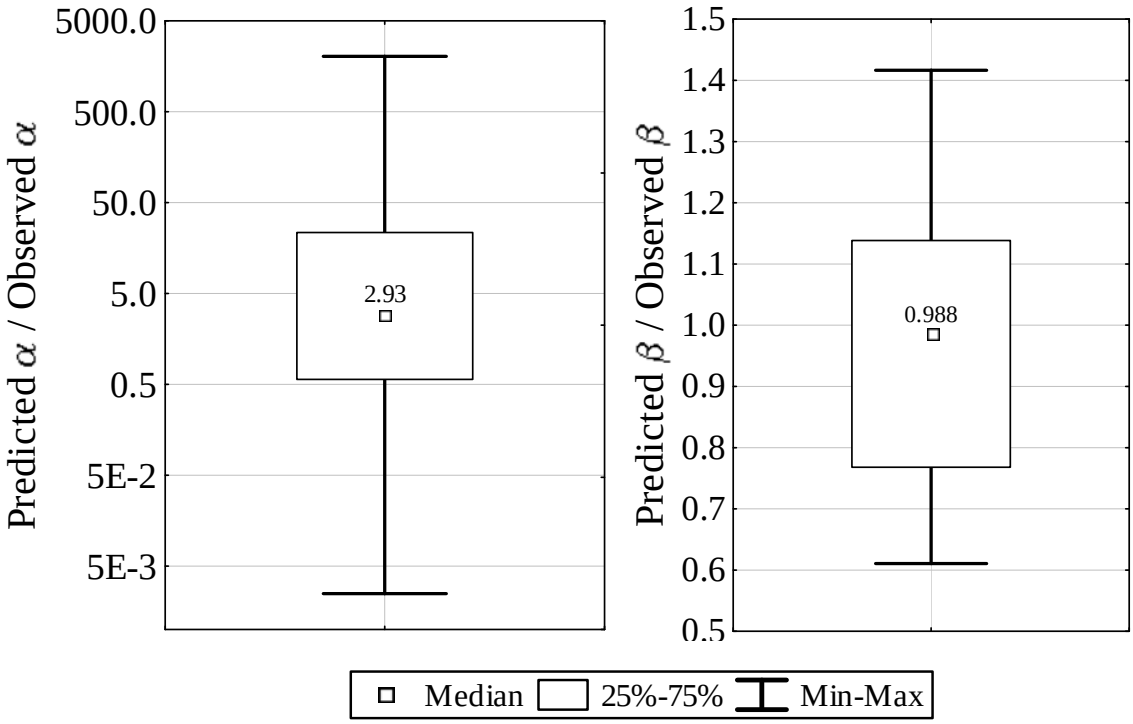

Figure 1.9. Box plots of predicted versus observed values of a) coefficient and b) exponent of our bed load transport function (1.6). Median values are specified.

The Oak Creek watershed is unique relative to the 24 Idaho study sites in that it is composed primarily of basalt, rather than granite, and has a climatic regime dominated by

rainfall, rather than snowmelt. Because (1.6) accurately predicts the exponent of the Oak Creek bed load rating curve, as discussed above, the over-prediction of total bed load transport at this site is principally due to prediction error of the transport coefficient (observed α of $1.9 \bullet 10^{-4}$ versus predicted α of 0.39), which may be due to differences in basin geology and sediment production rates. Basalt is typically less erosive and produces less sediment per unit area than the highly decomposed granites found in the Idaho batholith [e.g., *Lisle and Hilton*, 1999]. Consequently, one would expect (1.6) to over-predict the transport coefficient at Oak Creek, as observed. Alternatively, the bed load supply and transport coefficient may be influenced by climate and runoff regime; however the relationship between these two variables is not well documented. Previous studies suggest that in temperate climates bed load supplies may be higher in rainfall regimes than snowmelt-dominated ones [*Lisle et al.*, 2000]. Therefore, our α prediction, which is derived from snowmelt streams, would be expected to underpredict transport rates in the rainfall-dominated Oak Creek, contrary to what we observe. Consequently, differences in runoff regime do not appear to explain the observed error at Oak Creek. Regardless of the exact physical cause, the prediction error highlights the site-specific nature of our coefficient function (α) (discussed further in Section 1.5.7).

In contrast, the under-prediction of the transport coefficient at East Fork may be due to a difference in channel type. The East Fork site occurs at the gravel/sand transition and has a finer, more mobile bed than the coarser-grained Idaho sites. The gravel/sand transition represents a shift in the abundance of sand-sized material that likely increases the magnitude of Phase I transport and total sediment load compared to

gravel-bed channels. Consequently, one might expect (1.6) to under-predict the coefficient at East Fork, as observed.

The Oak Creek and East Fork sites also differ from the others in that bed load samples were obtained from channel-spanning slot traps, rather than Helley-Smith samplers. Recent work by *Bunte et al.* [in press] shows that differences in sampling method can dramatically affect bed load transport results, although *Emmett* [1980] demonstrates reasonably good agreement between slot and Helley-Smith samples at the East Fork site. Consequently, differences in sampling method do not explain the observed prediction error of the transport coefficient, at least at the East Fork site.

Differences in climate and runoff regime may also influence the rating-curve exponent (β). This is not a source of error in our analysis (β is accurately predicted by (1.6), even at Oak Creek), but rather a source of systematic variation in β. A rainfall-dominated climate produces greater short-term variability in the annual hydrograph (i.e., flashier hydrograph) than one dominated by snowmelt [*Swanston*, 1991; *Lisle et al.*, 2000] and typically generates multiple peak flows throughout the year versus the single, sustained peak associated with spring snowmelt. Consequently, the frequency and magnitude of bed load events differs between rainfall- and snowmelt-dominated hydrographs. The magnitude of flow associated with a given return period is typically greater in a rainfall-dominated watershed than in a similarly sized snowmelt-dominated watershed [*Pitlick*, 1994]. This is seen at our study sites in that the highest Q_2 unit discharge (0.44 m^3 km^{-2}) occurs at the rainfall-dominated Oak Creek test site and is almost twice the second highest Q_2 unit discharge (0.27 m^3 km^{-2}) at the snowmelt-dominated Dollar Creek study site. Furthermore, due to the greater short-term variability

of rainfall-dominated hydrographs, the duration of intermediate flows is reduced, which can lead to fining of the bed surface and a decrease in the degree of the channel armoring [*Laronne and Reid* 1993; *Lisle et al.*, 2000; *Parker et al.*, 2003]. Consequently, one might expect less armoring and lower bed load rating-curve exponents (β) in rainfall-dominated environments compared to snowmelt ones. However, β and the degree of armoring are also influenced by bed load supply and boundary shear stress (Section 1.5.4), so those parameters must be factored into any comparison of runoff regimes. Lack of data (only one rainfall-dominated site in our data set) precludes further examination of this issue here.

1.5.6. Comparison with Other Equations

To compare the accuracy of our bed load transport formula (1.6) to those presented in Section 1.5.1, we performed a test of six formulae (including (1.6)) at the 17 test sites. The test procedure was similar to that used in Section 1.5.1.3; however, we assume no transport observations are available for formula calibration (i.e., blind test) and, therefore, we do not include the two variants of the *Parker et al.* [1982] (d_i and d_{50ss}) equation or the *Bagnold* [1980] (d_{mqb}) equation which require measured bed load transport data. Consequently, only five of the eight variants of the formulae from Section 1.5.1 are included here, plus our power-law equation (1.6).

Similar to Section 1.5.1, incorrect zero-transport predictions are a problem for threshold-based equations, but the number of zero predictions is significantly less at the test sites (about 50% less compared to those shown in Figure 1.3 for the Idaho study sites). For both variants of the *Meyer-Peter and Müller* [1948] equation the median percentage of incorrect zero transport predictions is about 22%, while the median

percentage of incorrect zero predictions for the *Bagnold* [1980] (d_{mss}) equation is 28%. In contrast, the *Ackers and White* [1973] equation incorrectly predicted zero transport at only one test site (Oak Creek) for 35% of the observations. The significance of incorrect zero-transport predictions is similar at the 17 test sites as at the 24 Idaho sites. The Q_{max}/Q_2 ratio for both variants of the *Meyer-Peter and Müller* [1948] (d_{50ss} and d_i) equation had a median value of 32% and 28%, respectively, at the Idaho sites and about 30% at the test sites. The Q_{max}/Q_2 ratio for the *Bagnold* [1980] (d_{mss}) equation decreased slightly from a median value of 35% at the Idaho sites to 27% at the test sites.

Figure 1.10 shows the distribution of $\log_{10}$ differences across the 17 test sites and demonstrates a significant improvement in the performance of both versions of the *Meyer-Peter and Müller* [1948] equation and the *Bagnold* [1980] (d_{mss}) equation due to fewer incorrect zero transport predictions; median $\log_{10}$ differences improve from an under-prediction of almost 10 orders of magnitude at the 24 Idaho sites to an over-prediction of only 1.3 to 2.2 orders of magnitude at the test sites. The performance of both the *Parker et al.* [1982] (d_i via *Andrews* [1983]) equation and the *Ackers and White* [1973] equation decreased slightly at the test sites with median $\log_{10}$ differences increasing from 2.73 and 0.25, respectively, at the Idaho sites to 3.27 and 0.80, respectively, at the test sites. Our bed load equation (1.6) had the lowest median $\log_{10}$ difference (0.62) at the 17 test sites.

As in Section 1.5.1.3, the performance of each formula was evaluated using *Freese's* [1960] χ^2 test, with results similar to those of the Idaho sites; all formulae perform significantly worse than the specified accuracy (E = 1 $\log_{10}$ unit, $\alpha = 0.05$), including (1.6). We also evaluated the critical error, e^* [*Reynolds*, 1984], at each test site

and, like the Idaho study sites, we found that a given formula may occasionally provide the required accuracy, but generally no equation performs within the specified accuracy (Figure 1.11, all median e^*-values > E).

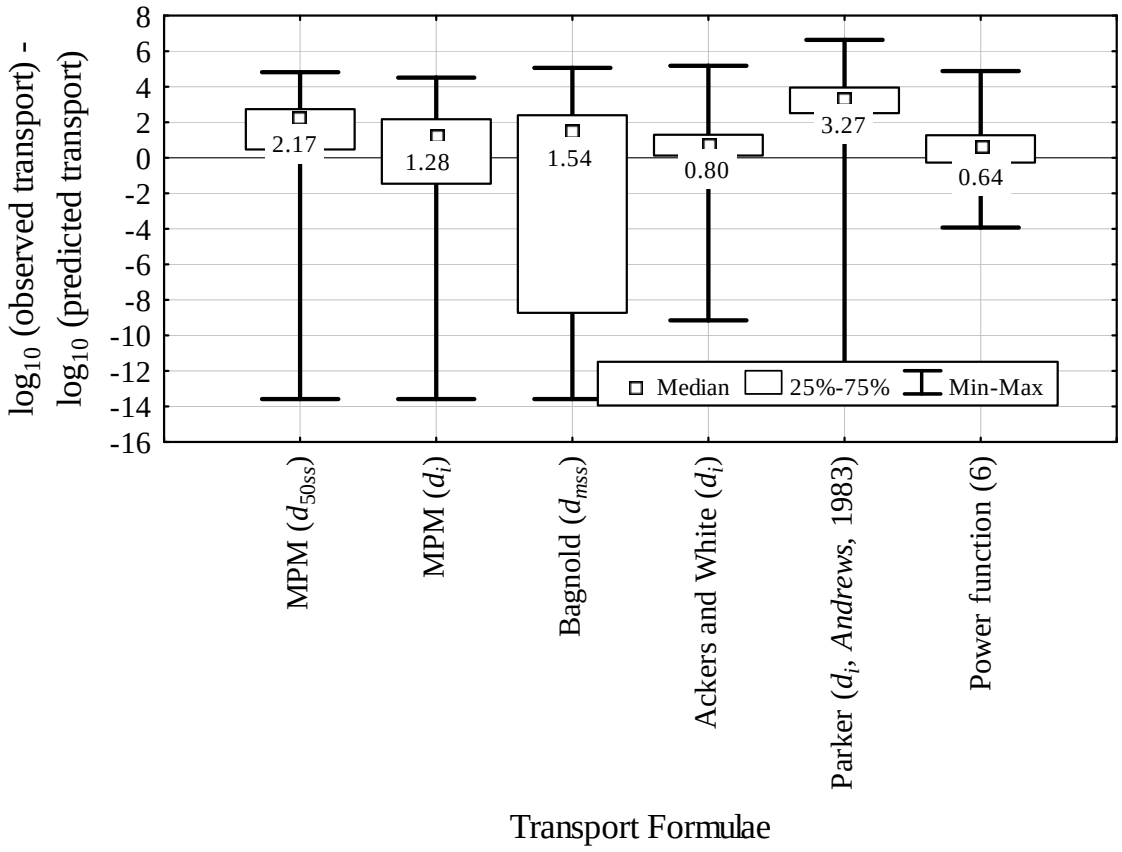

Figure 1.10. Box plots of the distribution of $\log_{10}$ differences between observed and predicted bed load transport rates at the 17 test sites. Median values are specified. MPM stands for Meyer-Peter and Müller.

Nevertheless, our bed load transport formula (1.6) outperformed all others at the 17 test sites, except for the *Ackers and White* [1973] equation which was statistically similar to ours (paired χ^2 test of e^* values, $\alpha = 0.05$) (Figure 1.11). As with the Idaho

sites, the worst performers were the *Bagnold* [1980] (d_{mss}) equation and both variants of the *Meyer-Peter and Müller* [1948] equation, both of which were similar to one another, but different from the *Bagnold* [1980] (d_{mss}) equation (paired χ^2 test, $\alpha = 0.05$). Critical errors for the *Parker et al.* [1982] (d_i via *Andrews* [1983]) equation were between these two groups of best and worst performers and statistically different from them (paired χ^2 test, $\alpha = 0.05$). Overall, the patterns of formula performance were similar to those of the Idaho study sites, but the 17 test sites tended to have lower values of critical error (cf. Figures 1.6 and 1.11).

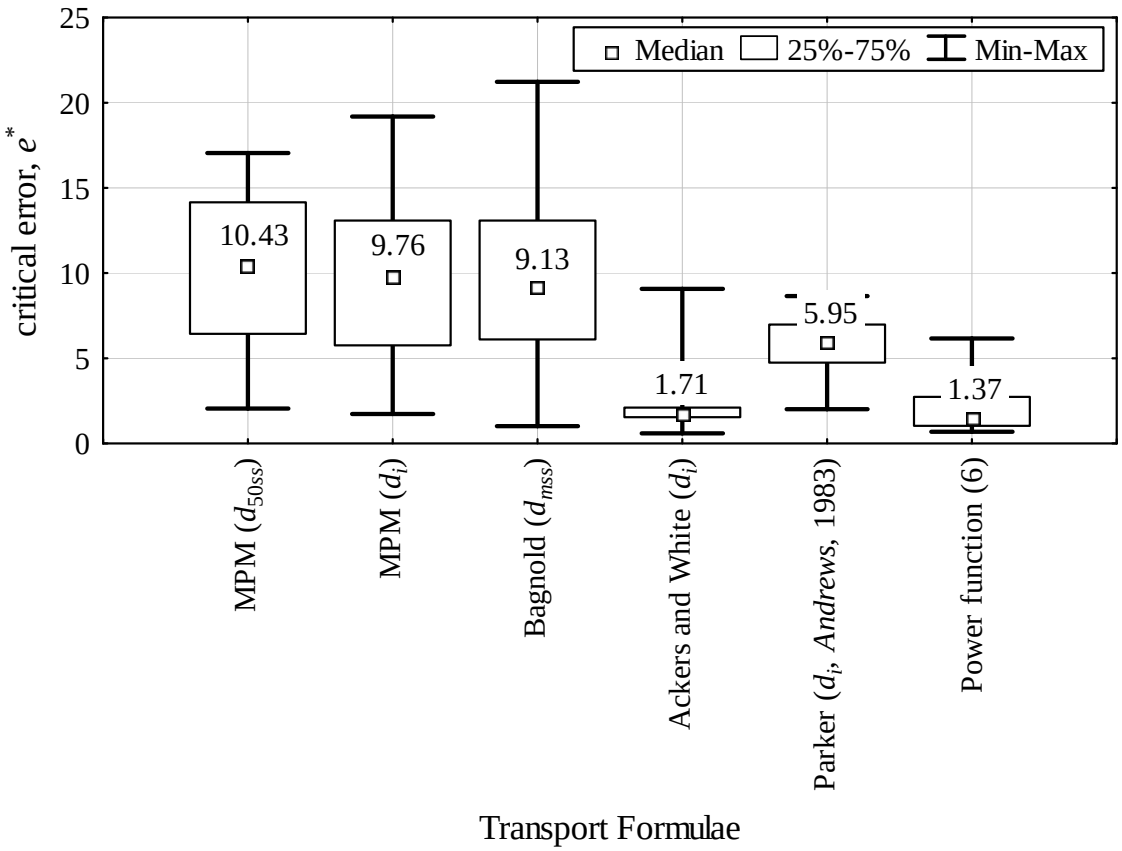

Figure 1.11. Box plots of the distribution of critical error, e^*, for the 17 test sites. Median values are specified. MPM stands for Meyer-Peter and Müller.

1.5.7. Formula Calibration

A principle drawback of our proposed bed load transport equation (1.6) appears to be the site-specific nature of the coefficient function (α). However, it may be possible to back-calculate a local coefficient from one or more low-flow bed load transport measurements coupled with prediction of the rating curve exponent as specified in (1.6), thus significantly reducing the cost and time required to develop a bed load rating curve from traditional bed load sampling procedures [e.g., *Emmett*, 1980]. A similar approach of formula calibration from a limited number of transport observations was proposed by *Wilcock* [2001]. Our suggested procedure for back-calculating the coefficient assumes that the exponent can be predicted with confidence (as demonstrated by our preceding analyses).

By way of example, we used (1.6) to calculate the exponent of the bed load rating curve at Oak Creek and then randomly selected 20 low-flow bed load transport observations to determine 20 possible rating curve coefficients. Low flows are defined as those less than the average annual value. The average predicted coefficient using this calibration method is 0.00032, which is much closer to the observed value (0.00019) than our original prediction (0.39) from (1.6). Thus, our calibration method better approximates the observed coefficient. Using the exponent predicted from (1.6) and the calibrated coefficient of 0.00032, we predict total transport for each observation made at Oak Creek. Results show that the critical error, e^*, improves from 6.17 to 1.53. Figure 1.12 illustrates the improved accuracy of our bed load formula with calibration to a limited number of low-flow transport observations.

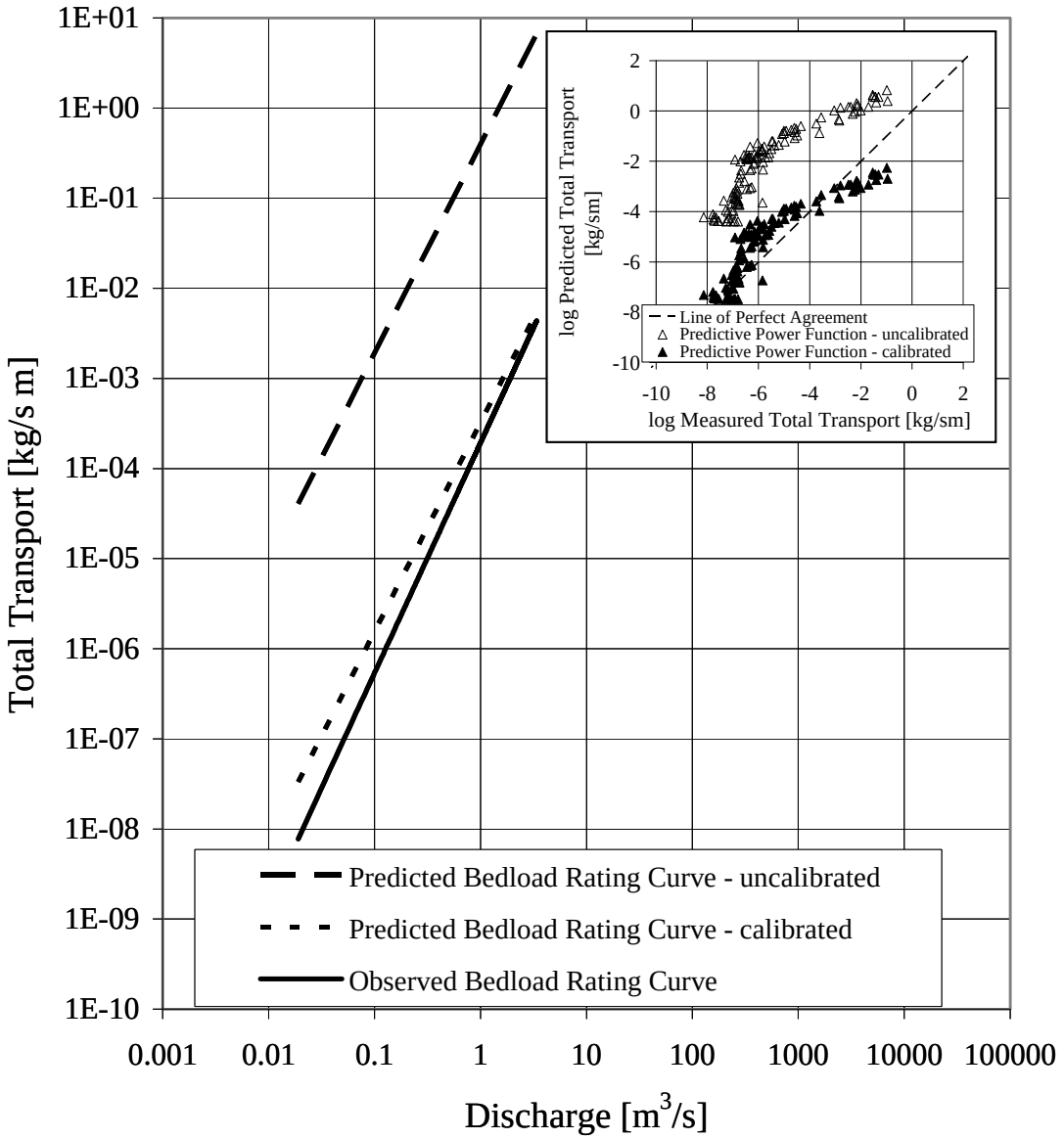

Figure 1.12. Observed versus predicted bed load transport rates at Oak Creek, illustrating improved performance by calibrating the coefficient of our equation (1.6) to a limited number of observed, low-flow, transport values.

1.6. Summary and Conclusions

The bed load transport datasets obtained from 24 study sites in central Idaho, USA, provide an opportunity to extend the analyses of *Gomez and Church* [1989] and

Yang and Huang [2001] into coarse-grained mountain rivers and to continue recent studies of those environments [*Almedeij and Diplas*, 2003; *Bravo-Espinosa et al.*, 2003; *Martin*, 2003]. We evaluated the performance of eight different formulations of four common bed load transport equations, each of which are calibrated to some degree with site-specific data and vary in their complexity and difficulty of use. Although we find considerable differences in formula performance, there is no consistent relationship between performance and degree of formula calibration or complexity at the 24 Idaho sites. However, formulae containing a threshold for bed load transport commonly predict a substantial number of incorrect zero-transport rates and typically perform worse than non-threshold formulae. Moreover, we find that a simple power function of discharge best describes the observed transport at the Idaho sites (*Freese's* [1960] χ^2, $\alpha = 0.05$). This result is expected because the power function is empirically fit to the observed data. Nevertheless, the simplicity of the equation is attractive, and we develop it into a predictive transport equation by parameterizing its coefficient and exponent in terms of channel and watershed conditions at the 24 Idaho study sites.

We find that the exponent of the bed load rating curve is inversely related to q^* which describes the degree of channel armoring relative to transport capacity and sediment supply [*Dietrich et al.*, 1989]. Because q^* is a relative index of supply-limited channel armoring we expect our exponent equation to be transferable to other physiographies and channel types. In contrast, we find that the coefficient of our bed load power function is inversely related to drainage area and is likely a function of site-specific sediment supply and channel type. As such, the coefficient equation may not be

as transferable to other locations, but can be locally calibrated (Section 1.5.7). We use an additional 17 independent data sets to test the accuracy of our bed load power function.

As expected, the exponent is better predicted than the coefficient at the 17 independent test data sets, with typical errors of less than 3% and almost 300%, respectively. We find that our coefficient function is sensitive to local geology and channel type. In particular, our bed load formula was developed from watersheds composed principally of granitics and coarse-grained channel types, and when applied to a less erosive lithology, such as basalt (Oak Creek), we tend to over-predict bed load transport. This is due to the site-specific nature of our coefficient function rather than errors associated with our exponent function (at Oak Creek the observed $\alpha = 1.9 \bullet 10^{-4}$, predicted $\alpha = 0.39$; observed $\beta = 2.55$, predicted $\beta = 2.43$). Conversely, when we apply our formula to a channel at the gravel/sand transition (East Fork River) we under-predict the amount of bed load transport for a given drainage area, again, due to the site-specific nature of our coefficient function (observed $\alpha = 8.26 \bullet 10^{-5}$, predicted $\alpha = 2.06 \bullet 10^{-7}$; observed $\beta = 2.19$, predicted $\beta = 1.82$).

Despite these concerns, we find that our bed load formula significantly outperformed three of the four transport formulae examined and was statistically similar to the *Ackers and White* [1973] equation at the 17 independent test sites.

Although our exponent function appears to be robust, a more thorough test of both the coefficient and exponent functions, covering a wider range of geologies and climatic regimes, is warranted. Moreover, our definition of q^* requires stage–discharge data to determine Q_2 from flood-frequency analyses and to determine the Q_2 flow depth from hydraulic geometry relationships. Because the cost and time involved in stream gaging

may be prohibitive, an alternative and simpler approach might be to define q^* based on field measurements of bankfull parameters. Bankfull depth can be determined from cross-sectional surveys, and bankfull discharge can be estimated from the *Manning* [1891] equation combined with channel surveys of slope, bankfull radius, and an appropriate estimate of channel roughness [e.g., *Barnes*, 1967].

Our proposed transport equation also has applications for channel maintenance flows [*Whiting*, 2002] which are often based on identifying discharges that transport the most sediment over the long term (i.e., effective flows [*Wolman and Miller*, 1960]). This type of analysis does not require knowledge of the actual amount of sediment in transport, but rather requires only an understanding of how bed load transport changes with discharge (i.e., quantifying the bed load rating-curve exponent). Consequently, our bed load formula offers a means to determine the exponent of the rating curve without the time or expense of a full bed load measurement campaign. For example, with the exponent of the bed load rating curve predicted from (1.6), the "effective discharge" can be calculated following the procedure outlined by *Emmett and Wolman* [2001] and does not depend on the coefficient of the bed load rating curve.

The bed load formulae examined here are all one-dimensional equations parameterized by reach-average hydrologic and sedimentologic variables. However, most natural channels exhibit patchy surface textures [e.g., *Kinerson*, 1990; *Paola and Seal*, 1995; *Buffington and Montgomery*, 1999a; *Laronne et al.*, 2000] and spatially variable hydraulics. Moreover, because transport rate is a nonlinear function of excess boundary shear stress, whole-channel transport rates based on reach-average conditions tend to under predict transport rates unless empirically adjusted [*Lisle et al.*, 2000;

Ferguson, 2003]. Thus, predictions of bed load transport rates ultimately would be more accurate and true to processes in natural channels if they were integrated over the distribution of excess shear stress for a given flow [*Gomez and Church*, 1989].

Nor does our analysis consider the short-term variability of the flux–discharge relationship. We relate the available bed load transport record of each site to channel and sediment-supply conditions at the time of field measurement. Hence, our analysis examines record-average transport phenomena, but does not consider annual, seasonal or flood-event variability (i.e., hysteresis). Nevertheless, the same computational procedure outlined here could be used to develop shorter-term values of α and β for use in (1.6).

1.7. References

Ackers, P., and, W. R. White (1973), Sediment transport: New approach and analysis, *J. Hydraul. Div., Am. Soc. Civ. Eng.*, 99, 2041-2060.

Almedeij, J. H., and, P. Diplas (2003), Bed load transport in gravel-bed streams with unimodal sediment, *J. Hydraul. Eng., 129*, 896-904.

Andrews, E. D. (1983), Entrainment of gravel from naturally sorted riverbed material, *Geol. Soc. Am. Bull., 94*, 1225-1231.

Andrews, E. D., and, J. M. Nankervis (1995), Effective discharge and the design of channel maintenance flows for gravel-bed rivers, in *Natural and Anthropogenic Influences in Fluvial Geomorphology, Geophysical Monograph 89*, edited by J.E. Costa, A.J. Miller, K.W. Potter and P.R. Wilcock, pp. 151-164, AGU, Washington, D.C.

Bagnold, R. A. (1980), An empirical correlation of bed load transport rates in flumes and natural rivers, *Proc. R. Soc. London, 372*, 453-473.

Barnes, H. H. (1967), Roughness characteristics of natural channels, *U.S. Geol. Sur. Water Supply Pap. 1849*, 213 pp.

Bravo-Espinosa, M., W. R. Osterkamp, and V. L. Lopes (2003), Bed load transport in alluvial channels, *J. Hydraul. Eng., 129*, 783-795.

Brown, C. B. (1950), Sediment transportation, in *Engineering Hydraulics*, edited by H. Rouse, pp. 769-857, John Wiley, New York.

Buffington, J. M., and D. R. Montgomery (1997), A systematic analysis of eight decades of incipient motion studies, with special reference to gravel-bedded rivers, *Water Resour. Res., 33*, 1993-2029.

Buffington, J. M., and D. R. Montgomery (1999a), Effects of hydraulic roughness on surface textures of gravel-bed rivers, *Water Resour. Res.*, *35*, 3507-3522.

Buffington, J. M., and D. R. Montgomery (1999b), Effects of sediment supply on surface textures of gravel-bed rivers, *Water Resour. Res.*, *35*, 3507-3522.

Bunte, K., S. R. Abt, J. P. Potyondy and S. R. Ryan, Measurement of coarse gravel and cobble transport using portable bed load traps, *J. Hydraul. Eng.*, in press.

Carling, P. (1988), The concept of dominant discharge applied to two gravel-bed streams in relation to channel stability thresholds, *Earth Surf. Processes Landforms*, *13*, 355-367.

Church, M. A., D. G. McLean, and J. F. Wolcott (1987), River bed gravels: Sampling and analysis, in *Sediment Transport in Gravel-bed Rivers*, edited by C.R. Thorne, J.C. Bathurst, and R.D. Hey, pp. 43-88, John Wiley, New York.

Cook, R. D. and S. Weisberg (1999), *Applied Regression Including Computing and Graphics*, 590 pp., John Wiley, New York.

Cui, Y., and G. Parker, Numerical model of sediment pulses and sediment supply disturbances in mountain rivers, *J. Hydraul. Eng.*, in press.

Day, T. J. (1980), A study of the transport of graded sediments, *Hydraul. Res. Stat. Rep. IT 190*, Wallingford, England, 10 pp.

Dietrich, W. E., J. Kirchner, H. Ikeda, and F. Iseya (1989), Sediment supply and the development of the coarse surface layer in gravel-bedded rivers, *Nature, 340*, 215-217.

Edwards, T. K. and, G. D. Glysson (1999), Field methods for measurement of fluvial sediment: Techniques of Water-Resources Investigations of the U.S. Geological Survey, Book 3, Applications of Hydraulics, Chapter 2, 89 p.

Einstein, H. A. (1950), The bed-load function for sediment transportation in open channel flows, *U.S.D.A. Soil Conservation Service, Tech. Bull. 1026*, 73 pp.

Emmett, W. W. (1980), A field calibration of the sediment-trapping characteristics of the Helley-Smith bed load sampler, *U.S. Geol. Surv. Prof. Pap., 1139*, 44 pp.

Emmett, W. W., and, M. G. Wolman (2001), Effective discharge and gravel-bed rivers, *Earth Surf. Processes Landforms, 26*, 1369-1380.

Fang, D. (1998), Book Review of: Sediment transport theory and practice by C.T. Yang, *Int. J. Sed. Res., 13*, 83-74.

Ferguson, R. I. (2003), The missing dimension: Effects of lateral variation on 1-D calculations of fluvial bed load transport, *Geomorphology, 56*, 1-14.

Ferguson, R. I., T. B. Hoey, S. J. Wathen, A. Werritty, R. I. Hardwick, and, G. H. Sambrook Smith (1998), Downstream fining of river gravels: Integrated field, laboratory and modeling study, in *Gravel-bed Rivers in the Environment*, edited by P. C. Klingeman, R. L. Beschta, P. D. Komar, and J. B. Bradley, pp. 85-114, Water Resources Publications, Highlands Ranch.

Freese, F. (1960), Testing accuracy, *Forest Science.*, 6, 139-145.

Gomez, B., and M. Church (1989), An assessment of bed load sediment transport formulae for gravel bed rivers, *Water Resour. Res., 25*, 1161-1186.

Gordon, N. (1995), Summary of technical testimony in the Colorado Water Division 1 Trial, *U.S. For. Serv. Gen. Tech. Rep., RMRS-GTR-270*, 140 pp.

Helley, E. J., and, W. Smith (1971), Development and calibration of a pressure-difference bed load sampler, *U.S. Geol. Surv. Open-File Rep.*, 18 pp.

Jackson, W. L., and, R. L. Beschta (1982), A model of two-phase bed load transport in an Oregon coast range stream, *Earth Surf. Processes Landforms*, *7*, 517-527.

Kinerson, D. (1990), Bed surface response to sediment supply, M.S. thesis, 420 pp., Univ. of Calif., Berkeley.

King, J. G., W. W. Emmett, P. J. Whiting, R. P. Kenworthy, and, J. J. Barry (2004), Sediment transport data and related information for selected gravel-bed streams and rivers in Idaho, *U.S. Forest Service Tech. Rep. RMRS-GTR-131*, 26 pp.

Laronne, J. B., and, I. Reid (1993), Very high rates of bed load sediment transport by ephemeral desert rivers, *Nature*, *366*, 148-150.

Laronne, J. B., C. Garcia, and, I. Reid (2000), Mobility of patch sediment in gravel bed streams: Patch character and its implications for bed load, in *Gravel-Bed Rivers V*, edited by M.P. Mosley, pp. 249-280, New Zealand Hydrological Society, Wellington, New Zealand.

Leopold, L. B., and, W. W. Emmett (1997), Bed load and river hydraulics – Inferences from the East Fork River, Wyoming, *U.S. Geol. Surv. Prof. Pap., 1583*, 52 pp.

Leopold, L. B., M. G. Wolman, and, J. P. Miller (1964), *Fluvial Processes in Geomorphology*, 552 pp., W.H. Freeman, San Francisco, California.

Lisle, T. E. and, S. Hilton (1999), Fine bed material in pools of natural gravel bed channels, *Water Resour. Res., 35*, 1291-1304.

Lisle, T. E., J. M. Nelson, J. Pitlick, M. A. Madej, and, B. L. Barkett (2000), Variability of bed mobility in natural, gravel-bed channels and adjustments to sediment load at local and reach scales, *Water Resour. Res., 36*, 3743-3755.

Manning, R. (1891), On the flow of water in open channels and pipes, *Trans. Inst. Civ. Eng. Ireland, 20*, 161-207.

Martin, Y. (2003), Evaluation of bed load transport formulae using field evidence from the Vedder River, British Columbia, *Geomorphology, 53*, 73-95.

Meyer-Peter, E., and, R. Müller (1948), Formulas for bed-load transport, in *Proceedings of the 2nd Meeting of the International Association for Hydraulic Structures Research*, pp. 39-64, Int. Assoc. Hydraul. Res., Delft, Netherlands.

Milhous, R. T. (1973), Sediment transport in a gravel-bottomed stream, Ph.D. dissertation, 232 pp., Ore. State Univ., Corvallis.

Montgomery, D. R. and, J. M. Buffington (1997), Channel-reach morphology in mountain drainage basins, *Geol. Soc. Am. Bull., 109*, 596-611.

Moog, D. B., and, P. J. Whiting (1998), Annual hysteresis in bed load rating curves, *Water Resour. Res., 34*, 2393-2399.

Neter, J., W. Wasserman, and, M. H. Kutner (1974), *Applied Linear Statistical Models*, 1181 pp., Richard D. Irwin, Inc., Burr Ridge, Illinois.

Paola, C., and, R. Seal (1995), Grain size patchiness as a cause of selective deposition and downstream fining, *Water Resour. Res., 31*, 1395-1407.

Parker, G. (1978), Self-formed straight rivers with equilibrium banks and mobile bed. Part 2. The gravel river, *J. Fluid Mech., 89*, 127-146.

Parker, G. (1979), Hydraulic geometry of active gravel rivers, *J. Hydraul. Div., Amer. Soc. Civ. Eng., 105*, 1185-1201.

Parker, G. (1990), Surface-based bed load transport relation for gravel rivers, *J. Hydraul. Res., 28*, 417-436.

Parker, G., and, Y. Cui (1998), The arrested gravel front: stable gravel-sand transitions in rivers, Part 1: Simplified analytical solution, *J. Hydraul. Res., 36*, 75-100.

Parker, G., and, P. C. Klingeman (1982), On why gravel bed streams are paved, *Water Resour. Res., 18*, 1409-1423.

Parker, G., P. C. Klingeman, and, D. G. McLean (1982), Bed load and size distribution in paved gravel-bed streams, *J. Hydraul. Div., Amer. Soc. Civ. Eng., 108*, 544-571.

Parker, G., C. M. Toro-Escobar, M. Ramey and, S. Beck (2003), Effect of floodwater extraction on mountain stream morphology, *J. Hydraul. Eng., 129*, 885-895.

Pitlick, J. (1994), Relation between peak flows, precipitation, and physiography for five mountainous regions in the western USA, *J. Hydrol., 158*, 219-214.

Reid, I., D. M. Powell, and, J. B. Laronne (1996), Prediction of bed-load transport by desert flash floods, *J. Hydraul. Eng., 122*, 170-173.

Reynolds, M. R. (1984), Estimating error in model prediction, *Forest Science.*, 30, 454-469.

Ryan, S. E., and, W. W. Emmett (2002), The nature of flow and sediment movement in Little Granite Creek near Bondurant, Wyoming, *U.S. For. Serv. Gen. Tech. Rep., RMRS-GTR-90*, 46 pp.

Ryan, S. E., L. S. Porth, and, C. A. Troendle (2002), Defining phases of bed load transport using piecewise regression, *Earth Surf. Processes Landforms, 27*, 971-990.

Sambrook Smith, G. H., and, R. I. Ferguson (1995), The gravel-sand transition along river channels, *J. Sed. Res., A65*, 423-430.

Schoklitsch, A. (1962), *Handbuch des wasserbaues*, Springer-Verlag, Vienna, 1, 173-177.

Smith, T. R., and, F. P. Bretherton (1972), Stability and the conservation of mass in drainage basin evolution, *Water Resour. Res., 8*, 1506-1528.

Strickler, A. (1923), Beitrage zur Frage der Geschwindigheistformel und der Rauhigkeitszahlen für Strome, Kanale und Geschlossene Leitungen, *Mitt. Eidgenossischer Amtes Wasserwirtschaft, Bern, Switzerland, 16*.

Swanston, D. N. (1991), Natural processes, in *Influences of Forest and Rangeland Management on Salmonid Fishes and Their Habitat*, edited by W.R. Meehan, pp. 139-179, Spec. Pub. 19, Amer. Fish. Soc., Bethesda.

United States Geological Survey (USGS) (1982), Guidelines for determining flood flow frequency, *U.S. Geol Surv., Interagency Advisory Committee Water Data, Bull. 17B Hydrol. Subcommittee*, 28 pp.

Vanoni, V. A. (1975), Sediment discharge formulas, in *Sedimentation Engineering*, edited by V.A. Vanoni, pp. 190-229, Amer. Soc. Civ. Eng., New York.

Whiting, P. J. (2002), Streamflow necessary for environmental maintenance, *Ann. Rev. Earth Planetary Sci., 30*, 181-200.

Whiting, P. J. and, J. G. King (2003), Surface particle sizes on armoured gravel streambeds: Effects of supply and hydraulics, *Earth Surf. Processes Landforms, 28*, 1459-1471.

Whiting, P. J., J. F. Stamm, D. B. Moog, and, R. L. Orndorff (1999), Sediment-transporting flows in headwater streams, *Geol. Soc. Am. Bull., 111*, 450-466.

Wilcock, P. R. (2001), Toward a practical method for estimating sediment-transport rates in gravel-bed rivers, *Earth Surf. Processes Landforms, 27*, 1395-1408.

Williams, G. P., B. Thomas, and, R. Daddow (1988), Methods for collection and analysis of fluvial-sediment data, *U.S. For. Serv. Tech. Pap., WSDG-TP-00012*, 85 pp.

Wolman, M. G. (1954), Method of sampling coarse river bed material, *EOS Trans. AGU, 35*, 951-956.

Wolman, M. G., and, J. P. Miller (1960), Magnitude and frequency of forces in geomorphic processes, *J. Geol., 68*, 54-74.

Yang, C. T., and, C. Huang (2001), Applicability of sediment transport formulas, *Int. J. Sed. Res., 16*, 335-353.

Zar, J. H. (1974), *Biostatistical Analysis*, 718 pp., Prentice Hall, Englewood Cliffs, New Jersey.

Appendix 1.1: Bed Load Transport Equations

1) *Meyer-Peter and Müller* [1948] (by d_{50ss}):

The *Meyer-Peter and Müller* [1948] formula is written as

$$q_b = 8\left[\frac{\rho_s}{\rho_s - \rho}\right]\sqrt{\frac{g}{\rho}}\left[\left(\frac{n'}{n_t}\right)^{3/2}\rho SD - 0.047(\rho_s - \rho)d_{50ss}\right]^{3/2} \quad \text{(A1.1)}$$

where q_b is the total specific bed load transport rate (dry mass per unit width and time), ρ and ρ_s are water and sediment densities, respectively (assumed equal to 1000 and 2650 kg/m^3 throughout), n'/n_t is the ratio of particle roughness to total roughness which corrects the total boundary shear stress to the skin friction stress (that portion applied to the bed and responsible for sediment transport), S is channel slope, D is average flow depth, 0.047 is the critical Shields stress, g denotes gravitational acceleration, and d_{50ss} is the subsurface particle size for which 50% of the sediment sample is finer. The original *Meyer-Peter and Müller* [1948] equation specifies the characteristic grain size as the mean particle size of the unworked laboratory sediment mixture, which is reasonably approximated by d_{50ss}.

The total roughness (n_t) is determined from the *Manning* [1891] equation as

$$n_t = \frac{S^{1/2}R^{2/3}}{V} \quad \text{(A1.2)}$$

where V is average velocity and R is hydraulic radius. The grain roughness (n') is determined from the *Strickler* [1923] equation as

$$n' = \frac{d_{90s}^{1/6}}{26} \quad \text{(A1.3)}$$

where d_{90s} is the surface particle size for which 90% of the sediment sample is finer.

2) *Meyer-Peter and Müller* [1948] (by d_i):

Here, we modify the *Meyer-Peter and Müller* [1948] formula for transport by size class

$$q_{bi} = 8 f_i \left[\frac{\rho_s}{\rho_s - \rho} \right] \sqrt{\frac{g}{\rho}} \left[\left(\frac{n'}{n_t} \right)^{3/2} \rho SD - \tau^*_{ci} (\rho_s - \rho) d_i \right]^{3/2} \quad \text{(A1.4)}$$

where q_{bi} is the size-specific bed load transport rate, f_i is the proportion of subsurface material in the i^{th} size class, τ^*_{ci} is the size-specific critical Shields stress, and d_i denotes mean particle diameter for the i^{th} size class. τ^*_{ci} is determined from the *Andrews* [1983] hiding function as

$$\tau^*_{ci} = 0.0834 \left(d_i / d_{50ss} \right)^{-0.872} \quad \text{(A1.5)}$$

We choose the *Andrews* [1983] function because it was derived from channel types and physiographic environments similar to those examined in this study.

3) *Ackers and White* [1973] (by d_i):

The *Ackers and White* [1973] equation as modified by *Day* [1980] for size-specific transport is

$$q_{bi} = G_{gri} f_i \rho_s d_i V \left(\frac{V}{u^*} \right)^n \quad \text{(A1.6)}$$

where u^* denotes shear velocity

$$u^* = \sqrt{gDS} \quad \text{(A1.7)}$$

and G_{gri} is the dimensionless transport rate of the i^{th} size class, defined as

$$G_{gri} = C \left[\frac{F_{gri}}{A_i} - 1 \right]^m \quad \text{(A1.8)}$$

F_{gri} is the dimensionless particle mobility parameter (analogous to a non-critical Shields stress), A_i is a dimensionless hiding function analogous to a critical Shields stress, and C and m are empirical values. F_{gri} is defined as

$$F_{gri} = \frac{u^{*n}}{\left(gD\frac{\rho_s - \rho}{\rho}\right)^{\frac{1}{2}}}\left[\frac{V}{\sqrt{32}\,log\left(\frac{10D}{d_i}\right)}\right]^{1-n} \tag{A1.9}$$

where n is an empirical parameter that accounts for mobility differences between the fine and coarse components of the bed load [*Ackers and White*, 1973]. A_i, C, m, and n are functions of dimensionless particle size (D_{gri})

$$D_{gri} = d_i\left[g\left(\rho_s - \rho\right)/\left(\rho\nu^2\right)\right]^{1/3} \tag{A1.10}$$

where ν denotes kinematic viscosity (water temperature assumed 15ºC throughout).

For $1 < D_{gri} \leq 60$

$$n = 1 - 0.56\log\left(D_{gri}\right) \tag{A1.11}$$

$$m = \frac{9.66}{D_{gri}} + 1.34 \tag{A1.12}$$

$$C = 10^{\left[2.86\log(D_{gri}) - \left(\log\left(D_{gri}\right)\right)^2 - 3.53\right]} \tag{A1.13}$$

$$A_i = \left[0.4\left(\frac{d_i}{D_A}\right)^{-1/2} + 0.6\right]A \tag{A1.14}$$

where

$$D_A = d_{50ss}\left[1.62\sqrt{\frac{d_{84ss}}{d_{16ss}}}^{-0.55}\right] \tag{A1.15}$$

$$A = \left(\frac{0.23}{\sqrt{D_{gri}}} \right) + 0.14 \tag{A1.16}$$

and d_{84ss} and d_{16ss} are, respectively, the subsurface particle sizes for which 84% and 16% of the sediment sample is finer. *Day* [1980] defines (A1.15) in terms of grain-size percentiles of the unworked laboratory sediment mixture, which we approximate here by the subsurface grain-size distribution.

For $D_{gri} > 60$

$$n = 0 \tag{A1.17}$$

$$m = 1.5 \tag{A1.18}$$

$$C = 0.025 \tag{A1.19}$$

$$A_i = \left[0.4 \left(\frac{d_i}{D_A} \right)^{-1/2} + 0.6 \right] A \tag{A1.20}$$

where

$$A = 0.17 \tag{A1.21}$$

4) *Bagnold* [1980] (by d_{mqb}):

The *Bagnold* [1980] formula is

$$q_b = \left[\frac{\rho_s}{\rho_s - \rho} \right] q_{b*} \left[\frac{\omega - \omega_0}{(\omega - \omega_0)_*} \right]^{3/2} \left(\frac{D}{D_*} \right)^{-2/3} \left(\frac{d_{mqb}}{d_*} \right)^{-1/2} \tag{A1.22}$$

where q_{b*} denotes the reference transport rate (0.1 kg s^{-1} m^{-1}), ω and ω_0 are the applied and critical values of unit stream power, respectively, $(\omega - \omega_0)_*$ denotes the reference excess stream power (0.5 kg s^{-1} m^{-1}), D_* is a reference stream depth (0.1 m), d_* denotes the reference particle size (0.0011 m), and d_{mqb} is the modal grain size of a given bed load transport observation.

Unit stream power is defined as

$$\omega = \rho DSV \tag{A1.23}$$

Note that this definition of stream power lacks a gravity term, which *Bagnold* [1980] factors out of all of his equations.

Critical unit stream power for unimodal sediments is defined as

$$\omega_0 = 5.75\left[\left(\frac{\rho_s}{\rho}-1\right)\rho 0.04\right]^{3/2}\left(\frac{g}{\rho}\right)^{1/2} d_{mss}{}^{3/2}\log\left(\frac{12D}{d_{mqb}}\right) \tag{A1.24}$$

For bimodal sediments, *Bagnold* [1980] replaces ω_0 with ϖ_0, the geometric mean of the critical stream power for the two modes

$$\varpi_0 = \left[(\omega_0)_1(\omega_0)_2\right]^{1/2} \tag{A1.25}$$

where $(\omega_0)_1$ and $(\omega_0)_2$ are solved individually from (A1.24), but with d_{mqb} replaced by the modes of the bed load size distribution (d_{m1} and d_{m2}, respectively). Separate computations of (A1.22) were made under bimodal conditions, replacing d_{mqb} with d_{m1} for one set of computations and d_{m2} for the second set of computations [*Bagnold*, 1980], which were then summed to determine the total bed load transport of each event.

5) *Bagnold* [1980] (by d_{mss}):

We use the same approach as above, but with the modal grain size defined from the subsurface material (d_{mss}) (a proxy for the high-flow bed load distribution).

6) *Parker et al.* [1982] (by d_{50ss}):

The *Parker et al.* [1982] formula is

$$q_b = \sqrt{g}(DS)^{3/2} G(\phi_{50ss}) W_r^* \frac{\rho_s}{\mathcal{R}} \tag{A1.26}$$

where W_r^* is the reference dimensionless transport rate (equal to 0.0025), $\mathcal{R}$ is the submerged specific gravity of sediment (ρ_s/ρ-1), and $G\left(\phi_{50ss}\right)$ is a three-part bed load transport function [as revised by *Parker* 1990] that depends on the excess Shields stress of the median subsurface grain size (ϕ_{50ss})

$$G\left(\phi_{50ss}\right)=\begin{cases}5474\left(1-\dfrac{0.853}{\phi_{50ss}}\right)^{4.5} & \phi_{50ss}>1.59\\ \exp\left[14.2\left(\phi_{50ss}-1\right)-9.28\left(\phi_{50ss}-1\right)^2\right] & 1\le\phi_{50ss}\le 1.59\\ \phi_{50ss}{}^{14.2} & \phi_{50ss}\le 1\end{cases} \qquad \text{(A1.27a-c)}$$

The excess Shields stress is defined as the ratio of the applied Shields stress (τ^*_{50ss}) to that of the reference value (τ^*_{50r}, that capable of producing the reference dimensionless transport rate, W_r^*=0.0025)

$$\phi_{50ss}=\left(\frac{\tau^*_{50ss}}{\tau^*_{50r}}\right) \qquad \text{(A1.28)}$$

The applied Shields stress is given by

$$\tau^*_{50ss}=\frac{\tau_0}{\rho g\,\mathcal{R}\,d_{50ss}} \qquad \text{(A1.29)}$$

where τ_0 is the total boundary shear stress calculated from the depth-slope product (ρgRS). The reference Shields stress (τ^*_{50r}) is empirically determined from site-specific bed load transport data following the procedure described by *Parker et al.* [1982]. Their approach involves regressing size-specific dimensionless transport rates (W^*_i)

$$W_i^*=\frac{\mathcal{R}\,q_{bi}}{f_i\sqrt{g}\left(DS\right)^{3/2}} \qquad \text{(A1.30)}$$

against corresponding Shields stress values (τ^*_i)

$$\tau_i^* = \frac{\tau_0}{\rho g \mathcal{R} d_i} \tag{A1.31}$$

and collapsing the size-specific curves into a single function

$$W_i^* = \alpha_i \tau^*_i{}^M \tag{A1.32}$$

where M is the weighted mean exponent of the size-specific functions of W^*_i versus τ^*_i, and α_i is the size-specific coefficient of regression [*Parker et al.*, 1982]. Finally, τ^*_{50r} is determined from (A1.32) for the reference transport rate (W^*_i=W^*_r=0.0025) and the site-specific value of α_{50}.

7) *Parker et al.* [1982] (by d_i):

The *Parker et al.* [1982] equation by size class (d_i) is

$$q_{bi} = f_i \sqrt{g} (DS)^{3/2} G(\phi_i) W_r^* \frac{\rho_s}{\mathcal{R}} \tag{A1.33}$$

where ϕ_i denotes the size-specific excess Shields stress

$$\phi_i = \left(\frac{\tau^*_i}{\tau^*_{ri}} \right) \tag{A1.34}$$

which replaces ϕ_{50ss} in (A1.27) for solution of $G(\phi_i)$. τ^*_{ri} values are determined from site-specific bed load transport data as described above for *Parker et al.* [1982] by d_{50ss}.

8) *Parker et al.* [1982] (by d_i via *Andrews* [1983]):

Here we use the same approach as above, but τ^*_{ri} values are determined from the *Andrews* [1983] hiding function (A1.5).

Appendix 1.2. Reply to Comment By C. Michel On "A General Power Equation for Predicting Bed Load Transport Rates In Gravel Bed Rivers"[2]

A1.2.1. Introduction

We thank *Michel* [2005] for the opportunity to improve our bed load transport equation (equation (6) of *Barry et al.* [2004]) and to resolve the dimensional complexity that he identified. However, we do not believe that the alternative bed load transport equation proposed by *Michel* [2005] provides either the mechanistic insight or predictive power of our transport equation.

A1.2.2. Results and Discussion

Although some bed load transport data exhibit non-linear trends in log-log plots of transport rate versus discharge, a simple linear function is sufficient to describe our data (*Barry et al.* [2004], paragraph 43). The Figure 7 data of *Barry et al.* [2004] could be fit by a non-linear function as suggested by *Michel* [2005], but we believe this to be an unnecessary complication, particularly given how well our simple equation predicts observed transport rates compared to other more complex equations, such as *Parker*'s [1991] three-part bed load transport function (*Barry et al.* [2004], Figure 11). Furthermore, an important aspect of our equation, that is not preserved in Michel's alternative, is the between-site variation in the exponent of the transport function that results from supply-related channel armoring (i.e., transport capacity in excess of bed load sediment supply) which provides a mechanistic understanding of the bed load

[2] Co-authored paper with John M. Buffington and John G. King published in Water Resources Research, 2005.

transport process [*Barry et al.*, 2004]. *Michel* [2005] proposes a bed load transport equation that mimics our equation in terms of the range of exponents that we observe (i.e., 1.5-4, Figure 8a of *Barry et al.* [2004]), but lacks the mechanistic insight and consequent predictive power. Moreover, Michel's equation requires a sufficient number of bed load transport observations across a broad range of discharges to empirically calibrate his α and β values.

Michel [2005] correctly points out a dimensional complexity of our transport equation that we resolve here by scaling discharge by the two-year flood (Q_2)

$$q_b = \alpha\left(\frac{Q}{Q_2}\right)^{\beta} = 0.0008A^{0.4982}\left(\frac{Q}{Q_2}\right)^{\left(-2.45q^{*}+3.56\right)} \qquad \text{(B1.1)}$$

giving the coefficient of the equation constant dimensions of kg m^{-1} s^{-1}. In our revised equation, the relationship between β and q^{*} remains the same as that of *Barry et al*. [2004], however the relationship between α and drainage area (A) changed substantially. The coefficient α represents the magnitude of bed load transport, which is a function of basin-specific sediment supply and discharge, both of which can be expressed as functions of drainage area. In *Barry et al*. [2004], we proposed an inverse relationship between α and drainage area because discharge increases faster then sediment transport rate (*Barry et al.* [2004], paragraph 51). However, we hypothesize here that a direct relationship exists between α and drainage area when we scale discharge by the two-year flow (Figure B1.1). This scaling incorporates basin-specific differences in water yield, causing the relationship between α and drainage area to be solely a function of how sediment yield increases with drainage area. We also find that equation (B1.1) performs better than the original equation in terms of predicting the observed bed load transport

rates at the 17 independent test sites (Figure B1.2). However, the performance of (B1.1) is not statistically different from equation (6) of *Barry et al.* [2004], nor is it statistically different from the performance of the *Ackers and White* [1973] equation. Consequently, our original assessments of formula performance remain unchanged.

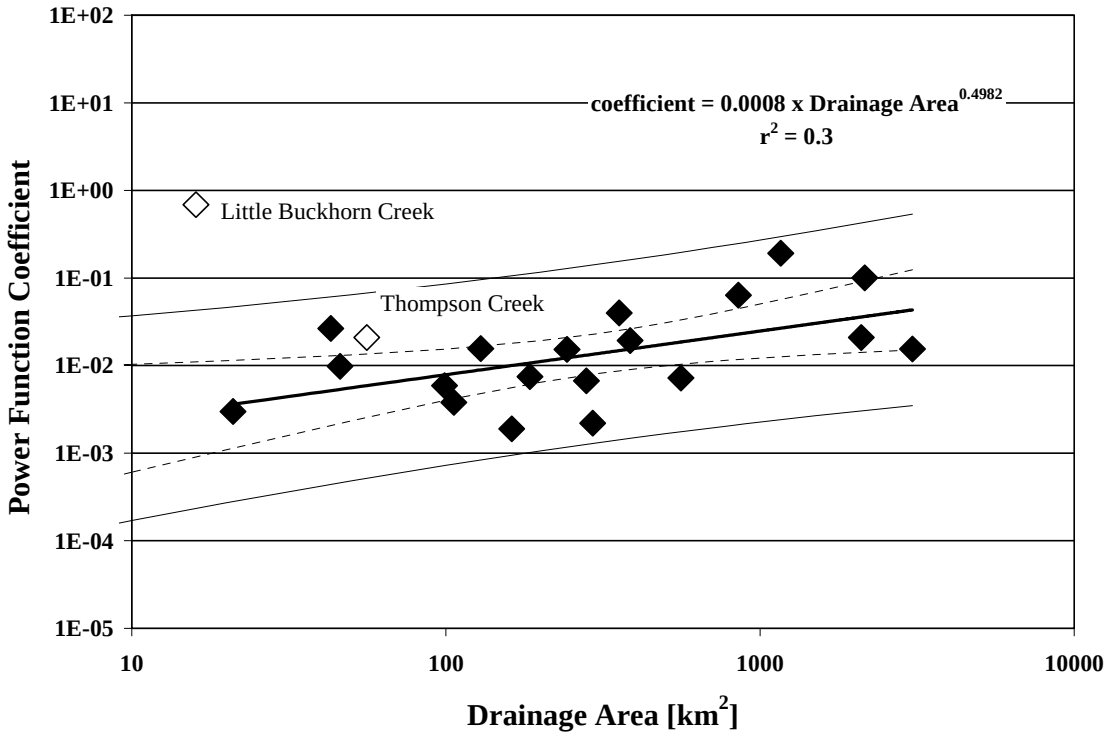

Figure B1.1. Revised relationship between drainage area and the coefficient of equation (B1.1) for the Idaho sites. Dashed lines indicate 95% confidence interval about the mean regression line. Solid lines indicate 95% prediction interval (observed values). Sites indicated by open diamonds are discussed by *Barry et al.* [2004].

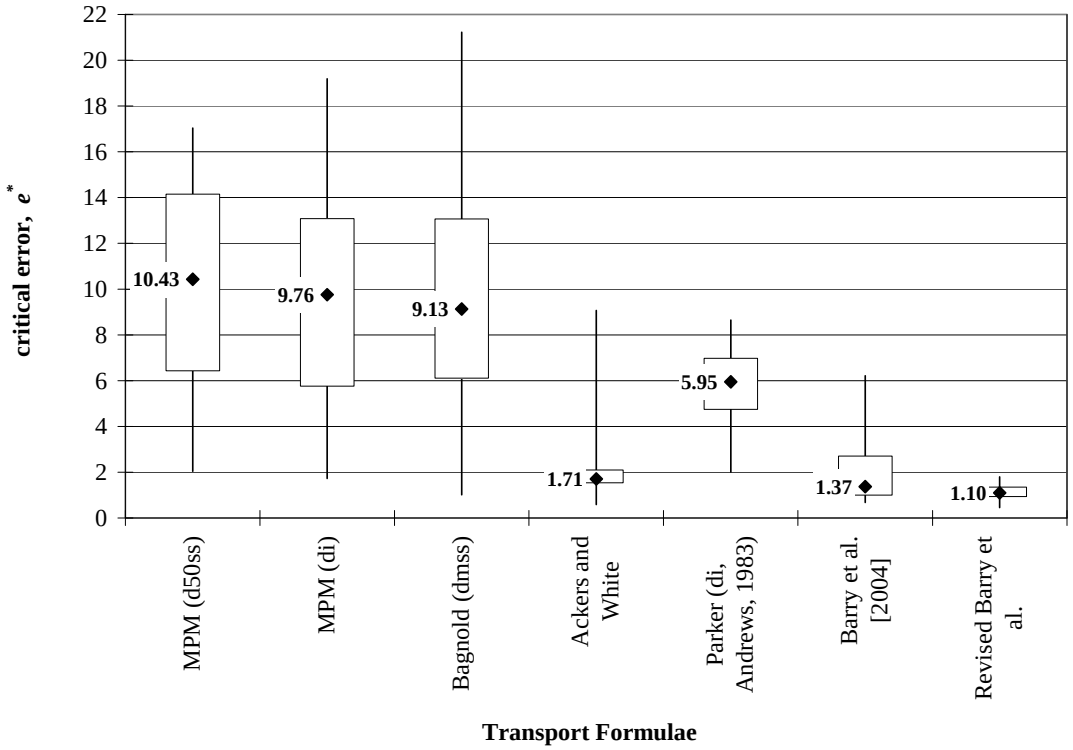

Figure B1.2. Box plots of the distribution of critical error, *e** [*Barry et al.*, 2004], for the 17 test sites. Median values are specified, box end represent the 75th and 25th percentiles, and whiskers denote maximum and minimum values. See *Barry et al.* [2004] for formulae citations.

A1.2.3. References

Ackers, P., and W.R. White (1973), Sediment transport: New approach and analysis, *J. Hydraul. Div., Am. Soc. Civ. Eng., 99,* 2041-2060.

Barry, J. J., J. M. Buffington, and J. G. King (2004), A general power equation for predicting bed load transport rates in gravel bed rivers, *Water Resour. Res., 40,* W10401, doi:10.1029/2004WR003190.

Appendix 1.3. Correction to "A general power equation for predicting bed load transport rates in gravel bed rivers" by Jeffrey J. Barry, John M. Buffington, and John G. King [3]

A1.3.1. Typographical Errors

In the paper "A general power equation for predicting bed load transport rates in gravel bed rivers" by Jeffrey J. Barry, John M. Buffington, and John G. King (Chapter 1) [*Water Resources Research, 40,* W10401, 2004], the y-axis for Figures 5 and 10 was incorrectly labeled and should have read "$\log_{10}$ (predicted transport) - $\log_{10}$ (observed transport)." In addition, flow depth (D) is incorrectly shown in the denominator of equation (A9) of *Barry et al.* [2004] and should be replaced by d_i, the mean particle diameter for the ith size class as shown below

$$F_{gri} = \frac{u^{*n}}{\left(g d_i \frac{\rho_s - \rho}{\rho} \right)^{1/2}} \left[\frac{V}{\sqrt{32} \log\left(\frac{10D}{d_i} \right)} \right]^{1-n} \qquad \text{(C1.1)}$$

Similarly, equation (A24) of *Barry et al.* [2004] incorrectly includes the modal grain size from the subsurface material (d_{mss}) which should be replaced with d_{mqb}, the modal grain size of a given bed load transport observation. The correct equation is

$$\omega_0 = 5.75[(\rho_s - \rho)0.04]^{3/2} \left(\frac{g}{\rho} \right)^{1/2} d_{mqb}{}^{3/2} \log\left(\frac{12D}{d_{mqb}} \right) \qquad \text{(C1.2)}$$

[3] Co-authored paper with John M. Buffington and John G. King submitted to Water Resources Research, 2007.

A1.3.2. Dimensions

We also correct two dimensional inconsistencies in equation (6) of *Barry et al.* [2004], 1) with drainage area (A) expressed in units of m^2 rather than km^2, and 2) by scaling discharge by the two-year flood (Q_2), which gives α constant units of kg m^{-1} sec^{-1} and improves the overall performance of our bed load transport equation [*Barry et al.*, 2005]

$$q_b = \alpha(Q/Q_2)^{\beta} = 8.13 \bullet 10^{-7} A^{0.49} (Q/Q_2)^{(-2.45q^*+3.56)} \quad \text{(C1.3)}$$

The units of the drainage area coefficient ($8.13 \bullet 10^{-7}$) depend on the site-specific regression between α and A; in our case, the units are kg $m^{-1.98}$ s^{-1}.

A1.3.3. Sensitivity of Equation Performance

We have also further tested the sensitivity of our results to selection of ε, the value that was added to bed load transport rates in order to include incorrect zero transport predictions in our log-transformed assessment of formula performance ($\log_{10}(P+\varepsilon) - \log_{10}(O+\varepsilon)$, where P and O are predicted and observed transport rates, respectively) [*Barry et al.*, 2004, section 4.1.3.]. Incorrect zero predictions can occur at low to moderate flows for transport equations that contain a threshold for the onset of bed load transport (i.e., the *Meyer-Peter and Müller* [1948], *Ackers and White* [1973], and *Bagnold* [1980] equations) [*Gomez and Church* 1989; *Habersack and Laronne* 2002; *Barry et al.* 2004]. We originally suggested that ε should be set equal to the lowest non-zero predicted transport rate at a given study site ($1 \bullet 10^{-15}$ kg m^{-1} s^{-1} for our analysis), recognizing that equation performance and degree of under-prediction for threshold equations would be influenced by the selected ε value when those equations erroneously predict zero transport [*Barry et al.*, 2004, paragraph 34]. Initial sensitivity analyses

showed that ε influenced absolute performance in terms of the magnitude of under-prediction reported for threshold equations when they predicted large numbers of incorrect zero transport rates [*Barry et al.*, 2004, Figure 5], but ε did not affect relative performance amongst the transport equations [*Barry et al.*, 2004, paragraph 38].

Further analyses demonstrate that significant numbers of incorrect zero predictions make the critical error, e^*, a function of ε, rather than an indicator of actual formula performance (Figure C1.1; see caption for e^* definition). This is particularly evident for the *Meyer-Peter and Müller* [1948] and *Bagnold* [1980] equations (Figure C1.1) due to their high number of incorrect zero predictions at our study sites [*Barry et al.* 2004, paragraph 62]. In contrast, the *Ackers and White* [1973], *Parker* [1990] and *Barry et al.* [2004] equations predict some degree of transport at most discharges, which makes their e^* values less susceptible to choice of ε (at least up to values of $1 \bullet 10^{-5}$ kg m^{-1} s^{-1}; Figure C1.2). The decline in prediction error toward zero as ε increases beyond $1 \bullet 10^{-5}$ kg m^{-1} s^{-1} is an artifact of ε becoming larger than the majority of the observed and predicted transport rates at our test sites. As ε becomes large, it masks the actual prediction error, with our assessment of formula performance effectively comparing the logarithmic difference of two very large numbers set by the magnitude of ε, resulting in vanishingly small differences and correspondingly small critical errors ($\log_{10}(P+\varepsilon) - \log_{10}(O+\varepsilon) \Rightarrow 0$ when $\varepsilon >> P$ and O). In summary, Figure C1.1 shows that the median critical errors, e^*, of the *Meyer-Peter and Müller* [1948] and *Bagnold* [1980] equations are influenced by ε regardless of its magnitude, while the selected value of ε only begins to influence the critical errors of the other equations when ε is greater than $1 \bullet 10^{-5}$ kg m^{-1} s^{-1}.

To avoid the analytical artifacts introduced by use of ε, we suggest that e^* values be determined from non-zero predictions (obviating the need for ε), but with results qualified by the proportion of incorrect zero predictions (Figure C1.2; see caption for e^* definition). Because equation performance varies with discharge [*Barry et al.*, 2004, their Figure 2], we show results binned by discharge as a percentage of Q_2. Furthermore, in this analysis we use the improved version of our bed load transport equation given in section A1.3.2 above. Results show that the *Ackers and White* [1973] and *Barry et al.* (C1.3) still outperform the others, with median critical errors near 1 across most discharge bins (Figure C1.2a). The performance of both the *Meyer-Peter and Müller* [1948] and *Bagnold* [1980] equations improves compared to that reported by *Barry et al.* [2004], with median e^* values typically between 3 and 4 for the *Meyer-Peter and Müller* [1948] equation and between 2 and 4 for the *Bagnold* [1980] equation. However, the frequency of incorrect zero predictions should be considered when evaluating the performance of those equations; both the *Meyer-Peter and Müller* [1948] and the *Bagnold* [1980] equations incorrectly predicted zero transport approximately 40% of the time at flows as large as 40-50% of Q_2 (Figure C1.2b). The performance of the *Parker* [1990] equation is essentially unchanged. The principal drawback of the approach shown in Figure C1.2 is that the user must select both an acceptable e^* value and an acceptable percentage of incorrect zero predictions. Nevertheless, having to do so highlights the frequently neglected error of threshold equations at low and moderate discharges.

An alternative method for evaluating equation performance that includes incorrect zero predictions is to compare ratios of untransformed values of predicted versus observed transport rates (P/O) [*Gomez and Church*, 1989; *Reid et al.*, 1996; *Habersack*

and Laronne, 2002]. However, this method skews the results to those equations that under-predict bed load transport. In terms of percentages, the maximum under-prediction is 100% (incorrect zero prediction), while the percentage of over-prediction can be infinite. Consequently, this approach creates a skewed error distribution that tends to favor equations that under predict.

Another method for evaluating equation performance that does not bias results is presented by *Bravo-Espinosa et al.* [2003]. They use an inequality coefficient, U, which can vary from 0 to 1, for evaluating equation performance based on untransformed values of predicted and observed transport rates. $U = 0$ corresponds with perfect agreement between observed and predicted values, while $U = 1$ indicates a complete lack of predictive power. The authors assume that equation performance is acceptable when $U \leq 0.5$, however the basis for this value is not given and the relative significance of different U values is uncertain. For example, how much better is $U = 0.4$ versus 0.5?

To our knowledge, there is no ideal method for assessing equation performance that allows for inclusion of incorrect zero predictions without either biasing results (i.e., creating a skewed error distribution) or requiring subjective qualification of results (i.e., determination of acceptable U values or acceptable percentages of incorrect zero predictions).

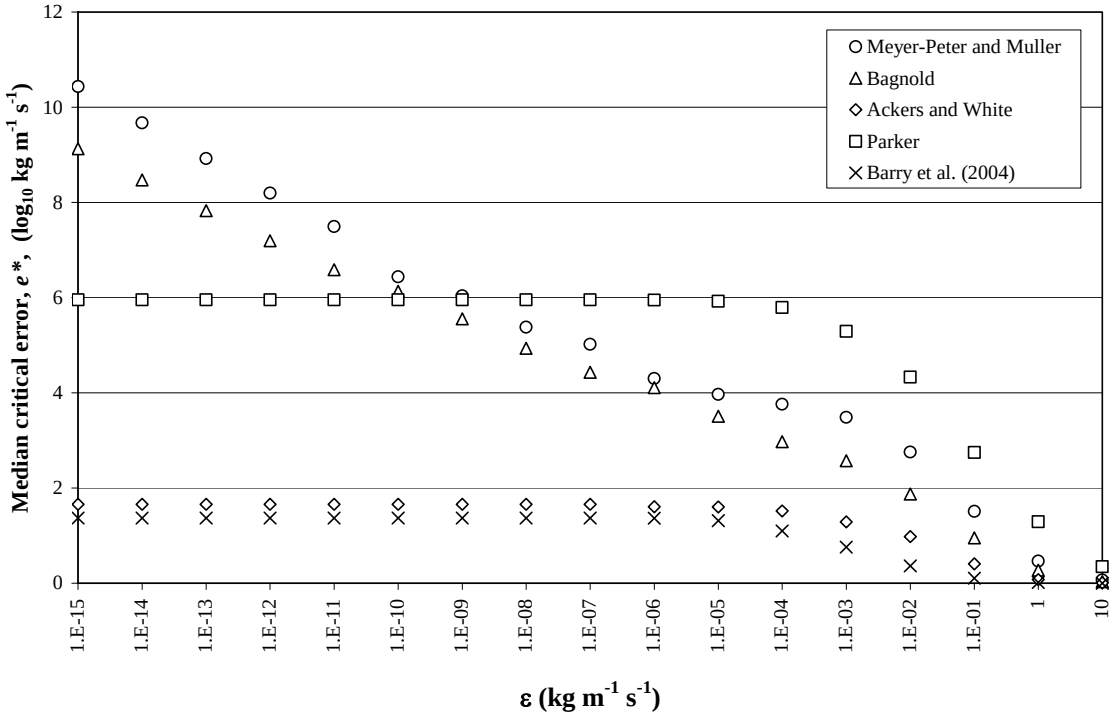

Figure C1.1. Sensitivity of median critical error, e^*, to changes in ε (constant added to preclude taking the logarithm of 0 when predicted transport rates are zero) at the 17 test sites. Sites described elsewhere [*Barry et al.*, 2004, section 3]. e^* is the amount of error that one would have to accept for equivalence between observed and predicted transport rates using *Freese*'s [1960] χ^2 test as modified by *Reynolds* [1984],

$$e^* = \sqrt{\frac{1.96^2}{\chi^2} \sum_{i=1}^{n} [\log(P_i + \varepsilon) - \log(O_i + \varepsilon)]^2} \ ,$$

where P_i and O_i are the i^{th} predicted and observed transport rates, respectively, n is the number of observations, 1.96 is the value of the standard normal deviate corresponding to a two-tailed probability of 0.05, and χ^2 is the two-tailed chi-squared statistic with n degrees of freedom.

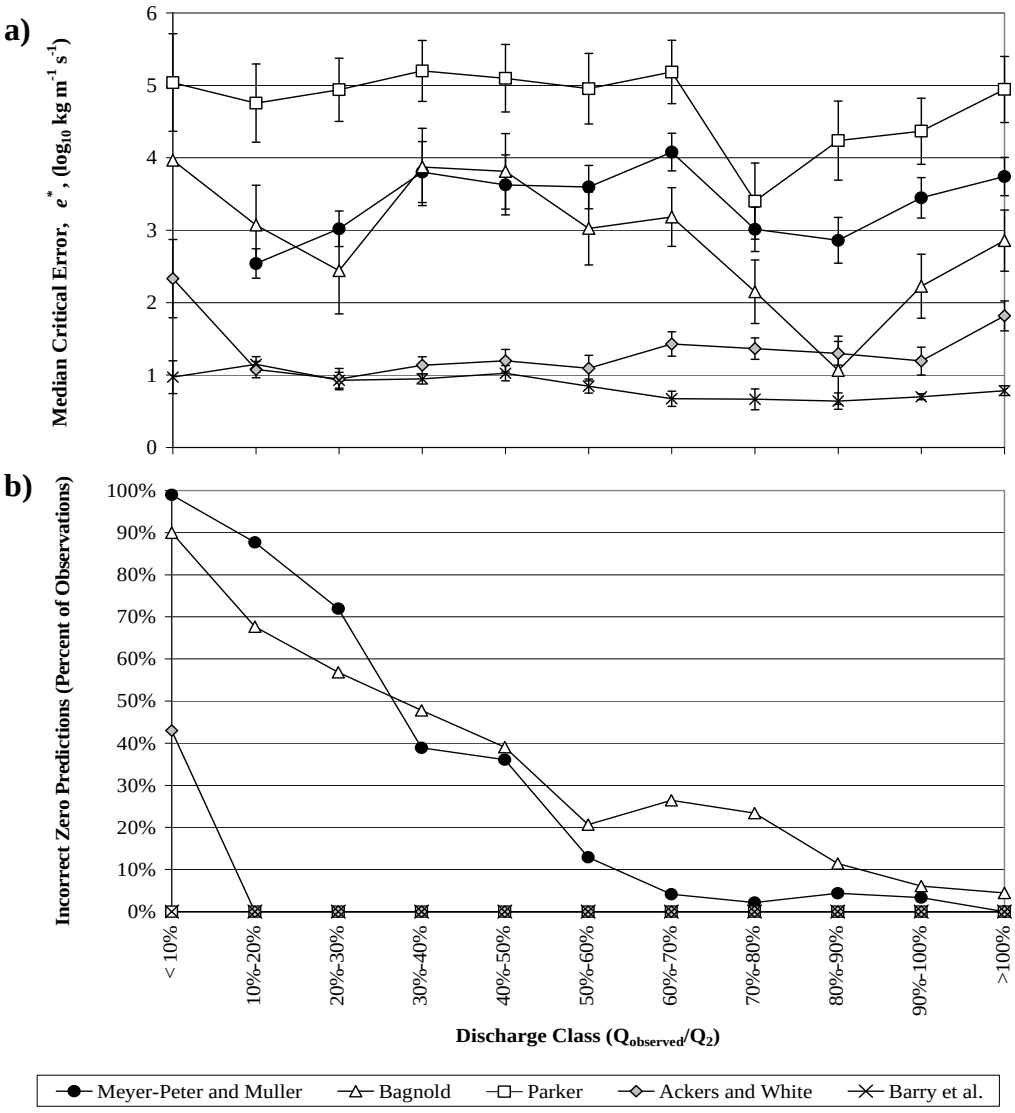

Figure C1.2. a) Median critical error, *e**, for non-zero predictions of bed load transport as a function of discharge scaled by Q_2, and b) frequency of incorrect zero predictions for same. Here, $e^* = \sqrt{\frac{1.96^2}{\chi^2}\sum_{i=1}^{n}(\log P_i - \log O_i)^2}$, with parameters defined in the caption for Figure 5.1. Whiskers in (a) indicate 95% confidence intervals around e^*. The *Meyer-Peter and Müller* [1948] equation predicted zero transport for all but one observation during flows < 10% of Q_2, consequently no median e^* value is shown in (a) for those flows.

A1.3.4. References

Ackers, P., and W. R. White (1973), Sediment transport: New approach and analysis, *J. Hydraul. Div. Am. Soc. Civ. Eng.*, *99*, 2041-2060.

Bagnold, R. A. (1980), An empirical correlation of bedload transport rates in flumes and natural rivers, *Proc. R. Soc. London*, *372*, 453-473.

Barry, J. J., J. M. Buffington, and J. G. King (2004), A general power equation for predicting bed load transport rates in gravel bed rivers, *Water Resour. Res.*, *40*, doi:10.1029/2004WR003190.

Barry, J. J., J. M. Buffington, and J. G. King (2005), Reply to Comment by C. Michel on "A general power equation for predicting bed load transport rates in gravel bed rivers", *Water Resour. Res.*, *41*, doi:10.1029/2005WR004172.

Bravo-Espinosa, M., W. R. Osterkamp, and V. L. Lopes (2003), Bedload transport in alluvial channels, *J. Hydraul. Eng.*, *129*, 783-795.

Freese, F. (1960), Testing accuracy, *For. Sci.*, *6*, 139-145.

Gomez, B., and M. Church (1989), An assessment of bedload sediment transport formulae for gravel bed rivers, *Water Resour. Res.*, *25*, 1161-1186.

Habersack, H. M., and J.B. Laronne (2002), Evaluation and improvement of bed load discharge formulas based on Helley-Smith sampling in an alpine gravel bed river, *J. Hydraul. Eng*., *128*(5), 484-498.

Leopold, L.B., M.G. Wolman, and J.P. Miller (1964), *Fluvial Processes in Geomorphology*, 552 pp., W.H. Freeman, San Francisco, CA.

Meyer-Peter, E., and R. Müller (1948), Formulas for bed-load transport, in *Proceedings of the 2nd Meeting of the International Association for Hydraulic Structures Research*, pp. 39-64, *Int. Assoc. Hydraul. Res.*, Delft, Netherlands.

Parker, G. (1990), Surface-based bedload transport relation for gravel rivers, *J. Hydraul. Res.*, *28*, 417-436.

Reid, I., D.M. Powell, and J.B. Laronne (1996), Prediction of bed-load transport by desert flash floods, *J. Hydraul. Eng.*, *122*, 170-173.

Reynolds, M.R. (1984), Estimating error in model prediction, *For. Sci.*, *30*, 454-469.

Chapter 2. Performance of Bed Load Transport Equations Relative to Geomorphic Significance: Predicting Effective Discharge and Its Transport Rate[4]

2.1. Abstract

Previous studies assessing the accuracy of bed load transport equations have considered equation performance statistically based on paired observations of measured and predicted bed load transport rates. However, transport measurements were typically taken during low flows, biasing the assessment of equation performance toward low discharges, and because equation performance can vary with discharge, it is unclear whether previous assessments of performance apply to higher, geomorphically significant flows (e.g., the bankfull or effective discharges). Nor is it clear whether these equations can predict the effective discharge, which depends on the accuracy of the bed load transport equation across a range of flows. Prediction of the effective discharge is particularly important in stream restoration projects, as it is frequently used as an index value for scaling channel dimensions and for designing dynamically stable channels. In this study, we consider the geomorphic performance of 5 bed load transport equations at 22 gravel-bed rivers in mountain basins of the western United States. Performance is assessed in terms of the accuracy with which the equations are able to predict the effective discharge and its bed load transport rate. We find that the median error in predicting effective discharge is near zero for all equations, indicating that effective

[4] Co-authored paper with John M. Buffington, Peter Goodwin, John G. King and William W. Emmett submitted to Journal of Hydraulic Engineering, 2007.

discharge predictions may not be particularly sensitive to one's choice of bed load transport equation. However, the standard deviation of the prediction error differs between equations (ranging from 10-60%), as does their ability to predict the transport rate at the effective discharge (median errors of less than 1 to almost 2.5 orders of magnitude). A framework is presented for standardizing the transport equations to explain observed differences in performance and to explore sensitivity of effective discharge predictions.

2.2. Introduction

Bed load transport is a fundamental physical process in alluvial rivers, building and maintaining a dynamically stable channel geometry that reflects both the quantity and timing of water and the volume and caliber of sediment delivered from the watershed [*Leopold et al.*, 1964; *Emmett and Wolman*, 2001]. Accordingly, *Leopold* [1994] describes alluvial rivers as the architects of their own geometry (also see *Parker* [1978]). Projects aimed at restoring the form and function of river ecosystems increasingly recognize the importance of channel geometry for dynamic equilibrium and the role of bed load transport in forming and maintaining it [*Goodwin*, 2004].

In these projects, the effective discharge is frequently used as an index value for scaling channel dimensions [*Goodwin*, 2004]. The effective discharge is defined as that which transports the greatest mass of sediment over time and is believed to control channel form in many alluvial rivers [*Wolman and Miller*, 1960]. The effective discharge is a fairly frequent event in sand- and gravel-bed rivers and is equivalent to the bankfull flow for channels in dynamic equilibrium [*Andrews*, 1980; *Carling*, 1988; *Andrews and Nankervis*, 1995; *Knighton*, 1998; *Emmett and Wolman*, 2001], which in temperate

climates tends to have a return period of 1-2 years [*Wolman and Leopold*, 1957; *Leopold et al.*, 1964; *Williams*, 1978].

Although the effective discharge is commonly used in restoration design, the accuracy of effective discharge predictions has not been widely examined. For a given flow record, effective discharge predictions depend on the performance of the chosen bed load transport equation across a range of flows. However, previous assessments of bed load transport equations [e.g., *Gomez and Church*, 1989; *Yang and Huang*, 2001; *Bravo-Espinosa et al*., 2003; *Barry et al*., 2004] have largely been based on low flow observations. For example, bed load datasets from these studies show that more than 80% of the observations at each site typically occur at flows less than the 2-year flood (Q_2, a bankfull-like flow [*Whiting et al*., 1999; *Barry et al*., 2004] similar to the effective discharge [*Emmett and Wolman*, 2001]) (Figure 2.1). Consequently, these previous assessments of equation performance are weighted toward low discharges that do not play a significant role in either building or maintaining the stable channel form, and thus have little geomorphic significance.

Because equation performance can vary with discharge (Figure 2 of *Barry et al*. [2004]; Figures 3-5 of *Bravo-Espinosa et al*. [2003]; Figure 5 of *Habersack and Laronne* [2002]), prior studies of performance, which are biased toward low flows, may not be representative of higher, geomorphically significant flows, such as the effective discharge. In addition, previous assessments of equation performance focus on comparing observed versus predicted magnitudes of bed load transport. However, accurate prediction of the effective discharge depends on how well a given transport equation predicts the rate of change in transport with discharge, rather than the absolute

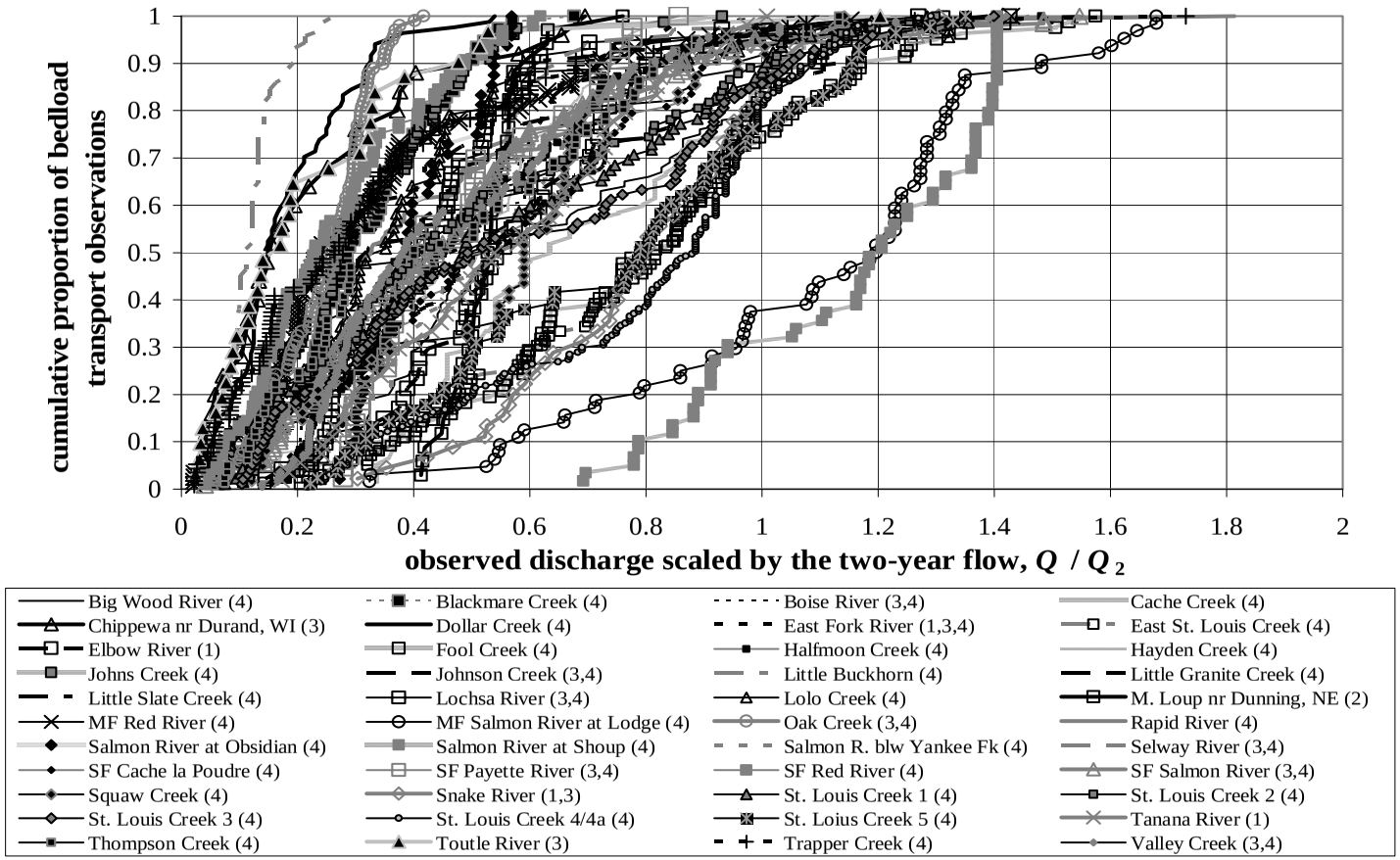

Figure 2.1. Discharge ranges over which bed load transport has been observed in gravel-bed rivers used in previous assessments of the performance of bed load transport equations. Numbers following each site name indicate specific performance studies using those data: 1) *Gomez and Church* [1989], 2) *Yang and Huang* [2001], 3) *Bravo-Espinosa et al*. [2003], and 4) *Barry et al*. [2004].

value of transport at a given discharge [*Emmett and Wolman*, 2001; *Goodwin*, 2004]. Hence, the ability of bed load transport equations to accurately predict the effective discharge and its transport rate remains to be tested.

A recent study by *Goodwin* [2004] developed analytical solutions for predicting effective discharge using generic forms of sediment transport equations and theoretical flow frequency distributions (normal, lognormal, and gamma). This study differs from his in that we examine the performance of specific transport equations, and we use observed flow frequency distributions because theoretical ones did not fit the data well.

Here, we consider the geomorphic performance of 5 different bed load transport equations at 22 gravel-bed rivers in mountain basins of the western United States. Performance is assessed in terms of the accuracy with which the equations are able to predict the effective discharge and its bed load transport rate. We also present a framework for standardizing the transport equations to explain observed differences in performance and to explore sensitivity of effective discharge predictions and their transport rates.

2.3. Effective Discharge

It is possible to directly compute the effective discharge at a site using the *Wolman and Miller* [1960] model if both the distribution of observed flows (from a nearby stream gauging station) and the sediment transport relationship (from direct measurements of bed load transport and stream discharge) are known and representative of current conditions (Figure 2.2). The product of discharge frequency (curve i) and bed load transport rate (curve ii) over the range of discharges in the flow record describes the work done by the channel during that period (curve iii). The discharge where this

product is maximized is termed the effective discharge [*Wolman and Miller*, 1960] (Figure 2.2). Controls on the prediction of effective discharge are examined below by parameterizing the Figure 2.2 curves of the *Wolman and Miller* [1960] model.

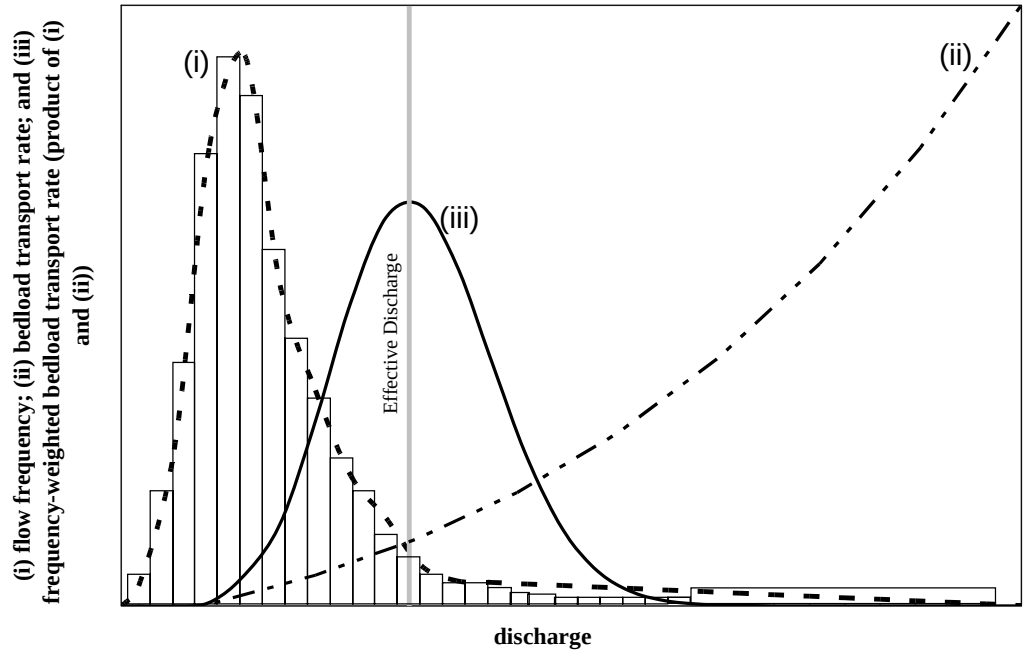

Figure 2.2. *Wolman and Miller* [1960] model for the magnitude and frequency of sediment transporting events (adapted from *Wolman and Miller* [1960]). Curve (i) is the flow frequency, curve (ii) is the sediment transport rate as a function of discharge, and curve (iii) is the distribution of sediment transported during the period of record (product of curves i and ii). The 26 arithmetic discharge bins used to describe the observed flow frequency distribution are shown as vertical boxes. The effective discharge is the flow rate which transports the most sediment over time, defined by the maximum value of curve (iii).

The bed load transport rate (curve ii) can be represented by a power function of discharge [e.g., *Gilbert*, 1914; *Vanoni*, 1975; *Emmett*, 1984; *Smith et al*., 1993; *Whiting et al*., 1999; *Emmett and Wolman*, 2001; *Bunte et al*., 2004]

$$Q_b = \alpha Q^{\beta} \tag{2.1}$$

where Q_b is the total bed load transport rate (kg sec^{-1}), Q is discharge (m^3 sec^{-1}), and α and β are empirical values. The total amount of bed load that is transported at a given discharge over the period of record (curve iii) can be represented by the parameter Φ, which is the bed load rating curve (2.1) multiplied by the frequency of occurrence of a given discharge, $f(Q)$, (curve i)

$$\Phi = \alpha Q^{\beta} f(Q) \tag{2.2}$$

The effective discharge (Q_e) occurs where Φ is at its maximum, such that $\partial\Phi/\partial Q = 0$ [*Nash*, 1994; *Goodwin*, 2004]. Upon setting the partial derivative of (2.2) to zero, the coefficient of the bed load rating curve, α, cancels out, with the effective discharge depending only on the exponent of the rating curve, β, and the characteristics of the flow distribution, $f(Q)$, [*Nash*, 1994; *Soar and Thorne*, 2001; *Goodwin*, 2004]. In addition to the overall shape of the flow frequency distribution, results can be particularly sensitive to adequate quantification of the frequency distribution in the range of flows close to the effective discharge [*Goodwin*, 2004].

The sensitivity of effective discharge predictions to the rating-curve slope (β) is shown in Figure 2.3. Larger values of β increase the predicted value of effective discharge for a given value of α (Figure 2.3a). In contrast, changes in α have no effect on the predicted value of effective discharge for a given value of β (Figure 2.3b); rather,

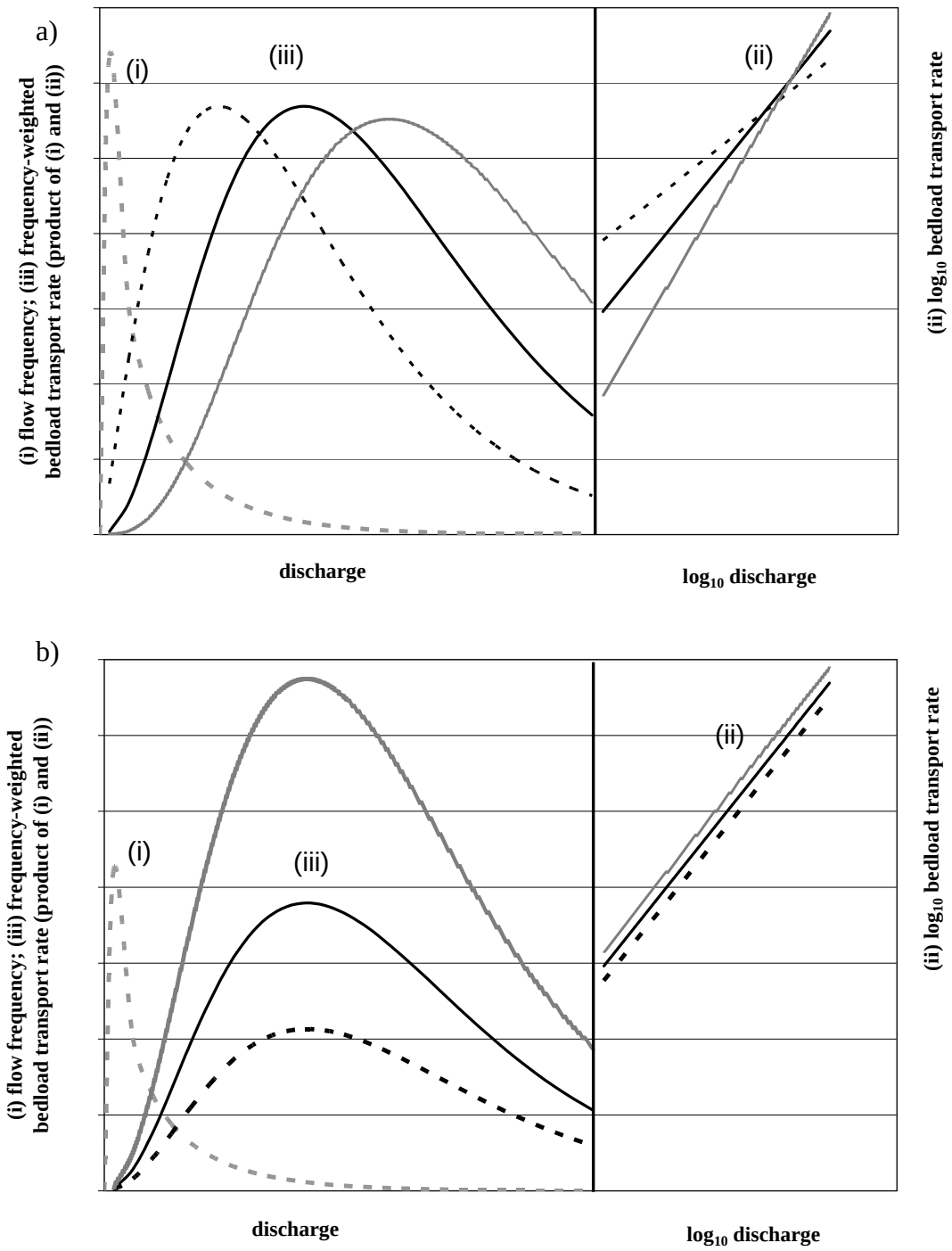

Figure 2.3. Effect of a) changing the exponent of the bed load rating curve, β, and b) changing the coefficient of the rating curve, α, on predictions of the effective discharge and bed load transport rate. Curve (i) is identical in both figures, α is constant in Figure 2.3a, and β is constant in Figure 2.3b.

as α increases, both the amount of transport at a given discharge and the bed load yield over the period of record increase. The exponent of the bed load rating curve is a function of supply-related channel armoring (transport capacity relative to sediment supply) [*Barry et al*., 2004; 2005]. Poorly-armored, fine-grained channels exhibit lower thresholds for bed load transport and, thus, lower rating-curve exponents compared to well-armored, coarse-grained channels; consequently, poorly-armored channels tend to have lower predicted values of effective discharge [*Emmett and Wolman*, 2001; *Goodwin*, 2004].

In this study, we are interested in assessing the ability of commonly used bed load transport equations to accurately predict effective discharges. However, the conceptual framework presented in Figure 2.3 for examining prediction sensitivity is complicated by that fact that most bed load transport equations are not written in terms of simple rating curves (2.1), but rather are expressed in complex terms of excess shear stress or excess stream power (e.g., Appendix A of *Barry et al*., 2004). Therefore, in our analysis we predict total bed load transport rates and consequent effective discharges in terms of the original formulations specified for each transport equation examined here. We then determine the equivalent bed load rating curves (2.1) for transport rates predicted from each of these equations to examine their performance in terms of the Figure 2.3 framework. Use of equivalent rating curves standardizes the diverse transport formulations to a common form that can be used in the Figure 2.3 framework to explain observed differences in performance.

2.4. Study Sites and Methods

2.4.1 Bed load Transport Equations and Study Site Selection

The equations examined in this analysis are: 1) the *Meyer-Peter and Müller* [1948] equation (calculated by median subsurface grain size, d_{50ss}), 2) the *Ackers and White* [1973] equation as modified by *Day* [1980] (calculated by individual size class, d_i), 3) the *Bagnold* [1980] equation (calculated by the mode of the subsurface material, d_{mss}), 4) the *Parker* [1990] equation (calculated by d_i), with site-specific hiding functions (paragraph 89 of *Barry et al*., [2004]) and 5) the *Barry et al.* [2004] equation as corrected in *Barry et al*. [in press] (summarized in Appendix 2.1). In each equation, we used the characteristic grain size as originally specified by the author(s) to avoid introducing error or bias. See *Barry et al*. [2004] for further detail of the equations used here.

We examined the performance of these equations in mountain gravel-bed rivers of the western United States studied by *Barry et al*. [2004]. Local discharge records were combined with the above equations to predict the effective discharge and its associated transport rate at each site, and then compared to observed values determined from site-specific rating curves (2.1). The analytical methods are described in detail later in the paper. To improve the accuracy of our analysis, we have only included those sites from *Barry et al*. [2004] where: 1) the observed record of daily mean discharge covers at least 10 years [*Biedenharn et al.,* 2001]; 2) the bed load transport observations were made over a wide range of low to high flows; and 3) the observed bed load transport data were adequately described by equation (2.1) (i.e., where the correlation coefficient (r^2) of the rating curve is greater than 0.70 and there is no obvious non-linearity to the observed transport data in $\log_{10}$ space) [*Nash*, 1994]. Only 22 of the 41 sites examined by *Barry et*

al. [2004] met these criteria and were used in the present analysis. The length of discharge observations at the study sites varies from 10-90 years, and the period of bed load transport observations ranges from 1-13 years (Table 2.1).

Bed load transport rates at these sites were observed across a range of flows from less than 10% to 180% of the 2-year flood (Q_2) (Figure 2.4). However, the maximum discharge for which bed load transport was measured at each site (Figure 2.4, square symbols) is typically less than the maximum discharge of record (Figure 2.4, diamond symbols). Consequently, in calculating the effective discharge, the observed bed load rating curves were extrapolated to flows 2-80% larger (30% on average) than the largest flow for which bed load observations were made. This extrapolation is unavoidable because few high-flow observations of transport are available due to unsafe field conditions during these events. Extrapolation error is likely reduced by our criteria for choosing sites with transport observations made over a broad range of discharges and with rating curves that have strong correlation coefficients ($r^2 > 0.7$).

2.4.2. Site Characteristics

The 22 sites are gravel-bed rivers located in mountain basins of Idaho, Colorado and Wyoming, with hydrographs dominated by snowmelt runoff (see Table 2.1 for a list of the sites and Figure 1 of *Barry et al*. [2004] for site locations). They are single-thread channels with pool-riffle or plane-bed morphology (as defined by *Montgomery and Buffington* [1997]). The stream banks of the study sites are typically composed of sand, gravel and cobbles with occasional boulders and are well vegetated. Median surface grain sizes and channel slopes vary between 38 and 185 mm and 0.0021 and 0.0108,

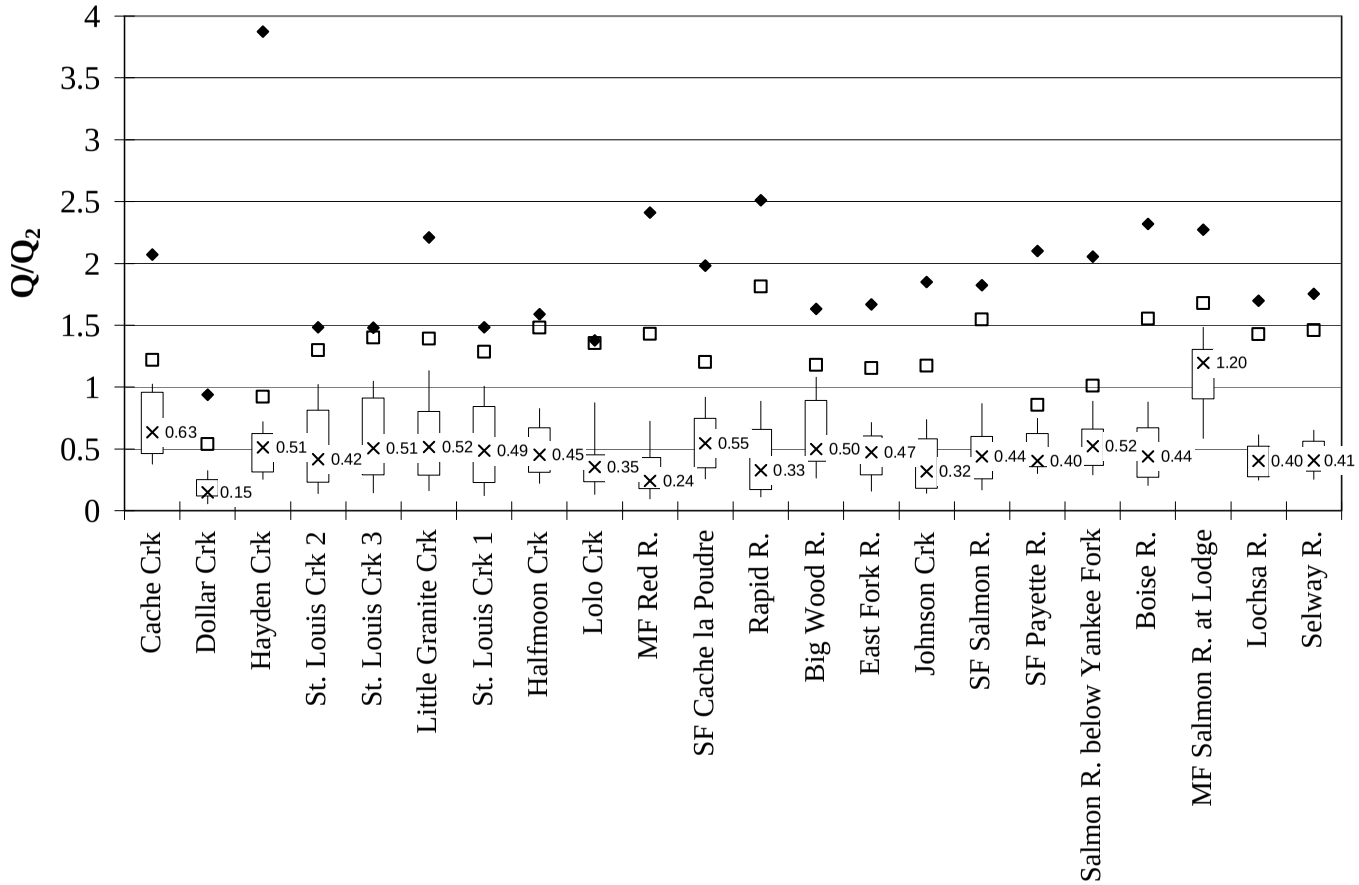

Figure 2.4. Box plots of the range of discharge, relative to Q_2, for which bed load transport was measured at each site. Median values are specified by "X". Upper and lower ends of each box indicate the inter-quartile range (25th and 75th percentiles). Extent of whiskers indicate 10th and 90th percentiles. Maximum discharges during the period of record are shown by solid diamonds, while maximum discharges for bed load transport observations are shown by open squares.

Table 2.1. Predicted and Observed Values of Effective Discharge.

Site	Number of years in discharge/bedload transport record	Observed effective discharge ($m^3 s^{-1}$)	Predicted Effective Discharge ($m^3 s^{-1}$)				
			Meyer-Peter and Müller [1948]	*Bagnold* [1980]	*Ackers and White* [1973]	*Parker* [1990]	*Barry et al.* [2004; in press]
Big Wood River	23/2	39.7	14.4	21.1	21.1	39.7	39.7
Boise River	90/4	175	115	18	127	175	139
Cache Creek	41/1	1.6	3.5	0.3	4.0	4.0	1.6
Dollar Creek	17/5	5.5	5.5	N.A.[a]	7.7	5.5	5.5
East Fork River	54/4	27.3	1.1	1.1	20.8	20.8	27.3
Halfmoon Creek	57/2	5.3	5.3	8.1	5.3	5.3	5.3
Hayden Creek	57/2	4.1	4.1	4.1	4.1	4.1	4.1
Johnson Creek	73/3	58.2	58.2	58.2	58.2	101.1	58.2
Little Granite Creek	11/13	6.52	5.4	5.4	9.4	13.3	6.52
Lochsa River	74/3	486.1	414.1	486.1	486.1	270.1	486.1
Lolo Creek	35/3	9.7	17.0	14.3	11.5	14.3	11.51
MF Red River	35/6	9.7	12.7	21.9	14.8	14.8	9.7
MF Salmon River at Lodge	10/1	362.9	160.3	362.9	227.8	362.9	362.9
Rapid River	88/7	21.2	17.1	3.0	25.2	25.2	21.2
Salmon River below Yankee Fork	67/2	166.5	120.6	97.6	166.5	178	166
Selway River	72/3	677.5	490.6	490.6	490.6	490.6	584
SF Cache la Poudre	23/2	9.0	9.0	11.6	9.0	9.0	9
SF Payette River	60/2	88.4	88.4	142.3	88.4	111.5	111.5
SF Salmon River	29/5	87.0	87.0	177.4	87.0	87.0	73
St. Louis Creek Site 1	69/5	4.9	3.5	3.5	4.9	4.9	4.9
St. Louis Creek Site 2	69/4	4.7	4.7	3.4	4.7	4.7	4.7
St. Louis Creek Site 3	69/4	4.7	4.7	4.7	4.7	4.7	4.7

[a] *Bagnold* [1980] equation predicted zero transport for all discharges in period of record.

respectively. See *Barry et al*. [2004] for complete details of site characteristics and field methods.

2.4.3. Calculating Effective Discharge and Bed Load Transport Rates

Flow frequency distributions at each of the 22 sites were discretized following the tabulation method of *Biedenharn et al*. [2001]. The observed discharges were divided into 25, equal-width, arithmetic discharge bins, with a 26^{th} bin for infrequent extreme events corresponding with the far right-hand tail of the flow distribution (Figure 2.2, curve i). The representative discharge for each interval is taken as the arithmetic mean of each discharge class (Figure 2.2).

The observed total bed load transport rates for each discharge bin (Q_{bi}) is estimated by applying the site-specific rating curve (2.1) developed from the measured total bed load transport data to the arithmetic mean of each discharge bin (Figure 2.2). The product of the total bed load transport rate and flow frequency within each discharge bin ($Q_{bi} \cdot f(Q_i)$) is the total bed load transport estimated for that bin (Φ_i). The effective discharge occurs where this product is maximized, and is taken as the arithmetic mean of that discharge bin. We assume that the transport rate for the average discharge of each bin is representative of the average transport rate across that bin, recognizing that this is an approximation that may not hold if bin sizes are too large, such that $\alpha\overline{Q}^{\beta}$ departs significantly from $\overline{\alpha Q^{\beta}}$.

Predicted values of effective discharge are determined in the same fashion, except with unit bed load transport rates within each discharge bin (q_{bi}) predicted in terms of the original formulations of each of the 5 transport equations [*Barry et al*., 2004; in press] multiplied by flow width (w) to estimate Q_{bi}, rather than in terms of rating-curve

functions. Flow width was determined from site-specific hydraulic geometry relationships. Shear stress and other necessary equation parameters for making these predictions were determined for each discharge following an approach similar to that used by *Barry et al*. [2004].

Other methods of estimating the effective discharge exist that do not require use of discharge bins, such as those presented by *Goodwin* [2004] and *Emmett and Wolman* [2001]. In addition, *Soar and Thorne* [2001] discuss various types of binning methods (e.g., logarithmic discharge intervals). Discharge binning is probably the most common approach used by practioners to estimate effective discharge [e.g., *Biedenharn et al*., 2001; *Soar and Thorne*, 2001], and so is used in this analysis. We have chosen to use arithmetic discharge intervals, rather than logarithmic ones, based on *Soar and Thorne's* [2001] finding that logarithmic binning tends to over-predict the effective discharge.

2.5. Results and Discussion

2.5.1. Estimating Effective Discharge

Figure 2.5 shows box plots of the percent difference between predicted and observed values of effective discharge across the 22 sites using the 5 equations discussed above, with site-specific values reported in Table 2.1. The median prediction error is 0% for all equations (Figure 2.5), indicating that effective discharge predictions may not depend on one's choice of bed load transport equation. However, the standard deviation of the prediction error differs across the equations, ranging from 10% error for the *Barry et al*. [2004; in press] equation to 60% for the *Bagnold* [1980] equation. The prediction errors for the *Ackers and White* [1973], *Meyer-Peter and Müller* [1948] and *Parker* [1990] equations have standard deviations of 40%, 44% and 49%, respectively.

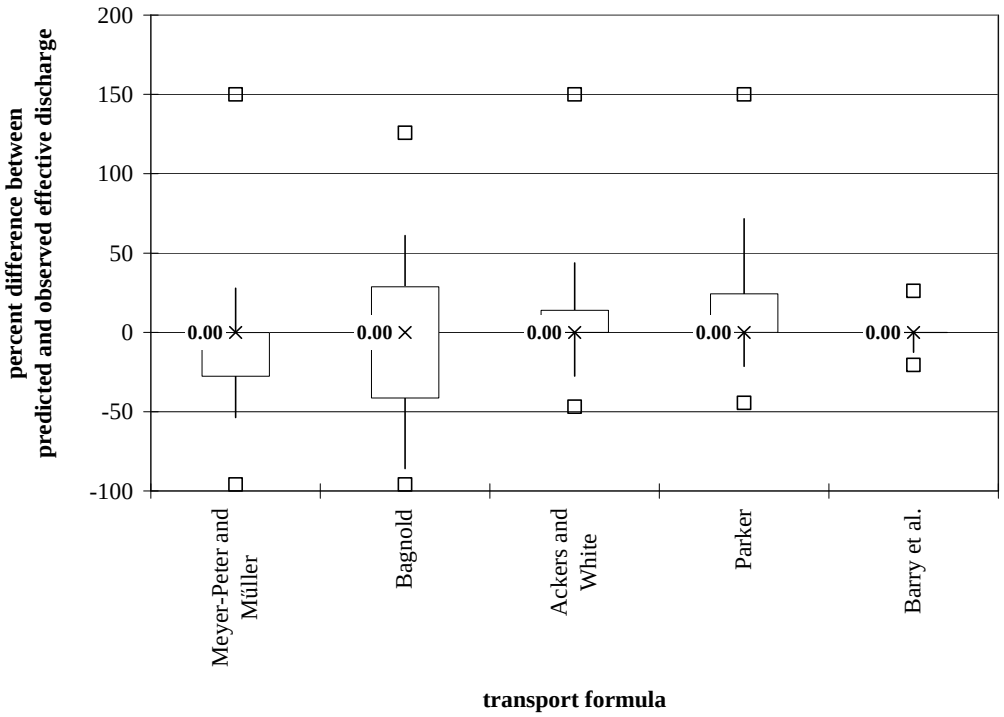

Figure 2.5. Box plots of the percent difference between predicted and observed effective discharge for each transport equation. Median values are specified by "X". Upper and lower ends of each box indicate the inter-quartile range (25^{th} and 75^{th} percentiles). Extent of whiskers indicates 10^{th} and 90^{th} percentiles. Maximum outliers are shown by open squares.

The performance of each equation was also assessed statistically using the methods of *Freese* [1960] and *Reynolds* [1984] to calculate the critical error, e^*, defined here as the percent difference between the predicted and observed effective discharge that one would have to tolerate to accept a given equation at a significance level of 0.05. The critical error is defined as

$$e^* = \sqrt{\frac{196^2}{\chi^2}\sum_{i=1}^{n}\left(\frac{P_i - O_i}{O_i}\right)^2} \tag{2.3}$$

where P_i and O_i are, respectively, the predicted and observed values of effective discharge at a given site, n is the number of observations, here equal to 22 (the number of sites), 196 is the value of the standard normal deviate corresponding to a two-tailed probability of 0.05 multiplied by 100, and χ^2 is the two-tailed chi-squared statistic with n degrees of freedom at a significance level of 0.05.

Values of the critical error, e^*, range from a low of 14% for the *Barry et al*. [2004; in press] equation to between 61% and 85% for the *Ackers and White* [1973] and *Bagnold* [1980] equations, respectively. Critical errors associated with the *Meyer-Peter and Müller* [1948] and *Parker* [1990] equations are 72% and 71%, respectively. These values of e^* differ from the median values of percent error shown in Figure 5 because e^* is more representative of the overall prediction error.

We find that all of the equations examined here provide good estimates of the effective discharge (Figure 2.5, median values), but performance can be quite variable across sites, with some equations performing better than others (Figure 2.5, whisker ranges; and *e** analysis).

2.5.2. Sensitivity of Effective Discharge Prediction to Rating Curve Slope

As shown in Figure 2.3, when using a simple bed load transport rating curve (2.1) to calculate the effective discharge for a given flow record, the predicted value is solely a function of β. As such, we would expect that transport equations with β values larger than the observed value will over-predict the effective discharge (i.e., differences greater than zero in Figure 2.5). Although only the *Barry et al*. [2004; in press] equation is

presented in the form of a rating curve (1) with specified values of β, equivalent rating-curve functions can be developed for the other transport equations examined here if a two-part fit of β is used. A weighted average exponent ($\overline{\beta}$) of the two-part fit can then be compared to observed β values and equation performance can be evaluated within the framework presented in Figure 2.3.

At each of the 22 sites, a weighted-average exponent, $\overline{\beta}$, was calculated for the *Meyer-Peter and Müller* [1948], *Ackers and White* [1973], *Bagnold* [1980] and *Parker* [1990] equations (Table 2.2). To do this, predicted bed load transport rates were plotted as a function of discharge and fitted by (2.1) using a two-part fit of β, one fit to low flows and a second to higher flows. A weighted-average exponent ($\overline{\beta}$) was then calculated as the sum of the two fitted slopes weighted by the proportion of the total bed load transported in each discharge class. To check the accuracy of our weighting procedure, we compared the effective discharge predicted from the original formulation to that predicted from (2.1) with $\overline{\beta}$. The resultant average error is just under 5%, with a standard deviation of 12%. Observed and predicted rating-curve exponents are shown in Table 2.2. Differences between predicted and observed values show that the *Meyer-Peter and Müller* [1948], *Bagnold* [1980], and *Barry et al*. [2004; in press] equations typically under-predict the observed exponent by about 7-12% (Figure2.6, median values). In contrast, both the *Ackers and White* [1973] and *Parker* [1990] equations tend to over-predict the observed exponent by about 16-29% (Figure 2.6, median values).

Table 2.2. Observed α and β Values Compared to Those Determined From Fitting (2.1) to Predicted Transport Rates For Each Equation.

Site	Observed		*Meyer-Peter and Müller* [1948]		*Bagnold* [1980]		*Ackers and White* [1973]		*Parker* [1990]		*Barry et al.* [2004; in press]	
	α (95% Confidence Interval)	β (95% Confidence Interval)	$\overline{\alpha}$ [a]	$\overline{\beta}$ [a]	$\overline{\alpha}$ [a]	$\overline{\beta}$ [a]	$\overline{\alpha}$ [a]	$\overline{\beta}$ [a]	$\overline{\alpha}$ [a]	$\overline{\beta}$ [a]	$\overline{\alpha}$ [a]	$\overline{\beta}$ [a]
Big Wood River	4.86E-06 (2.3E-6 – 1.0E-5)	3.54 (3.26 – 3.82)	0.63*	1.83*	7.70E-3*	2.60*	9.10E-3*	2.91*	5.98E-6	4.32*	1.30E-5*	2.94*
Boise River	1.78E-06 (6.6E-7 – 4.8E-6)	2.86 (2.63 – 3.08)	3.09E-2*	2.12*	0.20*	1.34*	5.76E-4*	2.44*	7.06E-6*	3.19*	3.03E-6	2.57*
Cache Creek	6.00E-04 (4.9E-4 – 7.5E-4)	2.81 (2.40 – 3.22)	0.0517*	4.51*	27.98*	1.67*	3.40E-4*	4.80*	1.08E-5*	5.38*	5.80E-3*	1.67*
Dollar Creek	8.98E-04 (7.0E-4 – 1.2E-3)	2.40 (2.10 – 2.69)	0.195*	3.56*	N.A. [b]	N.A. [b]	1.01E-3	4.36*	3.50E-3*	2.66	5.41E-5*	2.84*
East Fork River	1.20E-03 (5.1E-4 – 2.9E-3)	2.19 (1.88 – 2.51)	0.394*	1.05*	0.102*	1.16*	4.94E-2*	1.54*	0.18*	1.55*	4.00E-4*	1.82*
Halfmoon Creek	1.66E-03 (1.3E-3 – 2.1E-3)	2.82 (2.63 – 3.01)	0.159*	3.65*	5.29E-4*	6.70*	6.50E-4*	3.75*	6.47E-4*	3.81*	8.00E-4*	2.11*
Hayden Creek	6.00E-03 (5.3E-3 – 6.7E-3)	2.36 (2.12 – 2.59)	2.85*	2.29	1.16*	2.00*	0.133*	2.82*	2.83E-3*	3.34*	4.40E-3*	2.30
Johnson Creek	2.84E-07 (1.2E-7 – 6.5E-7)	3.03 (2.79 – 3.27)	0.139*	1.86*	7.42E-3*	2.13*	1.21E-3*	2.41*	1.48E-7	4.68*	1.67E-6*	2.85
Little Granite Creek	3.08E-04 (2.2E-4 – 4.4E-4)	2.93 (2.69 – 3.16)	0.60*	2.30*	1.04*	1.73*	3.98E-3*	3.31*	4.29E-4	3.99*	6.93E-4*	2.10*
Lochsa River	3.04E-11 (2.1E-12 – 4.3E-10)	3.89 (3.40 – 4.38)	8.41E-5*	2.01*	4.33E-7*	4.52*	1.66E-9*	4.38	1.90E-4*	1.86*	5.6E-10*	3.59
Lolo Creek	2.53E-04 (1.6E-4 – 4.1E-4)	1.83 (1.57 – 2.10)	8.49E-6*	7.49*	3.44E-4	4.89*	2.47E-4	2.35*	2.58E-5*	5.00*	1.89E-4	2.23*
MF Red River	3.75E-04 (2.7E-4 – 5.2E-4)	2.38 (2.16 – 2.60)	3.46E-2*	3.88*	5.34E-7*	6.68*	1.14E-4*	3.89*	2.90E-3*	3.53*	4.56E-5*	3.04*
MF Salmon River at Lodge	2.10E-14 (4.7E-16 – 9.4E-13)	5.75 (5.07 – 6.43)	1.95E-2*	2.47*	1.95E-7*	5.06*	6.85E-6*	3.00*	8.03E-12*	6.32	2.78E-9*	3.72*
Rapid River	1.01E-04 (6.3E-5 – 1.6E-4)	2.32 (2.08 – 2.56)	0.279*	2.34	0.32*	1.50*	4.68E-4*	3.26*	6.20E-6*	4.45*	7.46E-5	2.69*

[a] $\overline{\alpha}$ and $\overline{\beta}$ are weighted-average values (see *Estimating Effective Discharge*)

[b] *Bagnold* [1980] equation predicted zero transport for all discharges in period of record.

* Indicates predicted value outside 95% confidence interval.

Table 2.2, continued. Observed α and β Values Compared to Those Determined From Fitting (2.1) to Predicted Transport Rates For Each Equation.

Site	Observed		*Meyer-Peter and Müller* [1948]		*Bagnold* [1980]		*Ackers and White* [1973]		*Parker* [1990]		*Barry et al*. [2004; in press]	
	α (95% Confidence Interval)	β (95% Confidence Interval)	$\overline{\alpha}$ [a]	$\overline{\beta}$ [a]	$\overline{\alpha}$ [a]	$\overline{\beta}$ [a]	$\overline{\alpha}$ [a]	$\overline{\beta}$ [a]	$\overline{\alpha}$ [a]	$\overline{\beta}$ [a]	$\overline{\alpha}$ [a]	$\overline{\beta}$ [a]
Salmon River below Yankee Fork	4.04E-09 (2.6E-10 – 6.2E-8)	3.85 (3.21 – 4.49)	3.70E-3*	2.76*	2.24E-4*	3.16*	2.17E-7*	3.58	5.34E-9	4.86*	6.32E-8	3.40
Selway River	7.05E-13 (5.1E-14 – 9.7E-12)	4.43 (3.97 – 4.88)	3.55E-3*	2.47*	3.46E-5*	2.91*	5.81E-7*	3.12*	7.65E-5*	2.42*	2.6E-10*	3.59*
SF Cache la Poudre	4.11E-04 (2.5E-4 – 6.6E-4)	2.62 (2.38 – 2.86)	0.148*	2.59	2.05E-3*	4.11*	2.68E-3*	2.91*	5.59E-2*	2.43	3.47E-5*	3.21*
SF Payette River	5.97E-07 (9.0E-8 – 4.0E-6)	3.46 (2.98 – 3.93)	1.89E-2*	2.44*	1.90E-7	5.44*	4.08E-6*	3.44	1.87E-6	3.74	2.66E-8*	3.77
SF Salmon River	1.88E-06 (5.7E-7 – 6.2E-6)	3.06 (2.73 – 3.38)	4.34E-5*	3.86*	3.2E-16*	9.19*	6.46E-8*	3.75*	7.84E-5*	2.72*	4.59E-5*	2.14*
St. Louis Creek Site 1	3.39E-03 (2.5E-3 – 4.6E-3)	2.15 (1.88 – 2.41)	2.18*	2.08	0.858*	2.06	1.60E-3	4.06*	2.34E-3	4.44*	1.20E-3*	2.13
St. Louis Creek Site 2	2.25E-03 (1.7E-3 – 3.0E-3)	2.22 (1.94 – 2.50)	0.953*	2.41	0.467*	2.10	1.08E-2*	3.46*	1.95E-2*	2.94*	6.05E-4*	2.64*
St. Louis Creek Site 3	1.13E-03 (8.3E-4 – 1.5E-3)	2.84 (2.58 – 3.11)	1.81*	2.19*	0.234*	2.75	1.59E-2*	3.43*	1.34E-4*	5.09*	3.07E-4	3.20*

[a] $\overline{\alpha}$ and $\overline{\beta}$ are weighted-average values (see *Estimating Effective Discharge*)

[b] *Bagnold* [1980] equation predicted zero transport for all discharges in period of record.

* Indicates predicted value outside 95% confidence interval.

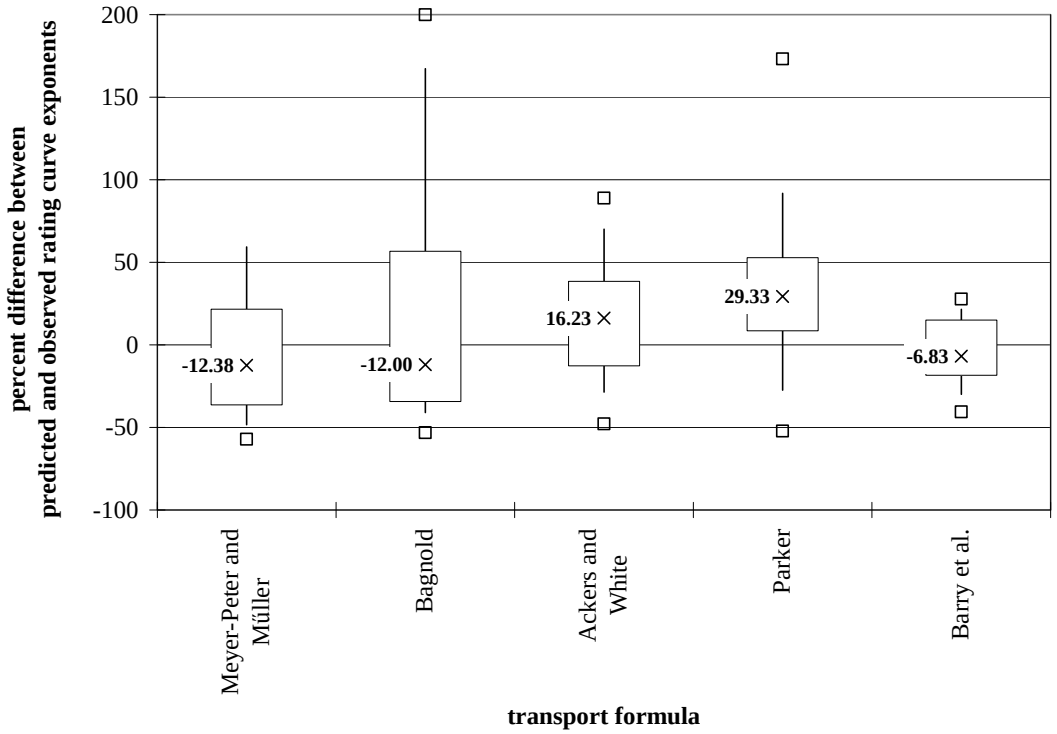

Figure 2.6. Box plots of the percent difference between predicted and observed bed load rating curve exponents for each transport equation. Median values are specified by "X". Upper and lower ends of each box indicate the inter-quartile range (25^{th} and 75^{th} percentiles). Extent of whiskers indicates 10^{th} and 90^{th} percentiles. Maximum outliers are shown by open squares.

As hypothesized, we see a generally increasing linear relationship between errors in the rating-curve slope and errors in the prediction of the effective discharge (Figure 2.7). However, many of the data are insensitive to errors in the rating-curve exponent and cluster along a line of zero error for prediction of effective discharge. This result is due to the characteristics of the underlying flow frequency distribution, which is explored further in Appendix 2.2.

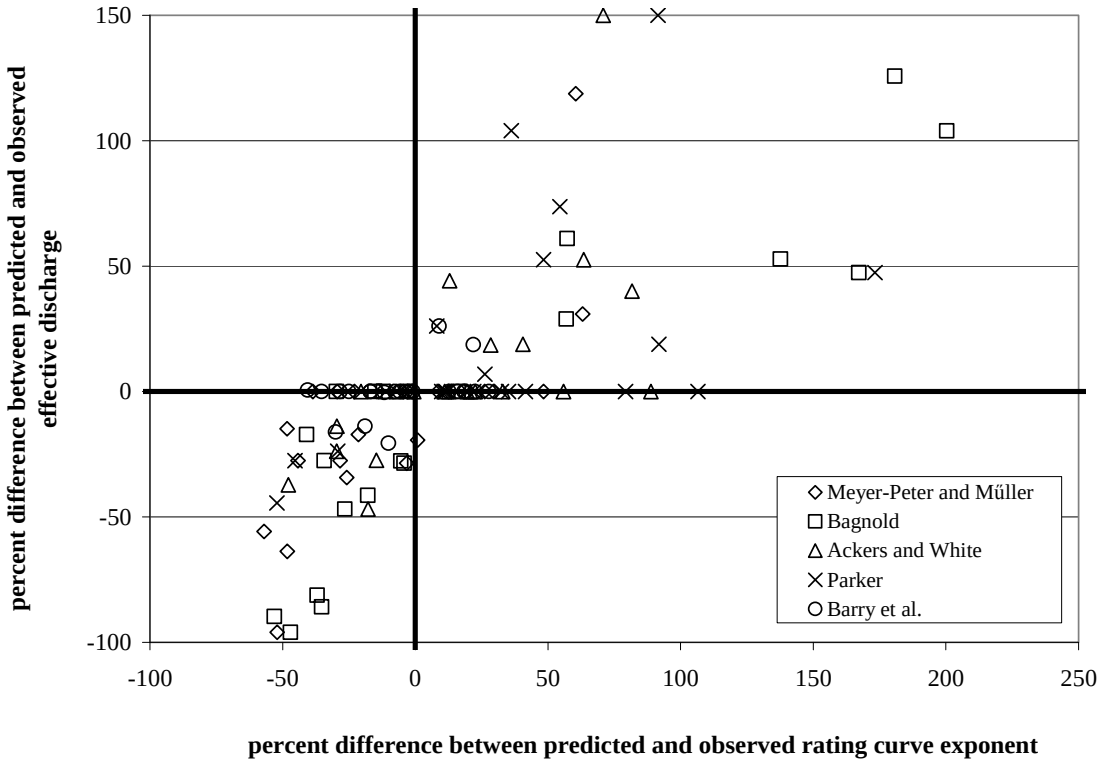

Figure 2.7. Relationship between errors in the predicted rating-curve exponent (Table 2.1) and errors in the predicted effective discharge, both expressed as a percent difference.

2.5.3. Bed load Transport Rate at the Effective Discharge

At each of the 22 sites we compared the predicted bed load transport rates from each equation, as originally formulated, to the observed transport rates at the observed effective discharge. We find that the performance of all 5 equations differs substantially in the accuracy with which they predict bed load transport rate at the observed effective discharge (Figure 2.8). Similar to previous studies [*Gomez and Church*, 1989; *Reid et al*., 1996; *Yang and Huang*, 2001; *Habersack and Laronne*, 2002; *Bravo-Espinosa et al*.,

2003; *Barry et al*., 2004], we find that most equations tend to over-predict. However, performance of a particular equation seems to be site-specific. For example, *Reid et al.* [1996] show the *Bagnold* [1980] equation under-predicting at the Nahal Yatir in Israel, while *Habersack and Laronne* [2002] show it over-predicting at the Drau River in Austria, and *Gomez and Church* [1989] show it having roughly equal probability of over- or under-predicting at their study sites in North America. Similarly, we find that the *Parker* [1990] equation over-predicts bed load transport at our study sites, while it was found to under-predict at study sites in both Austria [*Habersack and Laronne*, 2002] and Israel [*Reid et al*., 1996], but to have equal probability of over- or under-prediction at North American sites examined by *Gomez and Church* [1989; their Figure 2.4]. Consequently, equation performance varies across studies and sites. Furthermore, as discussed earlier, performance can vary with discharge. Our analysis focuses on performance at the effective discharge (a bankfull-like flow), while previous studies report average results across all observed flows, which are numerically biased toward a preponderance of low-flow observations. Hence, some of the discrepancy between studies may be due to the range of discharges used for assessing equation performance.

We also examined the critical error, e^*, in terms of $\log_{10}$ differences between predicted and observed transport rates [*Freese*, 1960; *Reynolds*, 1984]

$$e^* = \sqrt{\frac{1.96^2}{\chi^2} \sum_{i=1}^{n} [\log_{10} P_i - \log_{10} O_i]^2} \qquad (2.4)$$

where P_i and O_i are, respectively, the predicted and observed bed load transport rates for the observed effective discharge at a given site, n is the number of observations (i.e., number of sites), 1.96 is the value of the standard normal deviate corresponding to a two-

tailed probability of 0.05, and χ^2 is the two-tailed chi-squared statistic with *n* degrees of freedom at a significance level of 0.05. Only non-zero predictions are considered here, resulting in the exclusion of one predicted value (Table 2.1, Dollar Creek, Bagnold equation). Results show substantial differences in the amount of error one would have to tolerate to accept a given prediction of the bed load transport rate at the effective discharge. The *Ackers and White* [1973] and *Parker* [1990] equations have e^* values close to 1.75 orders-of-magnitude of error whereas the *Barry et al*. [2004; in press] equation has an e^* value less than 0.8 orders-of-magnitude of error (when discussing orders-of-magnitude, we use $\log_{10}$ units throughout). The e^* values for the *Bagnold* [1980] and the *Meyer-Peter and Müller* [1948] equations are equal to 2.1 and 3.2 orders-of-magnitude of error, respectively.

Accurate prediction of the total bed load transport rate at a given discharge depends on the overall performance of the transport equation and may be sensitive to a variety of factors, including performance of transport threshold functions embedded within the equation, inclusion and accuracy of roughness correction parameters, and degree of equation calibration to site-specific conditions [*Gomez and Church*, 1989; *Barry et al*., 2004]. In terms of bed load rating curves, this performance depends on the accuracy with which a given transport equation is able to reproduce the observed values of both α and β. We used the equivalent bed load rating curves (both $\overline{\alpha}$ and $\overline{\beta}$) fit to the transport values predicted for each equation (Table 2.2) to standardize the various equations and to compare performance in terms of these rating curve values and the Figure 2.3 framework. The *Bagnold* [1980] and *Barry et al.* [2004; in press] equations both have predicted rating-curve slopes similar to the observed value (median errors in

predicted β values of less than -0.056 and -0.032 orders of magnitude (or -12% and -7%), respectively; Figure 2.6, Table 2.2). However, the *Bagnold* [1980] equation over-estimates α with a median prediction error of 2.4 orders-of-magnitude, whereas the *Barry et al*. [2004; in press] equation has a median prediction error of less than -0.13 orders-of-magnitude (Table 2.2). As a result, the *Bagnold* [1980] equation over-predicts bed load transport with a median error of almost 1.3 orders-of-magnitude, whereas the *Barry et al*. [2004; in press] equation has a median prediction error of only -0.3 orders-of-magnitude (Figure 2.8). We also find that the *Ackers and White* [1973] and *Parker* [1990] equations predict β with similar degrees of accuracy (median prediction errors of 0.07 and 0.11 orders of magnitude (or 16% and 29%), respectively; Figure 2.6), however, the *Parker* [1990] equation predicts α more accurately than the *Ackers and White* [1973] equation (median prediction errors of 0.3 and almost 1.0 orders-of-magnitude, respectively). These differences in the relative accuracy of predicted α and β appear to be offsetting, in that both equations tend to over-predict bed load transport at the effective discharge by similar amounts; almost an order-of-magnitude (Figure 2.8).

2.5.4. Potential Error in the Observed Transport Data

The observed bed load rating curves at each site (2.1) are based on measured bed load transport data from either a channel-spanning bed load trap (East Fork River) or Helley-Smith samplers (all other sites). The channel-spanning trap captures essentially all of the bed load in motion, whereas the Helley-Smith samples collect only a subset of the sediment in motion up to the width of the sampler orifice (3 or 6 inches). Because Helley-Smith samples are collected as a series of point measurements of limited duration along a cross section, while bed load transport is a stochastic process in space and time,

Helley-Smith measurements may not accurately sample the bed load population, particularly the coarser sizes that move infrequently [*Wilcock*, 2001]. We assume that there is little error associated with the bed load trap, but we are unable to quantify the

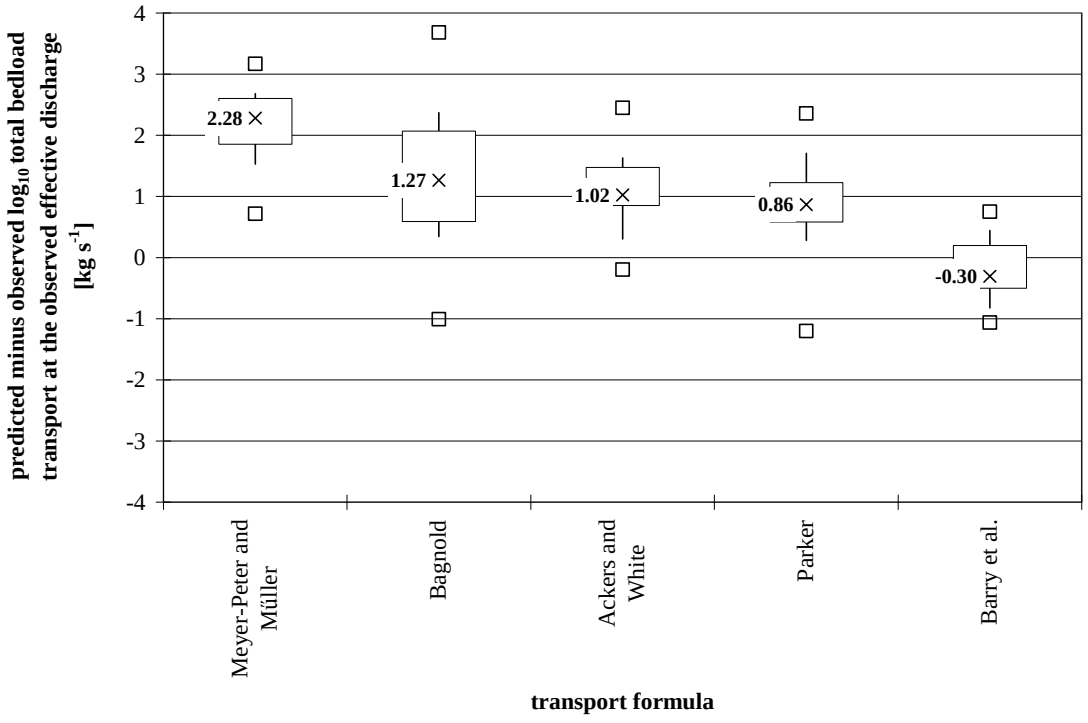

Figure 2.8. Box plots of the difference between predicted and observed $\log_{10}$ bed load transport rates at the observed effective discharge for each transport equation. Median values are specified by "X". Upper and lower ends of each box indicate the inter-quartile range (25^{th} and 75^{th} percentiles). Extent of whiskers indicates 10^{th} and 90^{th} percentiles. Maximum outliers are shown by open squares.

error associated with the Helley-Smith measurements at our study sites (this would require having both bed load trap and Helley-Smith samples at each site, which was not the case).

Habersack and Laronne [2002] did collect paired observations using a 6-inch Helley-Smith sampler and a pit-trap and found that the Helley-Smith sampler gave comparable results. Similarly, *Emmett* [1980] found that the Helley-Smith sampler has near-perfect sediment trapping efficiency for particles between 0.5 mm and 16 mm in size. However, based on a number of simplifying assumptions, *Hubbell and Stevens* [1986] suggest a maximum probable error of 40% when using a Helley-Smith sampler to measure bed load transport. Field studies by *Bunte et al*. [2004] indicate that Helley-Smith samples may overestimate transport rates by 3-4 orders of magnitude at lower flows (< 50% bankfull), but with transport rates converging toward those measured by fixed traps at higher flows. Hence, the two methods should yield comparable estimates of bed load transport at higher flows, which are the focus of this study. However, *Bunte et al*. [2004] show that bed load rating curves for Helley-Smith samples tend to have lower slopes than those of traps. Because effective discharge calculations are sensitive to rating-curve slopes, differences in sampling methods may yield different estimates of the "observed" effective discharge, and thus different results of equation performance when comparing observed versus predicted effective discharges.

Table 2.2 also reports the 95% confidence intervals for observed α and β values determined from (2.1), providing some sense of the uncertainty in the estimates of these values. The uncertainty in the observed rating-curve exponents varies from ±7-17%, while the uncertainty of the coefficient varies from ±2-14%. In contrast, between 70-90% of the predicted $\overline{\beta}$ values and 70-100% of the predicted $\overline{\alpha}$ values fall outside the 95% confidence intervals (Table 2.2 values marked with an asterisk). Despite the error in predicting rating-curve exponents, the predicted values of effective discharge are similar

to the observed effective discharge (Figure 2.5). Conversely, the tendency for predicted $\overline{\alpha}$ values to over-estimate observed rating-curve coefficients results in over-prediction of bed load transport at the observed effective discharge (Figure 2.8).

The length of bed load transport sampling records may introduce an additional source of uncertainty or error in the observed rating curves. For example, bed load transport observations made over a single year will not include any year to year changes in sediment loads [*Nordin*, 1980] and, depending upon when the samples were taken, may not incorporate the effect of annual hysteresis in bed load transport [*Moog and Whiting*, 1998]. At the 22 sites included in this analysis, bed load transport observations were collected over a 1 to 13 year period, with two sites having only a single year of record, and six sites having only two years of record (Table 2.1). However, there is no systematic relationship between length of record and uncertainty in observed β values at our study sites (Table 2.2). Furthermore, because transport observations were collected over a range of flows on both the rising and falling limbs of the spring hydrographs in these snowmelt rivers, any effects of hysteresis are likely included.

2.5.5. Potential Bias with the *Barry et al*. [2004, in press] Equation

Thirteen of the 22 sites included in this analysis were part of the data from which the *Barry et al*. [2004; in press] equation was derived. As a result, the portrayal of the *Barry et al*. [2004; in press] equation as "best", compared to the other transport equations considered here, may be an artifact of having included a number of the calibration data sets in this analysis of equation performance. If we restrict the analysis to the 9 sites not included in the development of the *Barry et al*. [2004; in press] equation, the relative performance of the 5 bed load transport equations shows only slight changes, with the

exception of the *Bagnold* [1980] equation, whose median percent error in predicting the effective discharge decreases from 0% to -17%. However, equation-specific critical errors (e^*) for prediction of the effective discharge do change, with critical errors for both the *Meyer-Peter and Müller* [1948] and the *Bagnold* [1980] equations changing from 72% and 85% to 81% and 57%, respectively. Similarly, the e^* values associated with the *Ackers and White* [1973] and *Parker* [1990] equations change from 61% and 71% to 71% and 82%, respectively. The e^* value associated with the *Barry et al.* [2004; in press] equation changes from 14% to 3%. Similar results are found when only the 9 independent test sites are included in predicting the total transport at the effective discharge. Regardless of whether we use all 22 sites, or the subset of 9 independent sites, the *Barry et al*. [2004] equation performs best for the rivers examined in this study. However, it remains to be seen how this equation performs in other gravel-bed rivers.

The superior performance of the *Barry et al*. [2004; in press] equation also may be due, in part, to the fact that it is expressed as a rating-curve function, similar to that used to describe the observed transport data (2.1). In particular, our estimates of the observed effective discharge and its transport rate may be influenced by the type of transport function fit to the observed data, which in turn could influence differences between observed and predicted values, and thus assessments of equation performance. In addition, the above 9 sites are from physiographic and hydrologic environments similar to those used to develop the *Barry et al.* [2004; in press] equation. Hence, they may not be geomorphically independent and further testing of our equation in different environments is warranted.

2.6. Conclusion

We find that prediction of the effective discharge is not particularly sensitive to the choice of bed load transport equation (at least for those equations and study sites examined here) and that all equations predict the observed effective discharge reasonably well (with median errors of 0%, Figure 2.5). However, equation performance differs both in terms of the range of effective discharge errors (Figure 2.5) and in calculated values of critical error, e^*. Similarly, the accuracy of predicted bed load transport rates at the effective discharge varies with equation selection with most equations over-predicting transport rates by almost 1 to over 2 orders-of-magnitude (Figure 2.8). Only the *Barry et al*. [2004; in press] equation under-predicts bed load transport (by -0.3 orders-of-magnitude) at the effective discharge.

Our finding that the prediction of effective discharge is insensitive to choice of bed load transport equation corroborates the analytical results of *Goodwin* [2004], and suggests that even when the absolute value of sediment transport cannot be predicted accurately, it is possible to determine the channel-forming or effective discharge. Consequently, the selection of an appropriate sediment transport equation depends on the intended application. For example, if the objective is modeling landscape evolution or the effective storage life of a dam, accurate prediction of the magnitude of sediment transport is critical, and therefore more care may be needed in selecting an appropriate transport equation. However, in channel restoration work, estimates of the requisite channel geometry and planform are sometimes obtained from empirical relations based on the effective discharge, rather than the magnitude of sediment transport at different flow conditions. For this case, our analysis suggests that any of the 5 equations examined here would provide a good estimate of the effective discharge on average, for the types of

streams analyzed. The insensitivity of effective discharge predictions to variability of the flow frequency distribution is further discussed in Appendix 2.2, where a relationship is derived that explains stability of effective discharge predictions as a function of discharge bin size, flow frequency, and β.

Although the effective discharge can be used as an index for restoration design, we emphasize that a suite of flows should be considered for successful restoration of physical processes and ecological function of rivers [*Kondolf et al*., 2001; *Buffington and Parker*, 2005; *Doyle et al.,* 2005; *Smith and Prestegaard,* 2005; *Wohl et al*., 2005].

2.7. References

Ackers, P., and, W. R. White (1973), Sediment transport: New approach and analysis, *J. Hydraul. Div., ASCE*, 99, 2041-2060.

Andrews, E. (1980), Effective and bankfull discharge in the Yampa River Basin, Colorado and Wyoming, *J. Hydrol*., 46, 311-330.

Andrews, E. D., and, J. M. Nankervis (1995), Effective discharge and the design of channel maintenance flows for gravel-bed rivers, *Natural and Anthropogenic Influences in Fluvial Geomorphology,* AGU Monograph Series 89, Washington, D.C., 151-164.

Bagnold, R. A. (1980), An empirical correlation of bed load transport rates in flumes and natural rivers, *Proc. R. Soc. London*, 372, 453-473.

Barry, J. J., J. M. Buffington, and, J. G. King (2004), A general power equation for predicting bed load transport rates in gravel bed rivers, *Water Resour. Res*., 40, W104001, doi:10.1029/2004WR003190.

Barry, J. J., J. M. Buffington, and, J. G. King (2005), Reply to Comment By C. Michel On "A General Power Equation for Predicting Bed load Transport Rates In Gravel Bed Rivers", *Water Resour. Res.*, 41, W07016, doi:10.1029/2005WR004172.

Barry, J. J., J. M. Buffington, and, J. G. King (in press), Correction to "A General Power Equation for Predicting Bed load Transport Rates In Gravel Bed Rivers" by Jeffrey J. Barry, John M. Buffington, and John G. King, *Water Resour. Res.*.

Biedenharn, D. S., C. R. Thorne, P. J. Soar, R. D. Hey, and, C. C. Watson (2001), Effective discharge calculation guide, *Int. J. Sediment Res*., 16(4), 445-459.

Bravo-Espinosa, M., W. R. Osterkamp, and, V. L. Lopes (2003), Bed load transport in alluvial channels, *J. Hydraul. Eng.*, 129, 783-795.

Buffington, J.M., and, D. R. Montgomery (1997), A systematic analysis of eight decades of incipient motion studies, with special reference to gravel-bedded rivers, *Water Resour. Res.*, 33, 1993-2029.

Buffington, J. M, and, G. Parker (2005), Use of geomorphic regime diagrams in channel restoration, *EOS, Trans. AGU*, 86(52): Fall Meeting Supplement, Abstract H13E-1359.

Bunte, K., S. R. Abt, J. P. Potyondy, and, S. R. Ryan (2004), Measurement of coarse gravel and cobble transport using portable bed load traps, *J. Hydraul. Eng.*, 130, 879-893.

Carling, P. (1988), The concept of dominant discharge applied to two gravel-bed streams in relation to channel stability thresholds, *Earth Surf. Proc. Landforms*, 13, 355-367.

Day, T. J. (1980), A study of the transport of graded sediments, *Hydraul. Res. Stat. Rep. IT 190*, Wallingford, England, 10.

Dietrich, W.E., J. Kirchner, H. Ikeda, and, F. Iseya (1989), Sediment supply and the development of the coarse surface layer in gravel-bedded rivers, *Nature*, 340, 215-217.

Doyle, M. W., E. H. Stanley, D. L. Strayer, R. B. Jacobson, and, Schmidt, J. C. (2005), Effective discharge analysis of ecological processes in streams, *Water Resour. Res.*, 41, W11411, doi:10.1029/2005WR004222.

Emmett, W. W. (1980), A field calibration of the sediment-trapping characteristics of the Helley-Smith bed load sampler, *U.S. Geol. Surv. Prof. Pap.*, *1139*, 44 pp.

Emmett, W. W. (1984), Measurement of bed load in rivers, in *Erosion and Sediment Yield: Some Methods of Measurement and Modelling*, edited by R. F. Hadley and D. E. Walling, Geo Books, Norwich, U.K., 91-109.

Emmett, W. W., and, M. G. Wolman (2001), Effective discharge and gravel-bed rivers, *Earth Surf. Processes Landforms*, 26, 1369-1380.

Freese, F. (1960), Testing accuracy, *Forest Sci.*, 6, 139-145.

Gilbert, G. K. (1914), The transportation of débris by running water, *U.S. Geol. Surv. Professional Paper 86*, 263 pp.

Gomez, B., and, M. Church (1989), An assessment of bed load sediment transport formulae for gravel bed rivers, *Water Resour. Res.*, 25, 1161-1186.

Goodwin, P. (2004), Analytical solutions for estimating effective discharge, *J. Hydraul. Eng.*, 130(8), 729-738.

Habersack, H. M., and, J. B. Laronne (2002), Evaluation and improvement of bed load discharge formulas based on Helley-Smith sampling in an alpine gravel bed river, *J. Hydraul Eng*., 128(5), 484-498.

Hubbell, D. W., and, H. H. Stevens (1986), Factors affecting accuracy of bed load sampling, Paper presented at 4th Federal Interagency Sedimentation Conference, Subcomm. on Sedimentation, Interagecny Advis. Comm. on Water Data, Las Vegas, Nevada.

Knighton, D. (1998). *Fluvial forms and processes: A new perspective*, Oxford University Press, New York, 400.

Kondolf, G. M., M. W. Smeltzer, and, S. Railsback (2001), Design and performance of a channel reconstruction project in a costal California gravel-bed stream, *Environ. Management*, 28, 761-776.

Leopold, L. B. (1994). *A view of the river*, Harvard University Press, Cambridge, Mass..

Leopold, L. B., M. G. Wolman, and, J. P. Miller (1964). *Fluvial Processes in Geomorphology*, Freeman, San Francisco.

Meyer-Peter, E., and, R. Müller (1948), Formulas for bed-load transport, *Proc., 2nd Meeting of the Int. Association for Hydraulic Structures Research*, pp. 39-64, Int. Assoc. Hydraul. Res., Delft, Netherlands, 39-64.

Montgomery, D. R., and, J. M. Buffington (1997), Channel-reach morphology in mountain drainage basins, *Geol. Soc. Am. Bull*., 109, 596-611.

Moog, D. B., and, J. P. Whiting(1998), Annual hysteresis in bed load rating curves, *Water Resour. Res*., 34, 2393-2399.

Nash, D. B., (1994), Effective sediment-transporting discharge from magnitude-frequency analysis, *J. Geol.*, 102, 79-95.

Nordin, C. F. (1980), Data collection and analysis, in *Application of stochastic processes in sediment transport*, edited by H. W. Shen and H. Kikkawa, Water Resources Publications, Littleton, Colorado, 2-1-2-25.

Parker, G. (1978), Self-formed straight rivers with equilibrium banks and mobile bed. Part 2. The gravel river, *J. Fluid Mech.*, 89, 127-146.

Parker, G. (1990), Surface-based bed load transport relation for gravel rivers, *J. Hydraul. Res.*, 28, 417-436.

Reid, I., D. M. Powell, and, J. B. Laronne (1996), Prediction of bed load transport by desert flash-floods, *J. Hydraul Eng.*, 122, 170-173.

Reynolds, M. R. (1984), Estimating error in model prediction, *Forest Sci.*, 30, 454-469.

Soar, P. J., and C. R. Thorne (2001), Channel restoration design for meandering rivers, *U.S. Army Corps of Engineers ERDC/CHL CR-01-1*.

Smith, R. D., R. C. Sidle, and P. E. Porter. (1993), Effects on bed load transport of experimental removal of woody debris from a forest gravel-bed stream, *Earth Surf. Processes Landforms*, 18, 455-468.

Smith, S. M., and K. L. Prestegaard (2005), Hydraulic performance of a morphology-based stream channel design, *Water Resour. Res.*, 41, W11413, doi:10.1029/2004WR003926.

Vanoni, V. A. (1975), Sediment discharge formulas, *Sedimentation Engineering*, ASCE, New York, 190-229.

Whiting, P. J., J. F. Stamm, D. B. Moog, and, R. L. Orndorff (1999), Sediment-transporting flows in headwater streams, *Geol. Soc. Am. Bull.*, 111, 450-466.

Wilcock, P. R. (2001), Toward a practical method for estimating sediment-transport rates in gravel-bed rivers, *Earth Surf. Processes Landforms*, 26, 1395-1408.

Williams, G. P. (1978), Bankfull discharge of rivers, *Water Resour. Res.*, 14, 1141-1154.

Wohl, E., P. L. Angermeier, B. Bledsoe, G. M. Kondolf, L. MacDonnell, D. M. Merritt, M. A. Palmer, N. L. Poff, and D. Tarboton (2005), River restoration, *Water Resour. Res.*, 41, W10301, doi:10.1029/2005WR003985.

Wolman M. G., and, L. B. Leopold (1957), River floodplains: some observations on their formation, *U. S. Geol. Surv. Prof. Paper 282-C*.

Wolman, M. G., and, J. P. Miller (1960), Magnitude and frequency of forces in geomorphic processes, *J. Geol.*, 68, 54-74.

Yang, C.T., and, C. Huang (2001), Applicability of sediment transport formulas, *Int. J. Sed. Res*., 16, 335-353.

Appendix 2.1. *Barry et al*. [2004; in press] Equation

The *Barry et al*. [2004] equation as modified by *Barry et al*. [in press] is

$$q_b = \alpha(Q/Q_2)^{\beta} = 8.13 \bullet 10^{-7} A^{0.49} (Q/Q_2)^{(-2.45q^*+3.56)} \quad \text{(A2.1)}$$

where q_b is the total bed load transport rate per unit width (kg m^{-1} sec^{-1}), α is parameterized as a power function of drainage area (A, m^2, a surrogate for the magnitude of basin-specific bed load supply), with the units of the drainage area coefficient ($8.13 \bullet 10^{-7}$) dependent on the site-specific regression between α and A (in our case, the units are kg $m^{-1.98}$ s^{-1}), and β is expressed as a linear function of q^* (a dimensionless index of channel armoring as a function of transport capacity relative to bed load supply [*Dietrich et al*., 1989; *Barry et al*. 2004]).

Barry et al. [2004] define q^* as,

$$q^* = \left(\frac{\tau_{Q_2} - \tau_{d_{50s}}}{\tau_{Q_2} - \tau_{d_{50ss}}} \right)^{1.5} \quad \text{(A2.2)}$$

where τ_{Q_2} is the total shear stress at Q_2 calculated from the depth-slope product (ρgDS, where ρ is fluid density, g is gravitational acceleration, D is flow depth at Q_2 calculated from site-specific hydraulic geometry relationships, and S is channel slope) and $\tau_{d_{50s}}$ and $\tau_{d_{50ss}}$ are the critical shear stresses necessary to mobilize the surface and subsurface median grain sizes, respectively, calculated from the Shields equation ($\tau_{d50} = \tau^*_{c50}(\rho_s - \rho)gd_{50}$) where the dimensionless critical Shields stress for mobilization of the median grain size (τ^*_{c50}) is set equal to 0.03, the lower limit for visually-based determination of incipient motion in coarse-grained channels [*Buffington and Montgomery*, 1997].

Appendix 2.2. Sensitivity of Effective Discharge to Flow Frequency Distribution and Number of Discharge Bins

The sensitivity of effective discharge predictions to changes in β (Figure 2.7) is largely determined by the variability of the flow frequency distribution surrounding the effective discharge bin. Moreover, the degree to which the effective discharge (Q_e) shifts to the left or right with changes in β depends on the flow frequency distribution that is used. When Q_e shifts to the left or right, it will move to the next largest Φ_i value of the work distribution (2.2). Work distributions derived from theoretical flow distributions [*Goodwin*, 2004] are smoothly varying, such that the next largest Φ_i values are adjacent to the Q_e bin, causing Q_e to shift one bin to the left or right as β changes. In contrast, observed flow and work distributions are irregular [e.g., *Goodwin*, 2004; his Figures 3 and 4], with the next largest Φ_i value sometimes occurring several bins to the left or right of Q_e, causing Q_e to jump multiple bins with altered β. For example, at our sites we find that the effective discharge typically jumps 4 discharge bins with changes in β when observed flow frequency distributions are used (divided into 26 bins).

It is possible to develop an analytical solution to further explore the sensitivity of effective discharge estimates to changes or errors in the rating-curve slope, β. The total bed load transport rate, Φ, is expressed as

$$\Phi_{L,e,R} = \alpha Q_{L,e,R}^{\beta} f(Q_{L,e,R}) \qquad \text{(B2.1)}$$

where the subscripts *e*, *L*, and *R* respectively indicate values for the effective discharge and those to the left and right of the effective discharge bin. The largest value of β before Q_e shifts to the right (i.e., to a larger discharge bin) occurs when $\Phi_e = \Phi_R$,

$$\alpha Q_e^{\beta} f(Q_e) = \alpha Q_R^{\beta} f(Q_R) \quad \text{(B2.2)}$$

Similarly, the smallest value of β before Q_e shifts to the left (i.e., to a smaller discharge bin) occurs when $\Phi_L = \Phi_e$,

$$\alpha Q_L^{\beta} f(Q_L) = \alpha Q_e^{\beta} f(Q_e) \quad \text{(B2.3)}$$

To allow for the possibility of Q_e shifting more than one discharge bin with changing β, Q_L and Q_R are generalized to Q_{nL} and Q_{nR}, where n is the number of discharge intervals, or bins ΔQ, that Q_e moves, with $Q_{nL} = Q_e - n\Delta Q$, and $Q_{nR} = Q_e + n\Delta Q$. Combining (B2.2) and (B2.3) and solving for β yields an expression describing the minimum and maximum β values before a change in the predicted effective discharge occurs (i.e., shifting Q_e to a neighboring discharge bin)

$$\frac{\log\left(f(Q_e) \big/ f(Q_{nL})\right)}{\log\left(1 - n\Delta Q / Q_e\right)} \le \beta \le \frac{\log\left(f(Q_e) \big/ f(Q_{nR})\right)}{\log\left(1 + n\Delta Q / Q_e\right)} \quad \text{(B2.4)}$$

This equation describes the sensitivity, or robustness, of the predicted effective discharge to changes or errors in the rating-curve slope (β) for a given flow frequency distribution ($f(Q_i)$) and discharge interval (ΔQ). In particular, the minimum and maximum values which β can take before a change in Q_e occurs depend on the flow frequency of the effective discharge relative to that of its neighboring discharge bins ($f(Q_e)/ f(Q_{nL})$ and $f(Q_e)/ f(Q_{nR})$) and on the dimensionless size of the discharge bins ($n\Delta Q/Q_e$). Figure B2.1 shows example plots of the upper and lower limits of β as a function of these parameters for n = 1 (i.e., for shifting Q_e to an adjacent discharge bin). Absolute values of β increase with dimensionless bin size ($\Delta Q/Q_e$), but the predicted range of values which β can take before a shift in Q_e occurs depends on the flow

frequency ratios (both in terms of their magnitude and asymmetry). For example, for a given value of $\Delta Q/Q_e$, the range in β values is smallest when $f(Q_L)/ f(Q_e) = f(Q_e)/ f(Q_R)$, and broader when $f(Q_L)/ f(Q_e) < f(Q_e)/ f(Q_R)$ (Figure B2.1). As such, the variability of the flow frequency distribution about the effective discharge has a strong influence on the allowable range of β values before Q_e shifts to a neighboring discharge bin and, thus, the sensitivity of effective discharge predictions to changes or errors in β (Figure 2.7). As expected, Figure B2.1 also shows that larger flow frequency ratios ($f(Q_L)/ f(Q_e)$, $f(Q_e)/ f(Q_R)$) are required to move the effective discharge to an adjacent bin as values of β increase for a given dimensionless bin size ($\Delta Q/Q_e$). However, smaller dimensionless bin sizes require smaller relative changes in flow frequency about the effective discharge to shift Q_e to a neighboring bin. This suggests that results may be sensitive to the number of discharge bins used. We examined this issue for both observed and theoretical flow frequency distributions.

At our study sites, we find that the number of discharge bins typically has little effect on the effective discharge predictions (at least for the range of bin sizes examined, 6-50) (Figure B2.2a). However, results vary depending on the type of flow distribution used, with fitted theoretical distributions (normal, lognormal, or gamma) typically under-predicting the effective discharge. A gamma distribution results in effective discharge estimates that are most similar to the observed values. We also find that the range of allowable β (difference between maximum and minimum β values before a shift in Q_e occurs, (B2.4)) depends on the number of discharge bins when theoretical frequency distributions are used, but is not a factor for observed flow distributions (Figure B2.2b). Furthermore, the observed flow distributions generally result in broader ranges of

allowable β, explaining the insensitivity of Q_e predictions to errors in β (Figure 2.7). These differences in behavior between observed and fitted theoretical flow distributions likely reflect differences in how the flow frequency ratios ($f(Q_L)/ f(Q_e)$ or $f(Q_e)/ f(Q_R)$) change with bin size and the irregular nature of observed flow frequency distributions compared to theoretical ones.

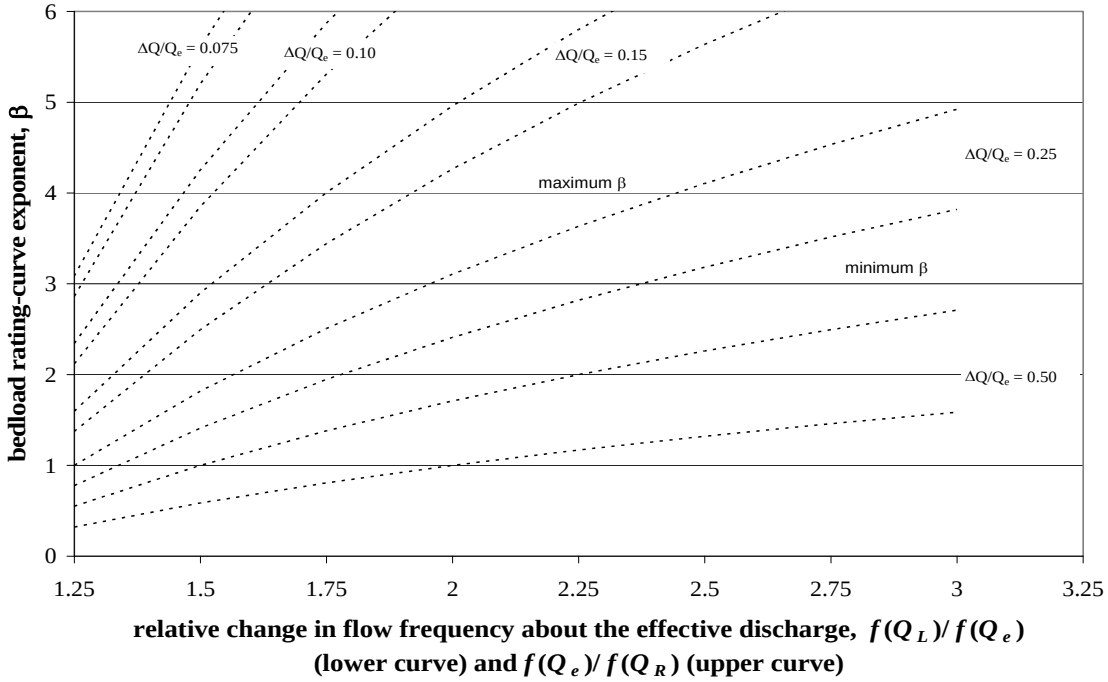

Figure B2.1. Predicted ranges of the bedload rating-curve slope (minimum/maximum β) before the effective discharge (Q_e) shifts to a neighboring discharge bin, expressed as a function of the relative change in flow frequency about the effective discharge ($f(Q_L)/ f(Q_e)$ and $f(Q_e)/ f(Q_R)$, where L and R indicate values for discharge bins to the left and right of the Q_e bin). For plotting convenience we inverted $f(Q_e)/ f(Q_L)$ ratio in (B2.4). Results are stratified by dimensionless bin size used for discretizing the flow frequency distribution ($\Delta Q/Q_e$). Each pair of curves represents maximum and minimum β values determined from solution of the left and right sides of (B2.4), respectively, with n=1.

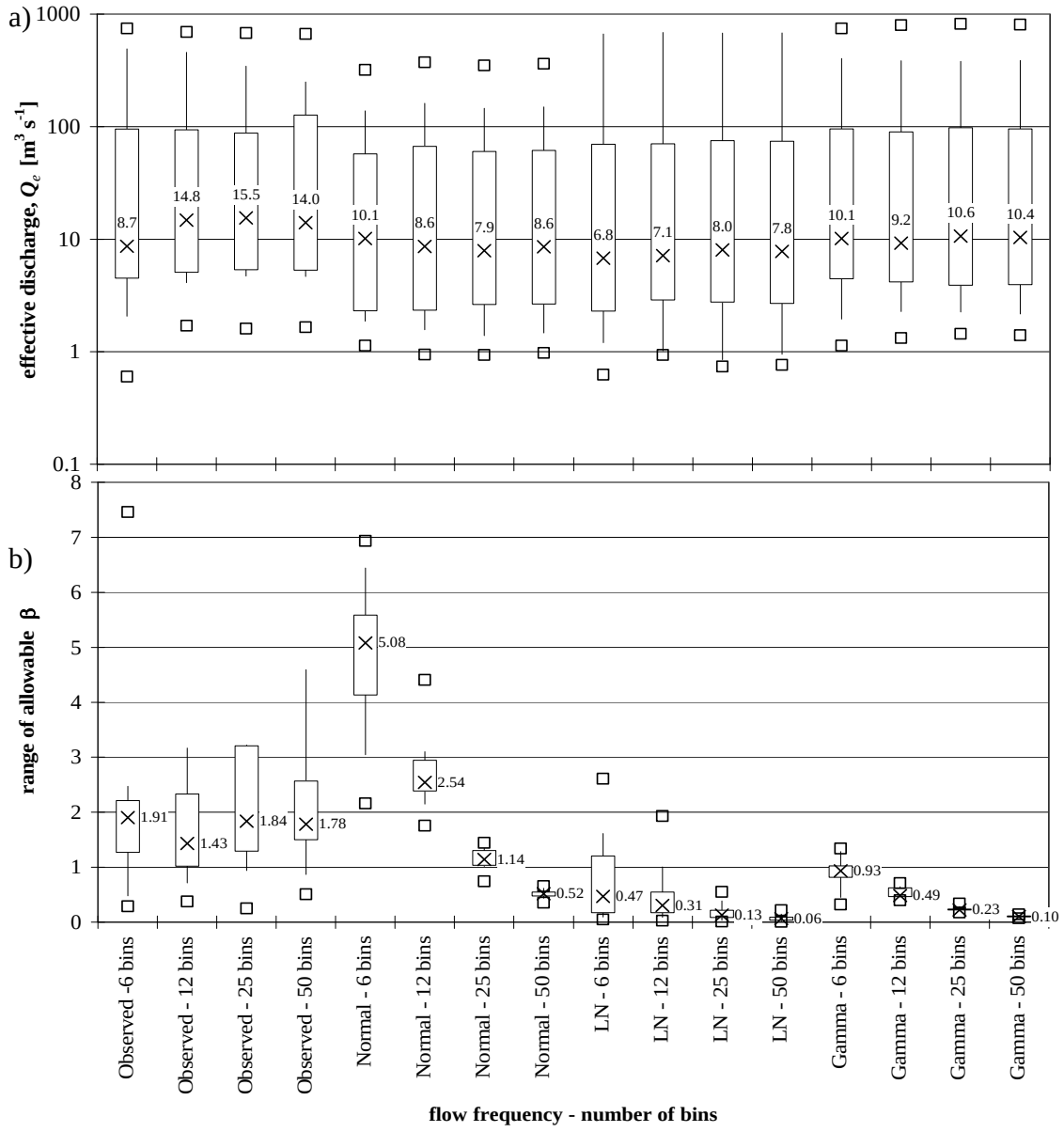

Figure B2.2. Box plots of a) effective discharge and b) the range of allowable β (difference between maximum and minimum values of β before Q_e shifts discharge bins, (B2.4)) at the 22 field sites as a function of the number of discharge bins (6-50) and flow frequency type (observed, normal, log normal, gamma). Median values are specified by "X". Upper and lower ends of each box indicate the inter-quartile range (25th and 75th percentiles). Extent of whiskers indicates 10th and 90th percentiles. Maximum outliers are shown by open squares.

Chapter 3. Identifying Phases of Bed Load Transport: An Objective Approach for Defining Reference Bed Load Transport Rates in Gravel-Bed Rivers [5]

3.1. Abstract

Previous studies have described three phases of bed load transport in armored gravel-bed rivers, though any given river might not demonstrate all three phases. Phase I motion is typically characterized by a low-sloped transport function, representing supply-limited movement of the most easily mobilized grains over a largely immobile armor layer during low flows. Phase II motion exhibits a steeper-sloped function characterized by transport-limited movement of surface and subsurface material during low to moderate flows (depending upon the degree of channel armoring) and is limited by the spatial and temporal variation of excess shear stress (a function of both boundary shear stress and grain size). Phase III motion is characterized by a decline in the slope of the transport function at moderate to high flows, which has several possible interpretations: 1) the channel is nearing transport capacity, 2) the channel has reached bank-full stage, such that additional flow spills onto the floodplain, increasing width rather than depth and transport rate, and 3) all available sediment sources have been accessed by the flow, such that further increases in discharge do not result in large increases in transport.

Here, we use a piecewise regression similar to that of *Ryan et al.* [2002] for objectively identifying transitions between phases of bed load transport observable within plots of dimensionless transport rate (W^*) versus Shields stress (τ^*) [*Parker et al.,* 1982].

[5] Co-authored paper with John M. Buffington, Peter Goodwin, and John G. King.

The approach is applied to data sets from Oak Creek, Oregon, and the East Fork River, Wyoming, providing contrasting physical conditions and transport processes. Oak Creek is a well-armored gravel channel that exhibits Phase I and II transport, while the East Fork River is a poorly-armored, sand-gravel channel that exhibits Phase II and III transport. We find that phase transitions vary by size class and that equal mobility for any given size class (defined as $p_i/f_i \approx 1$, the proportion of a size class in the bed load relative to that of the subsurface [*Wilcock and McArdell*, 1993; *Church and Hassan*, 2002]) can occur during any phase of transport. The identification of phase transitions provides a physical basis for defining size-specific reference transport rates (W^*_{ri}). In particular, the transition from Phase I to II transport may be an alternative to *Parker*'s [1990] constant value of W^*_{ri} =0.0025, and the transition from Phase II to III transport could be used for defining flushing flows or channel maintenance flows.

3.2. Introduction

The surface sediment of many gravel-bed streams is often significantly larger than the subsurface material. This coarse surface material, referred to as the armor layer [*Leopold et al*., 1964; *Parker et al*., 1982], acts as a physical barrier limiting the transport of the finer subsurface material [*Emmett*, 1976; *Jackson and Beschta*, 1982; *Ryan et al*., 2002; *Barry et al*., 2004]. Previous studies indicate that bed load transport in gravel-bed rivers can exhibit up to three phases of transport as a result of the coarse armor layer and the spatial and temporal variability in excess boundary shear stress (Figure 3.1) [*Emmett*, 1976; *Jackson and Beschta*, 1982; *Ashworth and Ferguson*, 1989; *Andrews and Smith*, 1992; *Warburton*, 1992; *Wilcock and McArdell*, 1993, 1997; *Hassan and Church*, 2001; *Church and Hassan*, 2002]. Each phase is briefly introduced here, followed by more

detailed discussion in subsequent paragraphs. Phase I transport is typically characterized by a low-sloped transport curve, consisting of fine sediments traveling over a largely immobile armor layer during low flow [*Jackson and Beschta,* 1982] and may be akin to *Andrews and Smith*'s [1992] marginal transport. Phase II transport exhibits a steeper-sloped function, characterized by partial transport of the surface material (i.e., a portion of the surface grains are immobile while others are in motion [*Wilcock,* 1997; *Wilcock and McArdell,* 1997]) and occurs at low to moderate flows, depending on the size of the surface sediment and the degree of channel armoring [*Jackson and Beschta,* 1982; *Wilcock,* 1997; *Wilcock and McArdell,* 1997]; however, an armor layer is not required for Phase II transport, as discussed below. Phase III motion shows a decline in the slope of the transport function at moderate to high flows. The cause for the Phase II/III transition is uncertain, but may indicate that 1) the flow is transporting sediment near capacity, 2) the flow has reached bankfull stage, with additional discharge spreading across the floodplain, rather than continuing to increase depth and transport rate, and 3) all available sediment sources have been accessed by the flow, such that further increases in discharge do not result in large increases in transport.

In armored channels where the supply of sediment is predominantly controlled by in-stream sources, Phase I transport is limited to the transport of the most easily mobilized grains over a largely immobile armor layer during low flows. In gravel-bed rivers, the Phase I load is often dominated by fine sediment [*Jackson and Beschta,* 1982; *Ryan et al*., 2002]. However, transport of medium-sized particles of high protrusion and low friction angle [*Buffington et al.*, 1992; *Johnston et al.*, 1998] may also be observed

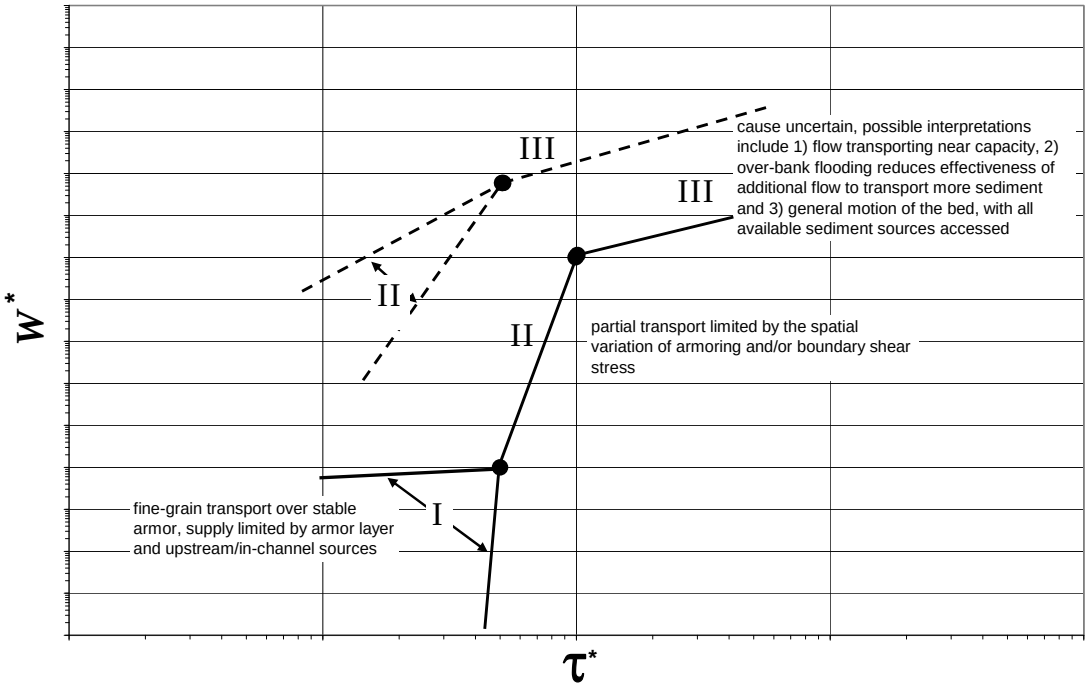

Figure 3.1. Schematic illustration of the phases of bed load transport possible in well-armored (solid lines) and poorly-armored (dashed lines) channels, where W^* is the dimensionless bed load transport rate [*Parker et al.,* 1982] and τ^* is the Shields stress.

during Phase I transport [*Andrews and Smith*, 1992; *Ryan et al*., 2002]. In such channels, the Phase I curve generally has a low slope typical of supply-limited transport (i.e., dimensionless transport rate, W^*, does not vary strongly with Shields stress, τ^*) (Figure 3.1) [*Wilcock* 1997; *Hassan and Church*, 2001]. The slope of the Phase I curve depends on the supply of fine material, with steeper slopes expected for higher supplies or poorly armored channels (Figure 3.1). For example, under conditions of extreme sediment loading, the coarse armor layer may be partially buried by finer material [*Borden*, 2001], which should result in transport-limited motion of the surface fines and a Phase I curve that is steeper than that of Phase II. In this case, the steep Phase I transport will continue

until the supply of fine material has been exhausted, or until the armor layer is mobilized, exposing the subsurface supply and altering the size distribution and mobility of the load. In contrast, Phase I transport should be absent from unarmored channels that, instead, will exhibit initiation of Phase II transport at low discharges, as typically observed for sand-bed channels (Figure 3.1). In unarmored sand-bed channels, the onset of motion typically occurs at lower Shields stresses than in well-armored channels [*Leopold et al.*, 1964; *Milhous*, 1972; *Buffington and Montgomery*, 1997], and the dimensionless transport rates are expected to be orders of magnitude larger than in similarly-sized gravel-bed rivers (Figure 3.1) [*Reid and Laronne*, 1995].

In contrast, Phase II motion is characterized by size-selective movement of bed material limited by the spatial and temporal variation of excess shear stress ($\tau^*/\tau^*_c > 1$, where τ^* is the applied Shields stress and τ^*_{ci} is the critical value for motion of a given particle size). In coarse gravel-bed streams, the surface particles are large enough that the applied Shields stress will not exceed the critical Shields stress until moderate flows [*Parker et al.*, 1982; *Wilcock and Kenworthy*, 2002]. Conversely, in unarmored, sand-bed streams, the applied Shields stress will typically exceed the critical Shields stress of the surface material even during low flows [*Wilcock and Kenworthy*, 2002] (Figure 3.1). The spatial and temporal variation in excess shear stress is a function of both boundary shear stress and grain size. Spatial variability in grain size may be expressed in terms of textural patches [*Paola and Seal*, 1995; *Buffington and Montgomery*, 1999; *Dietrich et al*., 2005] that can cause spatial variability in excess shear stress [*Lisle et al.* 2000], as finer sediment patches are mobilized before coarser ones. The presence of channel armoring may also reduce the areal extent of excess shear stress ($\tau^*/\tau^*_c > 1$) and alter the

timing of bed mobility [*Paola and Seal*, 1995; *Barry et al*. 2004] as discharge increases relative to an unarmored channel, but neither surface patches nor channel armoring are required for Phase II and III transport. Rather, as the discharge increases, the portion of the bed area experiencing excess shear stress expands, mobilizing more of the surface grains [*Wilcock and McArdell*, 1997] and exposing more of the subsurface material to the flow, providing additional sources of sediment for transport. However, the steepness of the Phase II transport relationship is a function of the degree of channel armoring as it regulates the supply of subsurface material [*Emmett*, 1976; *Barry et al.*, 2004]. As such, poorly-armored channels are expected to have lower-sloped Phase II curves than well-armored ones (Figure 3.1).

In well-armored channels, mobilization of the coarse armor layer is delayed (armor breakup occurs at larger flows) relative to a poorly armored channel (armor breakup occurs at smaller flows) and, consequently, is followed by a relatively larger increase in bed load transport rate compared to a similar channel with less surface armoring (Figure 3.1) [*Emmett and Wolman*, 2001; *Barry et al.*, 2004]. Movement of the armor layer exposes the subsurface supply, causing a rapid increase in transport rate and the steep Phase II transport relationship (Figure 3.1) typical of many gravel-bed streams [*Emmett*, 1976; *Jackson and Beschta*, 1982; *Hassan and Church*, 2001; *Church and Hassan*, 2002]. The relative change in slope of the transport function at the Phase I/II transition depends on both the degree of armoring (well-armored channels will produce steeper Phase II curves and a potentially larger contrast in slope between Phase I and II) and the amount of fine surface sediment available for transport (limited supplies of fine sediment will cause relatively shallow Phase I curves, with a potentially larger contrast in

slope) (Figure 3.1). In the case of an unarmored channel, the onset of Phase II transport begins at exceedingly small flows due to the low critical Shields stress required to mobilize the relatively finer surface sediment. The slope of the Phase II curve in unarmored channels is controlled by the supply of sediment and the spatial extent and variability of excess shear stress, such that steeper Phase II curves will occur when there is a readily available source of easily mobilized surface sediment and/or rapid expansion in the areal extent of excess shear stress with increasing discharge.

As suggested by *Hassan and Church* [2001], the relatively rapid increase in sediment transport rate associated with Phase II transport is likely to continue in both armored and unarmored channels as existing sources of sediment are further accessed and as new sources of sediment are mobilized with increasing discharge (i.e., sediment sources higher up on the channel banks or from new areas of the channel bed as the spatial extent of excess shear stress expands). However, once all available sediment sources have been accessed by the flow and conditions of general motion become established across the channel bed, no additional sources of in-channel sediment will be available for transport. We hypothesize that at this point the relatively rapid increase in transport rate seen during Phase II will slow, yielding the lower-sloped Phase III curve (Figure 3.1). The transition from Phase II to III transport is likely to occur sooner in an unarmored channel, as compared to an armored channel, due to more rapid expansion of the areal extent of excess shear (Figure 3.1).

An alternative (or perhaps complementary) explanation for the decrease in slope associated with Phase III transport may be that the channel is nearing transport capacity. Consequently, increasing discharge is no longer accompanied by rapid increases in the

transport rate. The decrease in slope at the Phase II/III transition may also be due to over-bank flooding. That is, once a channel reaches bankfull conditions, additional discharge tends to flow onto the floodplain increasing the width rather than the flow depth and transport rate.

Observed kinks in transport functions have been used by many authors to define phases of bed load transport [*Paintal*, 1971; *Wilcock*, 1997; *Wilcock and McArdell*, 1997; *Hassan and Church*, 2001; *Ryan et al.*, 2002]. However, identifying the transition from one phase of motion to another is imprecise and often occurs over a range of flows [*Wilcock*, 1997; *Wilcock and McArdell*, 1997; *Ryan et al.*, 2002]. The purpose of this paper is threefold: (1) to present an objective method for defining phases of bed load transport, (2) to apply this method to two contrasting field sites, and (3) to test the performance of the *Parker* [1990] equation using the identified Phase I/II transition as an alternative definition of the reference dimensionless transport rate, $W^*_{r.}$

3.3. Study Sites

We use bed load transport data from Oak Creek, Oregon [*Milhous*, 1973] and East Fork River, Wyoming [*Emmett*, 1980; *Leopold and Emmett*, 1997] for our analysis because they represent two well known data sets collected using channel-spanning traps, avoiding potential errors associated with point samples of sediment transport that are of limited spatial and temporal extent [*Wilcock*, 1992; *Hassan and Church*, 2001]. We have limited the Oak Creek data to those collected during the winter of 1971 based on *Milhous'* [1973] observation that these were the highest quality data collected at this site. These two channels also provide contrasting physical conditions that are expected to lead to differences in the phases of bed load transport observed at each site. Oak Creek is a

coarse gravel-bed stream (median surface grain size, d_{50s}, of 53 mm) with a wide range of particle sizes (sand to large cobble) and an armoring ratio (d_{50s}/d_{50ss}) of 2.65 (where d_{50ss} is the median subsurface particle), while the East Fork River site is located at the sand/gravel transition with a bed material made up primarily of sand ($d_{50s} \approx 1.3$ mm) and is essentially unarmored. The channel slopes of the Oak Creek and East Fork River sites also differ (0.0095 and 0.0007, respectively), as do their respective drainage areas (7 km^2 and 466 km^2). However, the bed load transport observations were made over similar ranges of flow at the two sites (about 1-110% of the 2-year flood (Q_2), which is typically a bankfull-like flow [e.g., *Barry et al*., 2004]).

3.4. Methods

3.4.1. Identifying the Transition from Phase I to Phase II Transport

We identify grain size-specific phase shifts in bed load transport within *Parker et al.*'s [1982] framework of dimensionless transport rate (W^*_i) versus Shields stress (τ^*_i) and test the performance of the *Parker* [1990] equation using the identified Phase I/II shifts as an alternative definition of the reference dimensionless transport rate, W^*_r

$$\tau^*_i = \frac{\tau_0}{\rho g R d_i} \tag{3.1}$$

$$W^*_i = \frac{q^*_{bi}}{\tau^{*1.5}_i} = \frac{Rq_{bi}}{f_i \sqrt{g}(DS)^{1.5}} \tag{3.2}$$

$$q^*_{bi} = \frac{q_{bi}}{f_i \sqrt{R g d_i} d_i} \tag{3.3}$$

where g is gravitational acceleration; S is the channel slope; d_i denotes the mean particle size for a given size range; q^*_{bi} represents the Einstein bed load parameter for the ith grain size range; q_{bi} is the volumetric bed load rate per unit width for the ith grain size

range; f_i denotes the fraction of the subsurface material for the *i*th size class; τ_0 is the boundary shear stress determined from the depth-slope product; *D* is the mean flow depth; and *R* denotes the submerged specific gravity of sediment ((ρ_s/ρ)-1, where ρ_s and ρ represent the density of sediment and water, respectively).

Parker et al. [1982] used *Milhous'* [1973] bed load measurements to describe the relationship between Shields stress (τ^*_i) and dimensionless transport rate (W^*_i) by size class. They limited their analysis to data collected during the winter of 1971 and at discharges greater then 1 $m^3 s^{-1}$, corresponding with the break up of the armor layer at Oak Creek [*Milhous*, 1973]. Figure 3.2 shows both the truncated data set (solid symbols, $Q > 1$ $m^3 s^{-1}$) and the full data set (solid and open symbols) for the winter of 1971.

From these relationships, *Parker et al.* [1982] identified a low reference dimensionless transport rate, arbitrarily chosen as $W^*_r = 0.0025$, for all grain sizes on the channel bed. They identified the corresponding reference Shields stress for each size class, τ^*_{ri}, at $W^*_r = 0.0025$ and developed the hiding function

$$\tau^*_{ri} = 0.0876 \cdot \left(\frac{d_i}{d_{50ss}} \right)^{-0.982} \tag{3.4}$$

and a bed load transport function, $G(\phi_i)$, modified by *Parker* [1990] as

$$G(\phi_i) = \begin{cases} 5474\left(1 - \dfrac{0.853}{\phi_i}\right)^{4.5} & \phi_i > 1.59 \quad (3.5a) \\ \exp\left[14.2(\phi_i - 1) - 9.28(\phi_i - 1)^2\right] & 1 \le \phi_i \le 1.59 \quad (3.5b) \\ \phi_i^{14.2} & \phi_i < 1 \quad (3.5c) \end{cases}$$

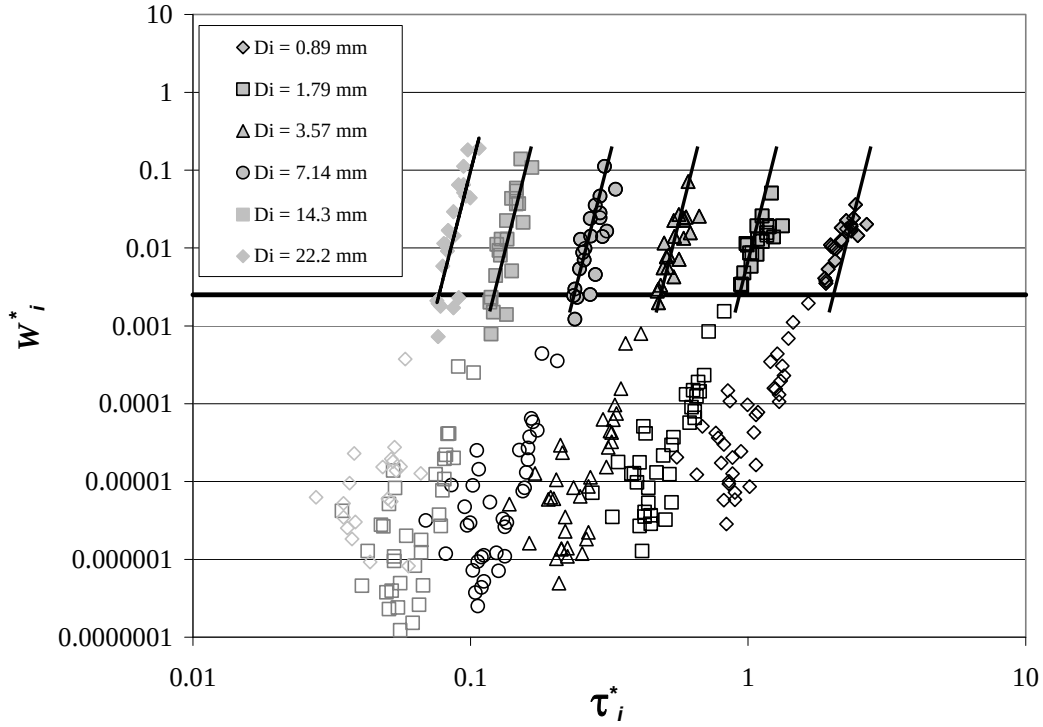

Figure 3.2. Dimensionless bed load transport rate (W^*_i) versus Shields stress (τ^*_i) for six grain-size classes, showing the truncated (solid points) and complete dataset for the winter of 1971 (solid and open points) at Oak Creek [*Milhous*, 1973]. Also shown, is *Parker*'s [1990] reference dimensionless transport value $W^*_r = 0.0025$ (horizontal line) and his bed load function for $\phi_i > 1$ (angled lines, equation (3.5b)).

where d_{50ss} is the median subsurface grain size, ϕ_i is the ratio of the applied Shields stress (τ^*_i) to the reference Shields stress (τ^*_{ri}). We interpret the three-part equation in (3.5) as representing Phase III, II and I transport, respectively. The second part of (3.5) was fit by *Parker et al.* [1982] to the observed Oak Creek data collected at discharges greater than 1 $m^3 s^{-1}$, but the first and third parts are assumed extensions of other transport equations [*Parker et al.*, 1982; *Parker*, 1990]. Because no transport observations were collected at $\phi_i > 1.59$ the first part of (3.5) is based on an extension of the *Parker* [1979] equation,

derived from experimental and field data from *Peterson and Howells* [1973], and matched to the second part of (3.5) at $\phi_i = 1.59$. The choice of a power law for the third part of (3.5) ($\phi_i < 1$) was based on work of *Proffitt and Sutherland* [1983] and *Paintal* [1971]. The exponent of 14.2 was selected such that the second and third parts of (3.5) match continuously at $\phi_i = 1$ and is very similar to the value obtained by *Paintal* [1971] at very low transport rates.

When the complete Oak Creek data set is considered, transitions, or kinks, in the transport relationships are observed at much lower dimensionless transport values (W^* near 0.00001) than *Parker et al.*'s [1982] value of $W^*_r = 0.0025$ (Figure 3.2). In addition, the kinks appear to vary by particle size. We propose that identifying the kinks in these plots of τ^*_i versus W^*_i provides an objective and physically-based method for selecting the reference dimensionless transport rate associated with the Phase I/II transition, $W^*_{ri\mathrm{II}}$, and, therefore, an alternative method for defining the corresponding reference Shields stress, $\tau^*_{ri\mathrm{II}}$.

Similar to the approaches used by *Paintal* [1971], *Hassan and Church* [2001] and *Ryan et al.* [2002], we use a two-piece model to describe the segmented τ^*_i - W^*_i relationship observed in Figure 3.2. We assume that the τ^*_i - W^*_i relationship is a continuous power function across the full range of observed τ^*_i values. The location of the transition between Phase I and II transport was selected to maximize the correlation coefficient (r^2) [*Ryan et al.*, 2002; *Ryan and Porth*, 2007]. Other methods for identifying the location of the phase shifts are available, such as fitting the regression lines by eye or using the method described by *Mark and Church* [1977] for optimizing regressions, and might produce different results.

3.4.2. Identifying the Transition from Phase II to Phase III Transport

Similar to the identification of the Phase I/II transition, we identify the reference dimensionless transport rate at the transition from Phase II to III transport, $W^*_{ri\mathrm{III}}$, and the associated reference dimensionless Shields stress, $\tau^*_{ri\mathrm{III}}$, by identifying the upper kink in the τ^*_i - W^*_i relationship (Figure 3.1). Identification of this flow could assist in selecting those discharges necessary for channel maintenance or flushing flows [*Reiser et al.*, 1989; *Whiting*, 1998; *Ryan et al.*, 2002] since it potentially represents a discharge that mobilizes the entire channel bed.

3.5. Results and Discussion

3.5.1. Phase I to II Transport

Results show that the reference dimensionless transport rate for the onset of Phase II transport, $W^*_{ri\mathrm{II}}$, varies by size class and is significantly less than the value proposed by *Parker et al.* [1982] ($W^*_r = 0.0025$) (Figure 3.3). We find that the onset of Phase II transport at Oak Creek occurs at flows between 0.27 and 0.51 $m^3 s^{-1}$, depending upon the grain size. These results suggest that breakup of the armor layer begins at discharges between 10 - 20% of Q_2. By comparison, *Milhous* [1973] observed the breakup of the surface layer did not begin until flows over 1 $m^3 s^{-1}$, or about 35% of Q_2. Both values are substantially less than observations made by *Ryan et al.* [2002] who identified the onset of Phase II transport around 60-100% of the bankfull discharge at 12 coarse-grained rivers in Colorado and Wyoming using an approach similar to ours. *Mueller et al.* [2005], using a different method, found that the discharge associated with the reference Shields stress, Q_r, at 35 gravel-bed rivers averaged 67% of the bankfull discharge (Q_b) (varied from 21% to 123% of Q_b).

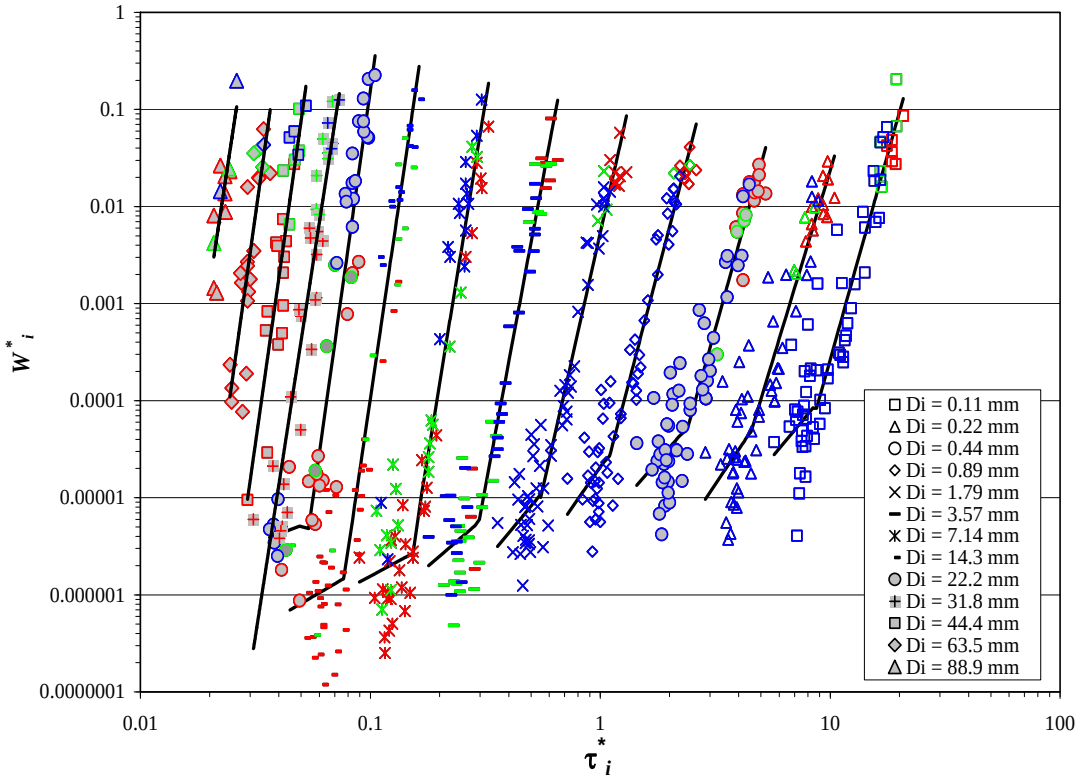

Figure 3.3. Dimensionless bed load transport rate (W^*_i) versus Shields stress (τ^*_i) for example size ranges at Oak Creek, showing our two-part regression of the data for identifying phases of bedload transport. Symbols highlighted with red indicate transport ratios (p_i/f_i) [*Wilcock and McArdell*, 1993] < 0.8; symbols highlighted with green indicate $0.8 \leq p_i/f_i \leq 1.2$; symbols highlighted with blue indicate $p_i/f_i > 1.2$. For clarity, not all of the smaller size classes are shown; however, their behavior is similar to those size classes that are shown.

The fact that Oak Creek exhibits a Phase I/II transition at lower flows than other gravel-bed rivers may indicate that the site is anomalous, as has been suggested in other investigations [*Buffington and Montgomery*, 1997; *Wilcock and Kenworthy*, 2002].

Therefore, caution should be used when applying results from these data to other gravel-bed rivers. However, the Oak Creek site is also relatively unique in that the bed load data were collected using a channel-spanning trap that avoids many of the potential sampling errors associated with point measurements (i.e., Helley-Smith samples) commonly used in bed load transport studies. Sampling errors may arise because bed load transport is a stochastic process in space and time, but Helley-Smith samples are collected as a series of point measurements of limited duration along a cross section. As a result, point measurements may not accurately sample the bed load population, particularly the coarser sizes that move infrequently [*Wilcock*, 2001].

The Oak Creek data also show a systematic decline in the slope of the Phase I curves with increasing grain size as one moves from right to left across Figure 3.3. As discussed in Section 3.2, the slope of the Phase I curve depends on the supply of bed load material, with steeper slopes expected for higher supplies. Hence, Figure 3.3 suggests a higher supply of fine grains than coarse ones during Phase I transport, as is commonly observed in bed load studies.

Because the data do not show a transition to Phase III transport, we conclude that either complete mobilization of the channel bed did not occur over the range of observed flows or that the channel did not reach transport capacity. The first possibility cannot be evaluated because data regarding the areal extent of bed mobilization are not available at Oak Creek. However, work by *Haschenburger and Wilcock* [2003] in Carnation Creek suggest that complete mobilization of the channel bed in coarse gravel-bed rivers may require flows >120% Q_2; in comparison, flows at Oak Creek only reached 110% Q_2.

The second possibility (flows below transport capacity) can be assessed using plots of unit total bed load transport rate versus unit stream power (Figure 3.4). An increase in unit total bed load transport rate with unit stream power indicates increasing transport efficiency [*Bagnold*, 1973; *Leopold and Emmett*, 1976; *Reid and Laronne*, 1995; *Gomez*, 2006] and this increase in efficiency is likely to continue until the flow approaches capacity and/or is transporting near its maximum potential efficiency *Gomez* [2006]. The maximum potential efficiency, as defined by *Gomez* [2006], is a function of sediment size and represents the maximum transport rate for a given unit stream power in the absence of constraints on the availability and supply of sediment and is likely synonymous with transport capacity. The maximum potential efficiency is always less than 100% given the losses and inefficiencies inherent in the transfer of energy and momentum from the fluid to the solid bed material [*Gomez*, 2006]. Once the flow is at capacity and/or transporting at maximum efficiency, we expect the bed load transport rates to level off [*Leopold and Emmett*, 1976] which is an alternative explanation for the Phase II/III transition.

At Oak Creek, we observe a rapid increase in transport efficiency with unit stream power to a maximum transport efficiency of less than 1% (Figure 3.4). However, we do not see a leveling off in efficiency. Furthermore, even at flows greater than Q_2, Oak Creek is still transporting sediment with an efficiency much less that the maximum potential efficiency of approximately 10%, as defined by *Gomez* [2006]. This suggests that the observed sediment transport rates in Oak Creek were not at capacity nor were the flows transporting sediment near their potential efficiency even at flows above Q_2 [*Gomez*, 2006].

A third explanation for the lack of Phase III transport at Oak Creek is that flows did not reach bankfull. However, since the bankfull stage at Oak Creek has not been reported, the influence of over-bank flows on transport capacity and the shape of the τ^*_i - W^*_i relationship is unknown.

A final issue is the relationship between phases of transport and equal mobility. There are numerous definitions of equal mobility, including (1) all particle sizes sharing the same critical shear stress for motion [*Parker et al.*, 1982], and (2) particle sizes moving in proportion to their availability [*Parker et al.*, 1982; *Wilcock and McArdell*, 1993]. We examine the latter, defining size-specific mobility in terms of the transport ratio, p_i/f_i, (where p_i and f_i are the proportions of a given size class within the bed load and subsurface material, respectively) [*Wilcock and McArdell*, 1993; *Church and Hassan*, 2002]. Values of p_i/f_i equal to one indicate equal mobility, while values less than one indicate under-representation (deposition) of a given size class, and values greater than one indicate over-representation (erosion). We find no systematic relationship between transport ratio and transport phase at Oak Creek (Figure 3.3). Furthermore, we find that transport ratios indicative of equal mobility (defined here as p_i/f_i, = 0.8-1.2) can occur during any phase of transport (Figure 3.3), with no indication that the transport ratios tend toward 1 with increasing Shields stress, nor that equal mobility is more likely during initial motion, as has been previously suggested [*Buffington et al.*, 1992].

3.5.2. Phase II to III Transport

Similar analyses for the East Fork site show an absence of Phase I transport (Figure 3.5), which is expected because the channel is unarmored and the fine-grained

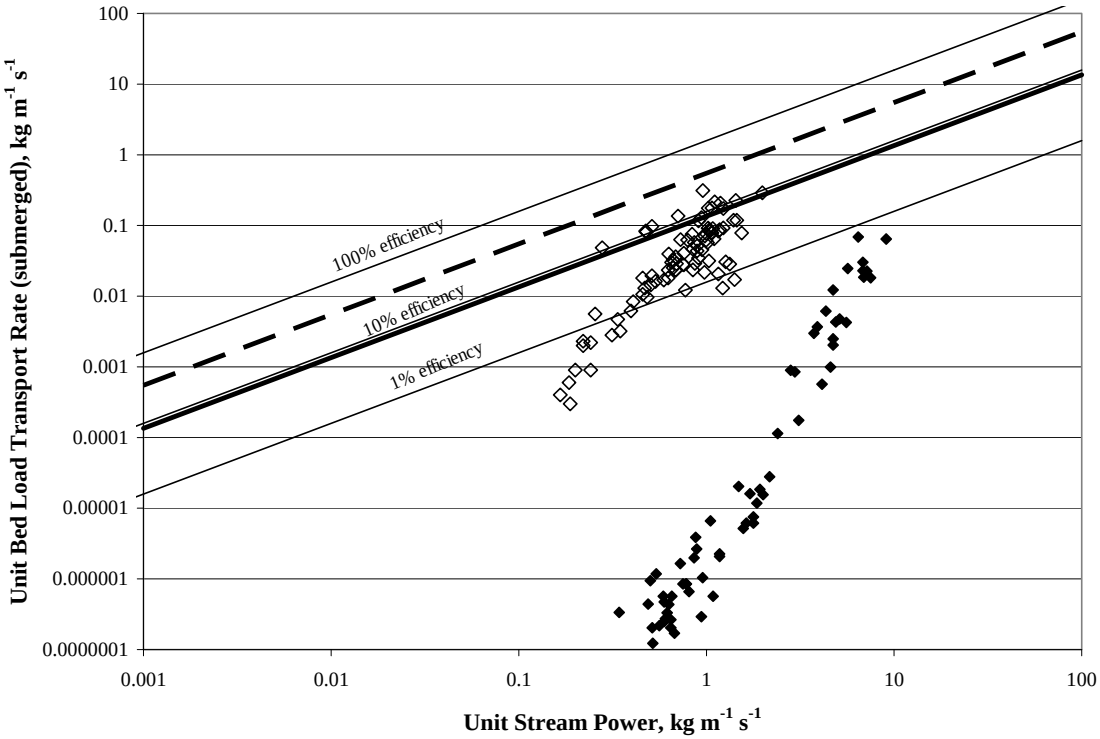

Figure 3.4. Unit total bed load transport rate versus unit stream power at Oak Creek (solid diamonds) and East Fork River (open diamonds). Selected levels of percent bed load transport efficiency are also shown [*Bagnold*, 1973; *Leopold and Emmett*, 1976; *Reid and Laronne*, 1995; *Gomez*, 2006]. Thick solid and dashed lines are the maximum transport efficiencies likely to occur at Oak Creek and East Fork, respectively [*Gomez*, 2006].

nature of the streambed provides a ready source of mobile sediment during all flows. In such fine-grained streams, partial transport is the general state of motion during low to moderate flows, with transport rates controlled solely by the aerial extent of excess shear stress, rather than a limiting armor layer. We interpret the observed kinks in the τ^*_i - W^*_i relationship at the East Fork site as representing the transition from Phase II to III transport. This transition to Phase III transport occurs at a flow near 9.0 $m^3 s^{-1}$, or 25% of

Q_2. This is a marked contrast to Oak Creek, which did not exhibit Phase III transport even at flows > 110% of Q_2. A series of marked sand particles placed across the channel bed at the East Fork site indicate that complete mobilization of the channel bed occurred at a flow that was approximately 80% of Q_2 [*Leopold and Emmett*, 1997]. However, because similar observations of bed mobilization were not made at lower flows, we are unable to determine it complete mobilization of the channel bed also occurred at the Phase II/III transition (9.0 $m^3 s^{-1}$, or 25% Q_2). Furthermore, because the observed Phase II/III transition occurs at flows significantly less than Q_2 we conclude it is un-related to over-bank flooding.

We also consider the effect of transport capacity as an alternative explanation for the Phase II/III transition. As at Oak Creek, the East Fork River data exhibit an initially rapid increase in transport efficiency with unit stream power (Figure 3.4). However, the East Fork River is much more efficient at transporting sediment, with an average efficiency of 4% compared to 0.05% at Oak Creek, and with much higher unit bed load transport rates. Unlike the Oak Creek data, the East Fork River observations begin to level off at values of unit stream power near 0.5 kg $m^{-1} s^{-1}$, corresponding with a discharge of approximately 11 $m^3 s^{-1}$ (slightly larger then the Phase II/III transition at 9.0 $m^3 s^{-1}$), which suggests that the Phase III curve at East Fork may be a transport capacity phenomenon.

The East Fork data also show a systematic decrease in the slopes of the Phase II transport curves with increasing grain size (moving from right to left in Figure 3.5), suggesting a lower supply of coarser particle sizes. This result seems to contrast with the Oak Creek findings, where the Phase II transport curves appear sub-parallel to one

another and indicate similar supplies of different particle sizes (Figure 3.3). The difference in behavior may reflect differences in armoring between the two sites and the effect of the armor layer in regulating the supply of particles, but further investigation of this issue is needed.

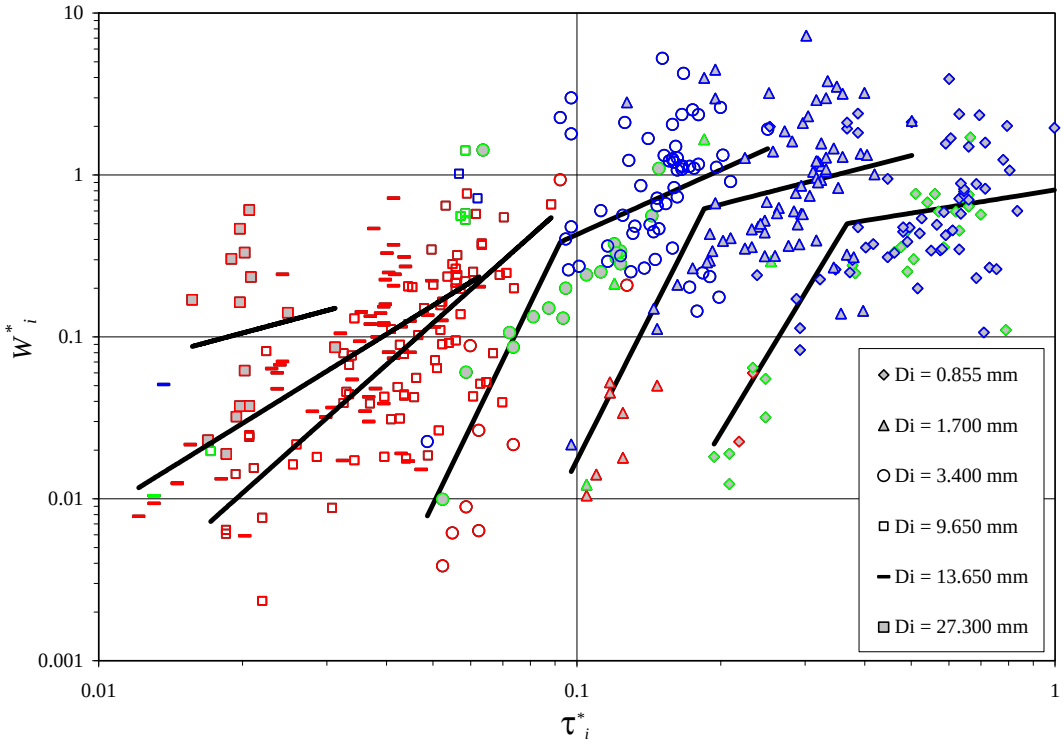

Figure 3.5. Dimensionless bed load transport rate (W^*_i) versus Shields stress (τ^*_i) for example size ranges at East Fork River, showing our two-part regression of the data for identifying phases of bedload transport. Symbols highlighted with red indicate transport ratios (p_i/f_i) [*Wilcock and McArdell*, 1993] < 0.8; symbols highlighted with green indicate $0.8 \leq p_i/f_i \leq 1.2$; symbols highlighted with blue indicate $p_i/f_i > 1.2$. For clarity, not all of the smaller size classes are shown; however, their behavior is similar to those size classes that are presented.

Again we find that transport ratios indicative of equal mobility (p_i/f_i = 0.8-1.2) occur across both phases of transport observed at the East Fork site and show no systematic trend with transport phase (Figure 3.5).

3.5.3. Dimensionless Transport Rates (W^*_{ri}) at Oak Creek and East Fork

We find that the sand-bed East Fork River exhibits dimensionless transport rates 1-5 orders of magnitude larger than Oak Creek for given grain size percentiles and comparable Shield stresses (τ^*_i) (Figure 3.6). Fine sediments (i.e., sand sizes and smaller) make up approximately 50% of the surface material at the East Fork River [*Emmett*, 1980] and 10% at Oak Creek [*Milhous 1973; Parker et al*., 1982]. This 40% difference in surface sand content could result in a 50% decrease in the dimensionless shear stress required to mobilize sand and gravel sized material [*Wilcock and Kenworthy*, 2002] at the East Fork River and may explain the significantly larger transport rates observed at this site. The grain-size specific transport rates shown in Figure 3.6 are given in terms of the subsurface size distribution because that distribution approximates the bed load size distribution over time, particularly at Oak Creek [*Parker et al.*, 1982].

3.5.4. Estimating Reference Transport Rates For All Sizes

A drawback of our approach for determining size-specific reference transport rates (W^*_{ri}) is that particle sizes larger than the d_{20} do not exhibit Phase I motion at Oak Creek (Figure 3.3, d_i > 22.2 mm, or d_i/d_{50s} = 0.40). It is unclear whether Phase I motion simply does not occur for large particles, or whether it is a rare occurrence that could not be detected with the sampling approach used. The long sampling times during low flows at Oak Creek (often over 24 hours) suggest that the later is unlikely. In any event, the lack of a Phase I/II transition for large particles means that reference dimensionless

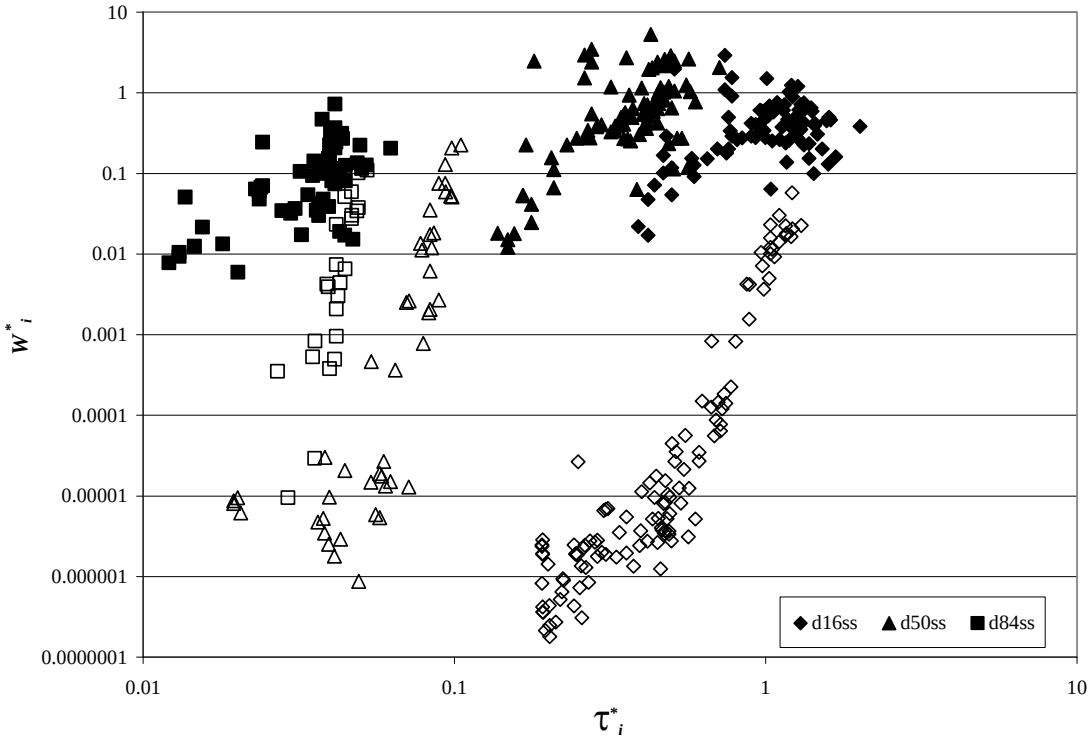

Figure 3.6. Dimensionless bed load transport rate (W^*_i) versus Shields stress (τ^*_i) for three different subsurface grain size percentiles at the East Fork River (solid symbols) and Oak Creek (open symbols).

transport rates ($W^*_{ri\mathrm{II}}$) cannot be determined for those sizes. However, these values are needed to test our proposed revision of the *Parker* [1990] equation (Section 3.5.5). To address this issue, we developed a relationship between dimensionless particle size (d_i/d_{50s}) and $W^*_{ri\mathrm{II}}$ (Figure 3.7), allowing prediction of reference dimensionless transport rates ($W^*_{ri\mathrm{II}}$) and associated Shields stresses ($\tau^*_{ri\mathrm{II}}$) for all size classes. A similar relationship was developed for the East Fork River to estimate $W^*_{ri\mathrm{III}}$ values (Figure 3.7) and associated $\tau^*_{ri\mathrm{III}}$ values for purposes of estimating channel maintenance or flushing flows [*Reiser et al.*, 1989; *Whiting*, 1998; *Ryan et al*., 2002]. Although these empirical

equations allow prediction of references dimensionless transport rates for all size classes, further work is needed to determine whether all grain sizes actually exhibit Phase I/II and II/III transitions.

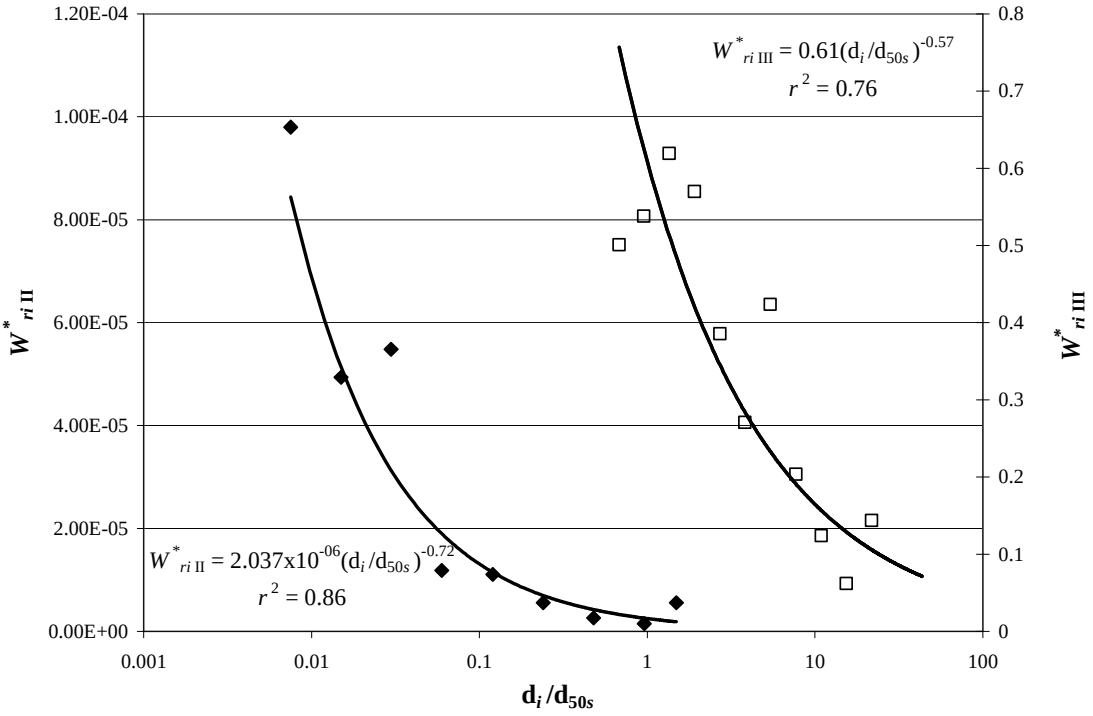

Figure 3.7. Reference dimensionless bed load transport rate for the Phase I/II ($W^*_{ri\mathrm{II}}$) and Phase II/III ($W^*_{ri\mathrm{III}}$) boundaries, as a function of particle size normalized by the surface median grain size, d_i/d_{50s}, at Oak Creek (solid diamonds) and the East Fork River (open squares).

3.5.5. Alternative Formulations of the *Parker* [1990] Transport Equation

Here we assess the performance of two alternative formulations of the *Parker* [1990] bed load transport equation using the observed kinks in the τ^*_i - W^*_i diagrams to

provide a physically-based definition of $W^*_{ri\mathrm{II}}$. Both formulations include a hiding function developed using predicted values of $W^*_{ri\mathrm{II}}$ (Figure 3.7) and corresponding values of $\tau^*_{ri\mathrm{II}}$ (Figure 3.8). There is only a 1% difference between the slope of our hiding function (Figure 3.8) and that developed by *Parker et al.* [1982] (-0.994 versus -0.982, respectively), but a 40% difference in the hiding function coefficient (0.0529 versus 0.0876, respectively). In both cases, the near -1 value of the exponent indicates equal mobility in terms of all sizes being mobilized at similar critical shear stresses, but the lower value of the coefficient in our approach implies a lower critical shear stress for mobilization of the armor layer than that predicted by *Parker et al.* [1982].

The first alternative formulation assumes *Parker*'s [1990] transport function (3.5), but with our hiding function (Figure 3.8). By predicting the reference Shields stress using our hiding function rather than *Parker*'s [1990], we are changing the distribution of ϕ_i values for the observed bed load data compared to that obtained by *Parker* [1990]. Consequently, we are also changing the distribution of flow conditions where equations 3.5a-c are applied. The first alternative formulation applies (3.5c) up to a flow of 0.4 m^3 s^{-1}, while use of the *Parker* [1990] equation with a constant W^*_r value results in application of (3.5c) up to flows of about 1.5 m^3 s^{-1}. Equation (3.5b) is used for flows between 0.4 m^3 s^{-1} and approximately 1.5 m^3 s^{-1} for the first alternative formulation, and between 1.5 m^3 s^{-1} and 5.5 m^3 s^{-1} for *Parker*'s [1990] equation. Equation (3.5a) was not used by *Parker* [1990] at Oak Creek because the largest ϕ_i value using his hiding function was < 1.59. But in our case, we use (3.5a) to predict transport for about 30% of the observations.

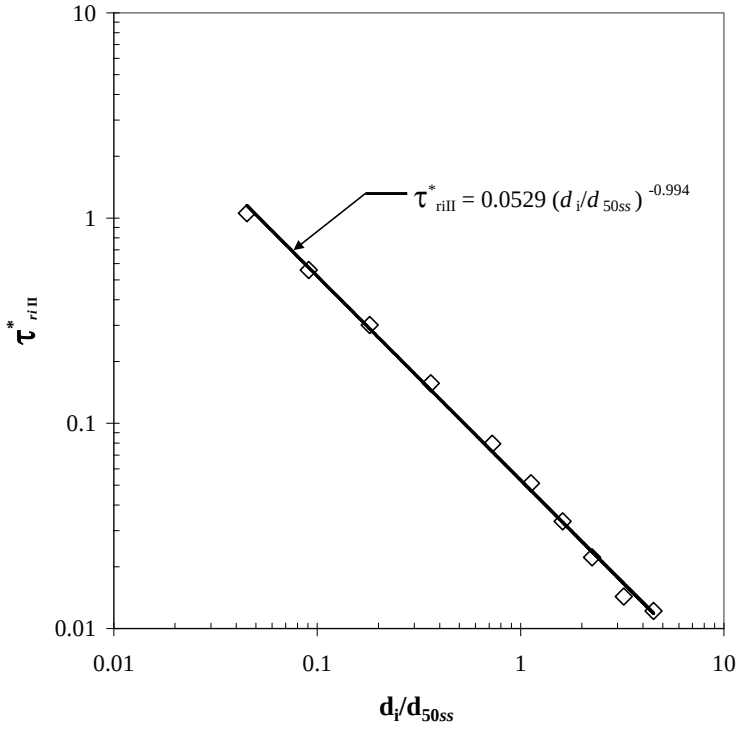

Figure 3.8. Oak Creek hiding function for reference Shields stress at the Phase I/II boundary (Figure 3.4). d_{50ss} represents the median particle size of the subsurface material.

The second alternative formulation also uses our hiding function (Figure 3.8), but includes a revised transport function based on a similarity collapse using our size-specific values of W^*_{riII} (rather than $W^*_r = 0.0025$) (Figure 3.9). Our similarity collapse analysis followed the procedure described by *Parker et al.* [1982]. From this analysis, we developed a site-specific transport relationship at Oak Creek across both Phase I and II transport (Figure 3.9), eliminating the need to assume a power law ($\phi_i^{14.2}$) for $\phi_i < 1.0$ (Equation 3.5c). Recall that *Parker*'s [1990] transport function was fit only to the Phase II transport at Oak Creek, with the Phase I relationship (3.5c) assumed from *Paintal* [1971] such that the two relations match continuously at $\phi_i = 1$. The revised transport

function shows a significantly different slope for Phase I transport than that assumed from *Paintal* [1971] (3.2 vs. 14.2, respectively) (Figure 3.9).

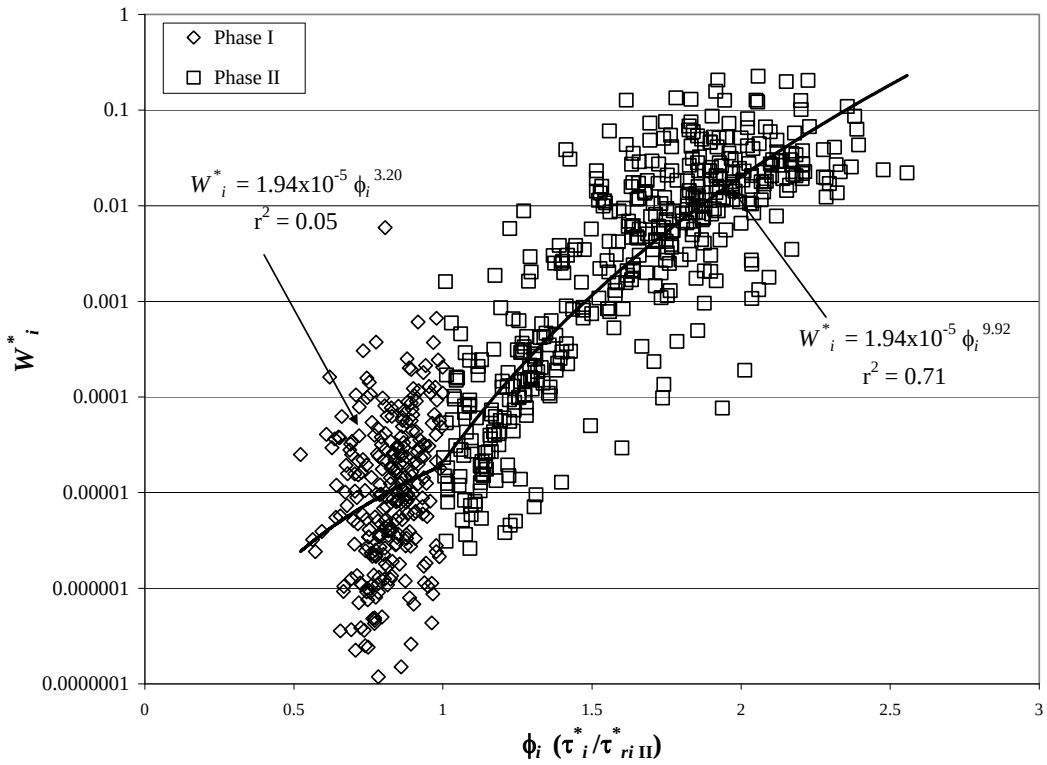

Figure 3.9. Alternative similarity transformation at Oak Creek and revised transport function.

Comparison of observed versus predicted transport rates shows that at low flows (i.e., $\phi_i < 1.0$) both the *Parker* [1990] transport equation and the first alternative formulation significantly under-predict the observed Oak Creek data by an average of -1.0 and -0.8 orders of magnitude, respectively (with standard deviations 0.83 and 0.63 orders of magnitude, respectively) (Figure 3.10). This occurs because both predictions employ equation (3.5c) at low flows, which significantly over-predicts the exponent of the transport function (14.2 vs. an observed value of 3.2, Figure 3.9) and can also be seen

in plots of predicted and observed transport rates as a function of discharge (Figure 3.11). In contrast, the second alternative transport formulation performs better at low flows, with an average error of approximately 0.2 orders of magnitude (standard deviation 0.40 orders of magnitude). The improved performance is expected because the second alternative equation is fit to all transport observations at Oak Creek (including the low-flow observations removed from *Parker*'s [1990] analysis).

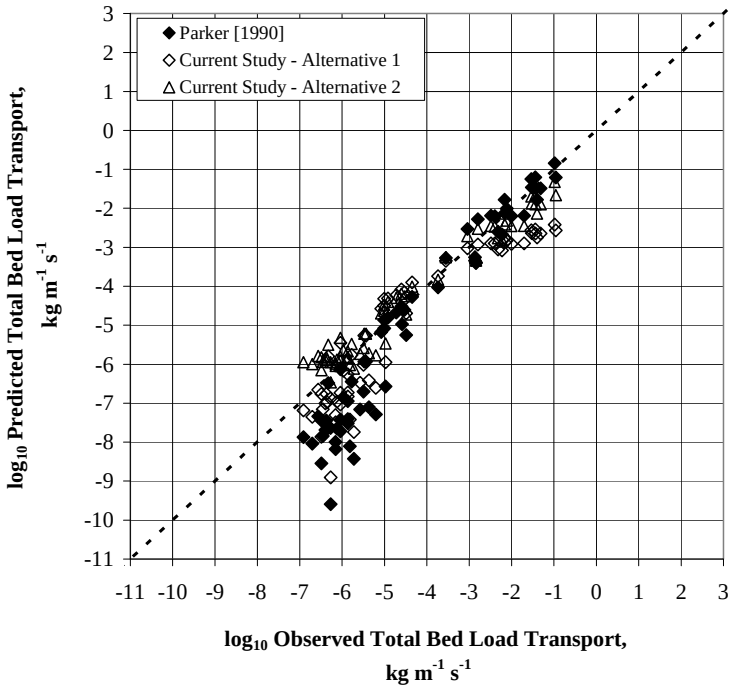

Figure 3.10. Observed versus predicted total unit bed load transport at Oak Creek using the *Parker* [1990] equation by size fraction as originally defined (W^*_r=0.0025) and the two alternative formulations discussed in the text.

The performance of all three equations is significantly improved during high flows (Figures 3.10 and 3.11), with the *Parker* [1990] equation out-performing both alternative formulations; average errors of 0.03 orders of magnitude for the *Parker*

[1990] equation (standard deviation of 0.31 orders of magnitude), compared to -0.34 and -0.05 orders of magnitude for the first and second alternative formulations, respectively (standard deviations of 0.70 and 0.41 orders of magnitude, respectively). Unlike the first alternative formulation, that has increasing prediction errors with discharge (Figure 3.11), neither the second alternative formulation nor the *Parker* [1990] equation show a trend toward positive or negative prediction errors at high discharges (Figure 3.11). The superior performance of the second alternative formulation and the *Parker* [1990] equation occurs because these formulations were fit to transport observations collected during high flow ($\phi_i > 1$) at Oak Creek, whereas the first alternative formulation applies equation (3.5a) which is based on data collected at sites other than Oak Creek.

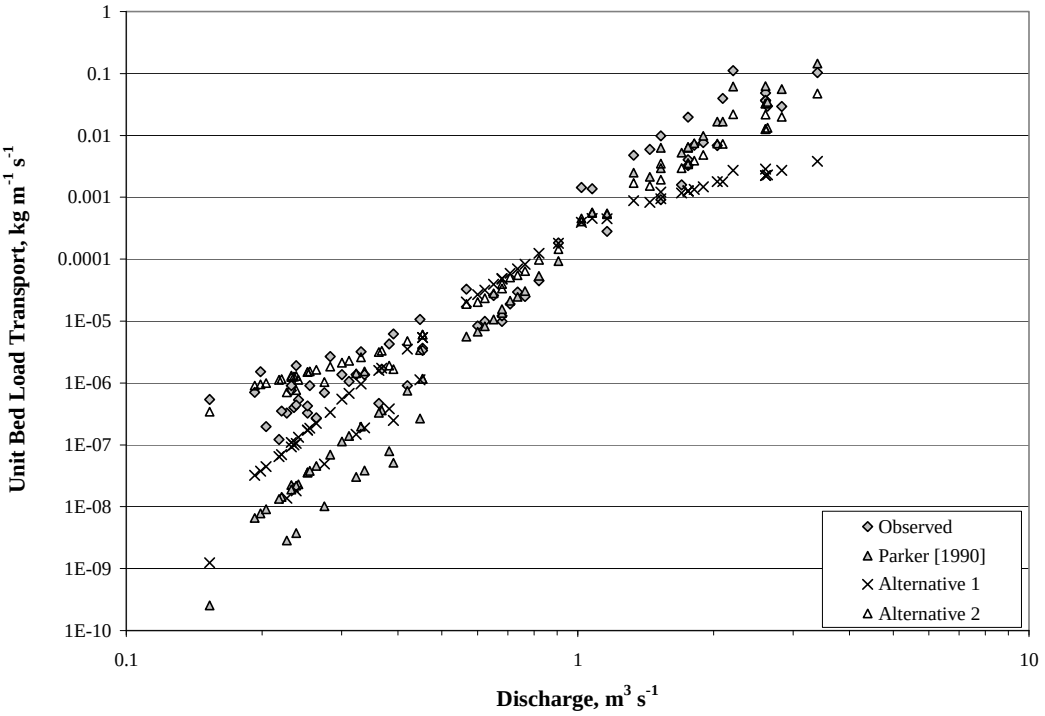

Figure 3.11. Observed and predicted unit bed load transport as a function of discharge at Oak Creek.

The superior performance of the first and second alternative formulations compared to the performance of the *Parker* [1990] equation only occurs during low flows. In fact, at higher flows the *Parker* [1990] equation performs best, suggesting that it is not particularly sensitive to the choice of $W^*_{ri\mathrm{II}}$, at least for the range of high flows examined here. Furthermore, it appears that application of our first alternative formulation may result in systematic prediction errors during both low and high flows (Figure 3.11). Nevertheless, our approach provides a more rationale definition of W^*_{ri} based on observed changes in transport processes.

3.6. Conclusion

Our analysis considers transitions between phases of bed load transport and uses a two-part regression to objectively identify changes in the slope of the transport functions, which we interpret as representing phase shifts (fundamental changes in boundary conditions for bed load transport). We use the observed kinks in plots of Shields stress versus dimensionless transport rate as a physical basis for defining reference transport rates by size class. We apply our method at Oak Creek to identify the transition from Phase I to II transport and to objectively define size-specific W^*_{ri}. Using these values, we offer two alternatives to the *Parker* [1990] bed load transport equation that improve performance at low flows (Phase I), but not at higher ones (Phase II).

We use the data set collected at the East Fork River site to identify the transition from Phase II to III transport. We limited our analysis to these two data sets because the data were collected using channel-spanning bed load traps which likely give best estimates of the actual bed load transport. In addition, these two sites provide contrasting

physical conditions (armored gravel-bed river vs. a poorly-armored, predominately sand-bed river) that allow us to investigate differences in the phases of bed load transport related to channel type and degree of armoring.

We find that the phase transitions at both sites vary by size class and that our identified values of $W^*_{ri\mathrm{II}}$ at the Oak Creek site occur at much lower dimensionless transport values (W^* near 0.00001) than *Parker's* [1990] $W^*_r = 0.0025$. In addition, we find that the onset of Phase II transport using our approach occurs at flows equal to 10 - 20% of Q_2. This is substantially less than observations made in other gravel-bed rivers by *Ryan et al.* [2002] who identified the onset of Phase II transport around 60-100% of the bankfull discharge. We also find that Phase III transport does not occur at Oak Creek even at flows larger than Q_2. At the East Fork River site, we observe that Phase I transport does not occur. Rather, in sand-bed channels such as the East Fork River, Phase II transport is the general state of motion until the spatial variability of excess shear stress has mobilized a majority of the channel bed and/or the flow approaches transport capacity. The transition to Phase III transport occurred at approximately 25% of Q_2. Objectively identifying the Phase II/III transition can assist in selecting the flow regime necessary for flushing of fine material from the surface sediment or for determining those flows necessary for channel maintenance purposes [*Reiser et al.*, 1989; *Whiting*, 1998; *Ryan et al*., 2002; *Schmidt and Potyondy*, 2004]. We suggest that the method presented here be applied at other locations to test the applicability and generality of our functions for predicting dimensionless reference transport rates (both $W^*_{ri\mathrm{II}}$ and $W^*_{ri\mathrm{III}}$) (Figures 3.7) and the Phase I/II and Phase II/III transitions. We also find that transport ratios (i.e., p_i/f_i)

indicative of equal mobility can occur during any phase of transport and there is no systematic trend in transport ratio with transport phase.

3.7. References

Andrews, E. D., and J. D. Smith (1992), A theoretical model for calculating marginal bedload transport rates of gravel, in *Dynamics of Gravel-Bed Rivers*, edited by P. Billi, R.D. Hey, C.R. Thorne, and P. Tacconi, 40-52, John Wiley & Sons, New York, New York.

Ashworth, P. J., and R. I. Ferguson (1989), Size-selective entrainment of bedload in gravel-bed streams, *Water Resour. Res.*, *25*, 627-634.

Barry, J. J., J. M. Buffington, and J. G. King (2004), A general power equation for predicting bed load transport rates in gravel bed rivers, *Water Resour. Res.*, *40*, doi:10.1029/2004WR003190.

Bagnold, R. A. (1973), The nature of saltation and of "bedload" transport in water, *Proc. R. Soc. London A*, *332*, 473-504.

Borden, J. C. (2001), A comparison of sediment monitoring to sediment facies mapping in the middle fork Payette river, central Idaho, M. S. Thesis, 120 pp., Boise State Univ, Boise, Id.

Buffington, J. M., W. E. Dietrich, and J. W. Kirchner (1992), Friction angle measurements on a naturally formed gravel streambed: Implications for critical boundary shear stress, *Water Resour. Res.*, *28*, 411-425.

Buffington, J. M., and D. R. Montgomery (1997), A systematic analysis of eight decades of incipient motion studies, with special reference to gravel-bedded rivers, *Water Resour. Res.*, *33*, 1993-2029.

Buffington, J. M., and D. R. Montgomery (1999), Effects of hydraulic roughness on surface textures of gravel-bed rivers, *Water Resour. Res.*, *35*, 3507-3522.

Buffington, J. M. (2000), Closure to discussion by Garcia, *J. Hydraul. Res., 9*, 721-723.

Church, M., and M. A. Hassan (2002), Mobility of bed material in Harris Creek, *Water Resour. Res*., *38*, doi:10.1029/2001WR000753.

Dietrich, W. E., J. Kirchner, H. Ikeda, and, F. Iseya (1989), Sediment supply and the development of the coarse surface layer in gravel-bedded rivers, *Nature, 340*, 215-217.

Dietrich, W. E., P.A. Nelson, E. Yager, J. G. Venditti, M. P. Lamb, and L. Collins (2005), Sediment patches, sediment supply, and channel morphology, in *River, Coastal and Estuarine Morphodynamics*, edited by G. Parker and M. Garcia, IAHR Symposium, Taylor and Francis, London, vol. 1, p. 79-90.

Emmett, W. W. (1976), Bedload transport in two large, gravel-bed rivers, Idaho and Washington, in *Proceedings of the Third Federal Inter-Agency Sedimentation Conference*, March 22-25, Denver, Colorado, 101-114.

Emmett, W. W. (1980), A field calibration of the sediment-trapping characteristics of the Helley-Smith bedload sampler, *U.S. Geol. Surv. Prof. Pap., 1139*, 44 pp.

Garcia, M. H. (2000), Discussion by Marcelo H. Garcia, *J. Hydraul. Res., 9*, 718-720.

Gomez, B. (2006), The potential rate of bed-load transport, *Proc. Natl. Acad. Sci., 73, 103*, 17170-17173.

Haschenburger, J. K., and, P. R. Wilcock (2003), Partial transport in a natural gravel bed channel, *Water Resour. Res*., *39*, doi:10.1029/2002WR001532.

Hassan, M. A., and M. Church (2001), Sensitivity of bed load transport in Harris Creek: Seasonal and Spatial Variation Over a Cobble-Gravel Bar, *Water Resour. Res*., *37*, 813-825.

Jackson, W. L., and, R. L. Beschta (1982), A model of two-phase bedload transport in an Oregon coast range stream, *Earth Surf. Processes Landforms, 7*, 517-527.

Johnston, C. E., E. D. Andrews, and, J. Pitlick (1998), In situ determination of particle friction angles of fluvial gravels, *Water Resour. Res., 34*, 2017-2030.

Lamberti, A.,and E. Paris (1992), Analysis of armouring processes through laboratory experimetns, in *Dynamics of Gravel-Bed Rivers*, edited by P. Billi, R.D. Hey, C.R. Thorne, and P. Tacconi, 225-250, John Wiley & Sons, New York, New York..

Leopold, L. B., M. G. Wolman, and, J. P. Miller (1964), Fluvial Processes in Geomorphology, 522 pp., W. H. Freeman, New York, New York.

Leopold, L. B., and W. W. Emmett (1976), Bed load measurements, East Fork River, Wyoming, *Proc. Natl. Acad. Sci., 73*, 1000-1004.

Leopold, L. B., and, W. W. Emmett (1997), Bedload and river hydraulics – Inferences from the East Fork River, Wyoming, *U.S. Geol. Surv. Prof. Pap., 1583*, 52 pp.

Lisle, T. E., J. M. Nelson, J. Pitlick, M. A. Madej, and, B. Barkett (2000), Variability of bed mobility in natural, gravel-bed channels and adjustments to sediment load at local and reach scales, *Water Resour. Res., 36*, 3743-3755.

Mark, D. M., and M. Church (1977), On the misuse of regression in earth science, *Math. Geol., 9*, 63-75.

Milhous, R. T. (1973), Sediment transport in a gravel-bottomed stream, Ph.D. dissertation, 232 pp., Oregon State Univ., Corvallis, Or.

Mueller, E. R., J. Pitlick, and, J. M. Nelson (2005), Variation in the reference Shields stress for bed load transport in gravel-bed streams and rivers, *Water Resour. Res., 41*, doi:10.1029/2004WR003692.

Paola, C., and, R. Seal (1995), Grain size patchiness as a cause of selective deposition and downstream fining, *Water Resour. Res., 31,* 1395-1408.

Paintal, A. S. (1971), Concept of critical shear stress in loose boundary open channels, *J. Hydraul. Res., 9*, 91-113.

Parker, G., P. C. Klingeman, and, D. G. McLean (1982), Bedload and size distribution in paved gravel-bed stream, *J. Hydraul. Div. Am. Soc. Civ. Eng., 108*, 544-571.

Parker, G. (1990). Surface-based bedload transport relation for gravel rivers, *J. Hydraul. Res., 28*, 417-436.

Peterson, A. W., and, R. F. Howells (1973), A compendium of solids transport data for mobile boundary channels, *Rep. No. Hy-1973-ST3*, University of Alberta, Alberta, Canada.

Proffitt, G. T., and, A. J. Sutherland (1983), Transport of non-uniform sediments, *J. Hydraul. Res., 21*, 33-43.

Reid, I., and J. B. Laronne (1995), Bed load sediment transport in an ephemeral stream and a comparison with seasonal and perennial counterparts, *Water Resour. Res., 31*, 773-781.

Reiser, D. W., M. P. Ramey, and, T. Wesche (1989), Flushing flows, in *Alternatives in Regulated River Management*, edited by J. A. Gore and G. E. Petts, 91-135, CRC Press, Boca Raton, Florida.

Ryan, S. E., L. S. Porth, and, C. A. Troendle (2002), Defining phases of bedload transport using piecewise regression, *Earth Surf. Processes Landforms, 27,* 971-990.

Ryan, S. E., and, L. S. Porth (2007), A tutorial on the piecewise regression approach applied to bedload transport data, *U.S. For. Serv. RMRS-GTR-189*, 41 pp.

Schmidt, L. J.; and, J. P. Potyondy (2004), Quantifying channel maintenance instream flows: an approach for gravel-bed streams in the Western United States, *U.S. For. Serv. RMRS-GTR-128*, 33 pp.

Tait, S. J., B. B. Willettes,and J. K. Maizels (1992), Laboratory observations of bed armouring and changes in bedload composition, in *Dynamics of Gravel-Bed Rivers*, edited by P. Billi, R.D. Hey, C.R. Thorne, and P. Tacconi, 205-224, John Wiley & Sons, New York, New York.

Warburton, J. (1992), Observations of bedload transport and channel bed changes in a proglacial mountain stream, *Arc. Alp. Res.*, *24*, 195-203.

Whiting, P. J. (1998), Floodplain maintenance flows, *Rivers*, *6*, 160-170.

Wilcock, P.R. (1992), Experimental investigation of the effect of mixture properties on transport dynamics, in *Dynamics of Gravel-Bed Rivers*, edited by P. Billi, R.D. Hey, C.R. Thorne, and P. Tacconi, 109-139, John Wiley & Sons, New York, New York.

Wilcock, P. W., and, B. W. McArdell (1993), Surface-based fractional transport rates: mobilization thresholds and partial transport of a sand-gravel sediment, *Water Resour. Res.*, *29*, 1297-1312.

Wilcock, P. W., and, B. W. McArdell (1997), Partial transport of a sand/gravel sediment, *Water Resour. Res.*, *33*, 235-245.

Wilcock, P. W. (1997), The components of fractional transport rate, *Water Resour. Res.*, *33*, 247-258.

Wilcock, P. R. (2001), Toward a practical method for estimating sediment-transport rates in gravel-bed rivers, *Earth Surf. Processes Landforms*, 26, 1395-1408.

Wilcock, P. W., and S. T. Kenworthy (2002), A two-fraction model for the transport of sand/gravel mixtures, *Water Resour. Res*., *38*, doi:10.1029/2001WR000684.

Copyright or Re-Print Permission

copy right or reprint permission From: PERMISSIONS [permissions@asce.org]

Sent: Wednesday, July 18, 2007 4:30 AM

To: Barry, Jeffrey/SEA

Subject: RE: copy right or reprint permission

Dear Mr. Jeff Barry

Permission is granted fro you to reuse your paper Performance of Bedload Transport Equations Relative to Geomorphic Significance in your dissertation. Please add the credit line to your paper (In review. With permission from ASCE).

Xi Van Fleet

Senior Manager, Information Services

Publication Division

American Society of Civil Engineers

1801 Alexander Bell Drive

Reston, VA 20191

(703) 295-6278-FAX

PERMISSIONS@asce.org

From: Michael Connolly [MConnolly@agu.org]

Sent: Wednesday, July 11, 2007 10:04 AM

To: Barry, Jeffrey/SEA

Subject: Re: copyright or reprint permission

We are pleased to grant permission for the use of the material requested for inclusion in your thesis. The following non-exclusive rights are granted to AGU authors:

- All proprietary rights other than copyright (such as patent rights).
- The right to present the material orally.
- The right to reproduce figures, tables, and extracts, appropriately cited.
- The right to make hard paper copies of all or part of the paper for classroom use.
- The right to deny subsequent commercial use of the paper.

Further reproduction or distribution is not permitted beyond that stipulated. The copyright credit line should appear on the first page of the article or book chapter. The following must also be included, “Reproduced by permission of American Geophysical Union.” To ensure that credit is given to the original source(s) and that authors receive full credit through appropriate citation to their papers, we recommend that the full bibliographic reference be cited in the reference list. The standard credit line for journal articles is:

"Author(s), title of work, publication title, volume number, issue number, page number(s), year. Copyright [year] American Geophysical Union."

If an article was placed in the public domain, in which case the words “Not subject to U.S. copyright” appear on the bottom of the first page or screen of the article, please substitute “published” for the word “copyright” in the credit line mentioned above.

Copyright information is provided on the inside cover of our journals.
For permission for any other use, please contact the AGU Publications Office at AGU, 2000 Florida Ave., N.W., Washington, DC 20009.

Michael Connolly
Journals Publications Specialist